NASA CR-72258
AMS TR-785

TECHNICAL REPORT

# A PRELIMINARY STUDY OF THE EFFECTS OF VAPORIZATION AND TRANSVERSE OSCILLATIONS ON LIQUID JET BREAKUP

by

James A. Newman

approved by

Luigi Crocco and David T. Harrje

prepared for

NATIONAL AERONAUTICS AND SPACE ADMINISTRATION

July 1967

CONTRACT NASr-217

Technical Management
NASA Lewis Research Center
Cleveland, Ohio
Chemistry and Energy Conversion Division
Marcus F. Heidmann

Guggenheim Laboratories for the Aerospace Propulsion Sciences
Department of Aerospace and Mechanical Sciences
PRINCETON UNIVERSITY
Princeton, New Jersey

TABLE OF CONTENTS

## FOREWORD AND ACKNOWLEDGEMENTS

In describing nonlinear (triggered) transverse mode combustion instability, the mechanism of vapor displacement provides the key to many of the phenomena observed. The experimental studies described in this report are pointing toward a quantitative assessment of the factors involved in the vapor generation and displacement associated with the tangential modes. This report describes the breakup of the liquid jets under various environments. Preliminary data involving the use of the vibrating "hyperdermic tube injector" to produce droplets, which are sufficiently separated to show individual vapor sheaths and hence the associated sheath and droplet histories, are described in the annual report (NASA CR-72270).

The author would like to express his gratitude to Mr. David Harrje, Senior Research Engineer, for his cooperation and patience in this endeavor and to Mr. Ken Gadsby and his technical staff for the assistance received in the construction of the experimental apparatus. Appreciation is also extended to Professor L. Crocco and Dr. W. Sirignano for their assistance in the completion of this work.

Support for this research was provided by NASA under Contract Number NASr-217.

## SUMMARY

An experiment has been performed to investigate the breakup of a vaporizing liquid jet. Behavior of the jet has been studied under a variety of steady and oscillatory pressures.

It has been observed that chamber pressure in the pseudo rocket has no significant effect on jet length in the laminar regime so long as the fluid is not rapidly evaporating. For the fluid whose vaporization rate is substantial, a decrease in chamber pressure and the subsequent increase in vaporization, leads to a slight decrease in jet length. This effect becomes more pronounced the larger the jet diameter. In the turbulent region the effect of pressure depends on the fluid under observation, the jet velocity and jet diameter. For a very slowly evaporating fluid, chamber pressure always accelerates jet breakup. This can be attributed to the increased effect of air friction. The length of a vaporizing Freon jet, however, sometimes decreases with chamber pressure and under other circumstances increases. Generally, the evaporation process becomes more important than air friction in controlling jet length when the jet diameter is large and the jet velocity is high.

When the gas in the chamber is subjected to acoustic oscillations, jet breakup is generally enhanced regardless of whether the fluid is rapidly evaporating or not. The effect, however, is only measurable in the laminar regime for the range of oscillation amplitudes employed. At low steady-state chamber pressures, oscillatory pressure (standing mode at a pressure antinode) and oscillatory velocity are both about as effective in promoting the breakup of a non-evaporating fluid. At higher steady pressure levels, pressure oscil-

lations (standing mode at a pressure antinode compared to the spinning mode) appear to be more effective than velocity oscillations. The behavior of a vaporizing fluid is essentially the same as a non-vaporizing fluid except that velocity oscillations become as effective in promoting breakup as pressure oscillations at high chamber pressure. As chamber pressure is lowered and vaporization rates increase, velocity oscillations become more effective than pressure oscillations.

Under none of the circumstances encountered in the pseudo rocket experiment did the spinning mode enhance jet breakup to a greater extent than the standing mode.

Viewing the results of droplet spray fan mixing in a hot rocket environment, tangential displacements resulting from velocity variations were observed. A sodium seeded jet was used as a tracer and indicated no detectable unidirectional motion within the range of the test conditions.

## INTRODUCTION

The combustion process in a liquid propellant rocket engine is never perfectly steady. During combustion, random fluctuations and/or organized oscillations may occur in the combustion chamber. Three distinct categories of combustion instability can exist: low frequency or chugging instability, intermediate frequency and high frequency instability. Chugging, which is caused by a coupling between the propellant feed system and the combustion chamber, is well understood. Intermediate (entropy wave) instability is seldom observed and the effects are usually manifested only as performance losses. High frequency instability, generally the most destructive, can occur in the longitudinal, transverse or mixed modes. As thrust levels have risen, chamber diameters have increased appreciably while the chamber lengths have changed much less. The increase of the chamber diameter relative to the length favors the occurence of the transverse modes of instability. These modes may be present in the radial or tangential form or as a combination of the two. In addition, as chamber diameters increase and oscillation frequency decreases, the effect of the propellant feed system (normally disregarded in the high frequency case) may play a significant role in the combustion instability problem.

One important aspect of combustion instability is the behavior of the liquid propellants when injected into the combustion chamber. The purpose of this study is to investigate this behavior under conditions of simulated transverse combustion instability with attention focused on the vaporization process and how it affects jet breakup and droplet dispersion. The experimental observations were made using a cold flow pseudo rocket motor (i.e., an optical motor where no combustion is taking place) in which were excited

standing and spinning first tangential acoustic modes.

Many investigations into the breakup of liquid jets have been made in the past. Rayleigh[1] investigated the collapse of a round cylindrical liquid column under the influence of surface tension. Rayleigh's analysis is not applicable to high pressure injection because it refers to a nonviscous liquid which is assumed to have a velocity potential. Under pressure, the liquid flows through the orifice with considerable velocity. Laminar flow of a nonviscous liquid through a pipe or orifice is unstable and actually can never occur because the smallest disturbance changes it into a turbulent flow. Therefore, for conditions such as encountered in liquid rocket injection systems, the Rayleigh theory is not applicable. Castleman[2], however, did apply Rayleigh's theory successfully to the atomization of liquids in an air stream and as such offers a reasonable explanation of the disintegration of a high speed liquid jet. According to this theory, "a portion of the mass of the liquid is caught up by the passing air at a point where its surface is ruffled and, being anchored at the base end, is drawn out into a fine ligament. This ligament is cut off by the rapid growth of a dent in its surface, and the detached mass, being very small, is quickly drawn up into a drop." If the ligaments formed are of such lengths as to be unstable, the disturbances caused by the resistance of the passing air are sufficient to initiate their immediate collapse.

Another early investigator, Haenlein[3], published, after the photographic investigation of the breakup of continuous jets of several different liquids, what is probably the most complete quantitative treatment of the theory of jet dispersion. He showed that when a jet of liquid issues from a

circular nozzle into gaseous surroundings, the stream (under the influence of certain disturbances) eventually separates into small particles. These disturbances may be due to such factors as vibration of the injector, imperfect roundness of the orifice, particles of dust in the nozzle, and the influence exerted on the jet by the surrounding gas. Such initial disturbances cause certain characteristic deformations to appear on the surface of the liquid column, the nature of the deformations being a function of the jet velocity and the liquid properties. Haenlein arrived at the conclusion that there were four separate and distinct processes responsible for the eventual disintegration: 1) Drop formation at very low velocities, when the influence of the surrounding gas is negligible and dispersion occurs as a result of the action of capillary forces of the liquid. Disintegration under these conditions is fairly regular and the resultant droplets thus formed are relatively large. 2) Drop formation under the weak influence of the surrounding gas. The aerodynamic action of the gas in passing over the liquid surface results in a rapid intensification of the initial disturbances in a symmetrical manner about the axis of the jet. 3) Wave formation of the jet shape due to stronger aerodynamic influence of the passing gas. The initial disturbances now develop in a lateral direction, giving the jet a wavy appearance, which contributes to a still more rapid disruption of the solid jet. 4) Complete disintegration of the jet due to the chaotic dispersion of the liquid under the influence of the gas through which it is passing. Here Haenlein suggests that this may be due to "internal vaporization of the liquid and the formation of vortices in the nozzle". As each of the above characteristic stages becomes evident, the accompanying injection velocity

must be greater and the droplets become smaller.

In Haelin's experimental study he did not include any liquids which rapidly evaporate. This exclusion cannot be overlooked, since in a rocket chamber, cryogenic propellants begin to vaporize as soon as they are injected. To incorporate this effect does not suggest any other categories other than the above four will exist, but the distinction between each process is no longer clear, since if the evaporation process has an effect on jet breakup (and this study shows that it does), each category will be affected in a different manner. For example, Category 1), though it still may result in relatively large droplets, is now directly influenced by the surrounding gas since the characteristics of the gas dictate the evaporation rate.

With the advent of the liquid propellant rocket engine, a good deal more theoretical and experimental work has been carried out in recent years in an attempt to explain even more clearly the breakup of liquid jets and droplets in both stable and unstable environments. Priem[4] has demonstrated the breakup of drops by a shock wave. Lane, Gordon and Morrel [5,6,7] have studied the breakup of droplets in an air stream. Analytical and experimental studies by Morrell, Provinelli and Clark[8-11] have considered the breakup of liquid jets due to the influence of a gas flow. In Clark's study[11], jets of high Weber numbers have been shown to spread in a direction transverse to the gas flow in response to the pressure distribution on the liquid surface. Drops and ligaments tear off along the edges of the thinned jet and breakup is resisted only by the inertia of the fluid. A semi-empirical correlation was derived to predict jet length and breakup time under his experimental conditions.

The behavior of liquid jets under conditions of simulated instability has been studied by Meisse[12] and Reba and Brosilow[13]. In both cases attention was paid primarily to the longitudinal mode of oscillation and the resultant fluid behavior. Photographic observations of liquid propellants in stable and unstable combustors have been made by Heidmann[15], Rossman[17] and Ingebo[18]. A theoretical analysis by Dityakin and Yagodkin[19] shows that under oscillatory chamber conditions; 1) there is a change in the character and in the wavelength of the unstable perturbation and instead of a single region (characteristic in the absence of fluctuations) an infinite number of separate disturbances arise and 2) the optimum wave length is less than that for the case of absence of fluctuations, that is, the fluctuations of the flow velocity and of the density of the gas lead to a decrease in the droplet dimensions obtained in the jet disintegration. The latter conclusion has been recently verified experimentally by Ingebo[18]. In a study of ethanol jets in a combustor with oscillatory combustion gas flow, a decrease in the volume-number mean drop diamter, $D_{30}$, from 217 microns to 62 microns was recorded.

Rocket motor designers, it is apparent, have long been concerned with the injection process and how it affects combustion instability. Of the experiments performed in the past, few if any have considered the effect of propellant vaporization except those studies which utilized a photographic investigation of actual firing rockets. Here, of course, the propellants do evaporate but the role played by the evaporation process as compared to the other jet breakup mechanisms cannot be ascertained. It is the purpose of this study to clarify this question and to determine under what circumstances evaporation of the propellant is a significant jet breakup parameter. This

study concerns itself, however, not only with jet breakup of a vaporizing fluid in a quiescent environment, but also examines the influence of oscillatory gas velocity and pressure. An analytical treatment examines the directional behavior of the resultant droplets and discusses its effect on combustion instability.

## EXPERIMENTAL APPARATUS

The apparatus used in the experimental portion of this work consisted primarily of a "pseudo" rocket motor with its associated instrumentation and a spark photography system. The term pseudo rocket motor is a carry-over from an earlier work[20] and will be used throughout this thesis. In the former study the intent was to simulate as closely as possible the significant rocket engine parameters present during the tangential mode of combustion instability and to observe the displacement of liquid and vapor in the chamber. Though the simulation was good, the experiment did not permit an accurate description of the prevalent jet breakup and displacement mechanisms. Because such a large number of variables were simultaneously present; i.e., axial gas flow, transverse gas flow, oscillatory gas flow, variable injection velocity, variable chamber pressure, variable pulse strength and variable fluid properties; it was not possible to categorically separate the individual effects. As a result the pseudo rocket was modified in an attempt to more rigidly control these variables and in fact to eliminate some of them.

Remaining essentially unchanged is the chamber itself. Nine inches in diameter and six inches long, the pseudo rocket chamber has the same nominal dimensions as the 1500 lb. thrust transverse rocket hardware used at Princeton. The original intent was to utilize data from both experiments for mutual benefit. The acoustic environment of the chamber is such that at room temperature the first tangential mode (the one of interest) occurs at approximately 890 cps, the first longitudinal

at 1130 cps, while the second tangential and first longitudinal-first tangential combined modes occur at just over 1400 cps.

To facilitate photographic and visual observations, the chamber is fitted with two diametrally opposed, rectangular, flush-mounted, optically ground and polished plate glass windows. The chamber was such that protuberances of any kind inside the chamber were kept to a minimum. This was to insure that the acoustic waves generated within were as ideal as possible and that no adverse damping or wave reflection took place.

Among those variables mentioned previously, the first to be eliminated was the axial gas flow. This was done to avoid the undesirable pressure fluctuations caused by turbulence in the gas and was accomplished by merely closing off the multiple nozzle chamber exit. A flat smooth cover plate was installed so as to guarantee that the numerous nozzles, though plugged, may not act as a damping device. When the multi-orifice nozzle is plugged the resulting combustion is similar to an acoustic absorbing liner, many of which have been found so successful in damping out combustion instability in jet engines.[21] Except for possible unexplained coupling effects between the transverse and axial gas flow[20], one would expect that the effect of axial gas flow would be very similar to the effects of the injection velocity of the fluid entering the stagnant atmosphere. That is, if gas flow along the axis of the jet can influence jet breakup, whether the gas or the liquid is in motion should make little difference. The capability of conducting experiments with flow through is still a feature of the equipment, however, and can be utilized with only minor changes to the system. The next important modification was to the method by which the gases in the

chamber were oscillated. Gartner's procedure was to use a nitrogen pulse gun. This gun had a side-ported slide ram which moved past a limited volume plenum chamber. When actuated the gun introduced tangentially into the chamber a nitrogen gas pulse thus momentarily exciting the first tangential acoustic mode. Unfortunately, the acoustic oscillations did not persist for long ($\sim$ 10 millisec) and in addition a severe vortex type motion was imported to the chamber gasses by the nitrogen pulse. Consequently it was difficult to distinguish between the effects of the vortex gas motion and the effects of oscillatory gas motion on jet breakup. Since in an unstable combustion chamber the energy to drive the wave is supplied continuously by the combustion process, and no severe tangential unidirectional motion is present[#], it was felt that a continuous energy input to the pseudo rocket would be a more accurate analogy and also would permit detailed examination of the jet behavior for a substantial length of time. In this regard the pulse gun mechanism was discarded and two 60 watt Universal horn driver units were installed. The horns were driven by a Knight audio oscillator through a Technology Instrumentation Corp., phase shifting network via a Bogen, MO 100A power amplifier and a Dukane 100 watt power amplifier. The placement of the horns (at right angles to each other) and the use of the phase shifting network gave the system considerable versatility. By proper phasing it was possible to obtain the first tangential standing mode with the pressure node at the injector (allowing specific observations of velocity effects). Also, the acoustic field could be established such that the injector was positioned at the

---

[#] A photographic investigation into the processes occurring near the injector face of the nine-inch diameter transverse rocket hardware did not show any significant tangential flux of gases. (See Appendix A)

pressure antinode thereby permitting the observation of pressure effects alone. In order to examine the combined effects of oscillatory pressure and velocity the first tangential spinning mode could also be established by setting the signal to one horn ninety degrees out of phase with the other. Acoustic field intensities of up to 165 db were attainable with this set-up resulting in peak-to-peak velocity oscillations of up to eighty feet per second. A photograph of the pseudo rocket appears in Figure 1 and a schematic is in Figure 2.

By changing to this system, it was found that the Kistler crystal pressure transducers previously utilized were no longer adequate for accurate pressure measurements.# In their place were installed two lead zirconate-lead titanate piezoelectric ceramic transducers. (See Figure 3) These devices, which were designed and constructed at Princeton, when used in conjunction with Kistler Model 565 charge amplifiers, produced signals which were remarkedly stable, with an extremely low noise to signal ratio. To calibrate these transducers a calibrated General Radio sound survey meter was utilized. Unfortunately the limited range of this instrument (135 db) necessitated the extrapolation to the higher field intensities encountered in the chamber. Attempts to improve the calibration with other available transducers whose output was known, were not successful primarily because of frequency response limitations of those instruments.

The measurement of oscillating velocities was made with a

---

# This was because of the low pressures involved, 1 psi, which would have required microphone-type transducers as contrasted with the 0 - 5000 psi Kistlers on hand.

constant temperature hot-wire anemometer system manufactured by Thermo-Systems, Inc. A radially oriented tungsten hot-wire sensor was located at the same axial and angular position as one of the pressure transducers and at the same radial positions as the fluid injector. By monitoring the signals from the-hot wire and the pressure probes it was possible to ascertain the type, and the amplitude and direction of the acoustic wave in the chamber. When necessary the hot-wire and pressure transducer signals were recorded using a scope camera and the Tektronix type 551 oscilloscope. Calibration of the hot-wire system was performed using facilities available at Princeton in which known velocities could be supplied. Unfortunately it was only possible to calibrate the system at one steady-state pressure level, however by utilizing King's law which has the form,

$$Nu = \frac{1}{\pi} + \sqrt{\frac{2}{\gamma}}\sqrt{Pr}\sqrt{Re}$$

it was possible to analytically correct the calibration curve so that velocity measurements, at all the steady chamber pressures encountered in this work, could be obtained.

Photographic records of the vapor and liquid displacement were secured with the aid of a 15KV spark source. The high intensity and short duration of the light emitted by the spark system was necessary to produce photographs of good clarity and detail. Shadowgraphs which were taken to specifically observe vapor displacement, were found to be of good photographic quality when the light output from the spark was attenuated with a 4X neutral density filter, and the film was Kodak Royal Pan or Polaroid type 52 sheet film. A variable delay trigger circuit was used to control the time during the acoustic cycle when the

film was exposed. In operation, this circuit was activated by the gate output from a Tetronix type 551 oscilloscope (see Figure 3). The intent here was that by taking several shadowgraphs at distinct intervals during the acoustic cycle it would be possible to determine to what extent fluid vaporization was promoting or hindering jet breakup. The photographs were taken with a bellows type studio camera fitted with a 200 mm focal length, f-1 lens. Of the approximately one hundred pictures taken during this study, several appear for illustrative purposes in this report.

The third major modification to the existing set-up was to the fluid injector itself. In the past the injected fluid, Freon 114, was steadily introduced through a cylindrical tube into the chamber resulting in a turbulent jet of size comparable to that of a typical rocket engine showerhead injector (orifice diameter = 0.120"). Though some data regarding the displacement of liquid and vapor were gathered, insufficient information was obtained pertaining to relative (between vapor and liquid) displacements. In addition it was not determined (a) how specifically the vaporization process was affected by the oscillatory gas motion and (b) how the vaporization process itself affected jet breakup and droplet dispersion. This was due to poor reproducibility and the high turbulence level and jet irregularity associated with streams of high Reynolds and Weber numbers. In what was initially an attempt to investigate (a), a capillary droplet generator was designed. However, the extent to which the oscillatory gas motion affects droplet vaporization rates has not been studied extensively. Should the desire arise to investigate this particular area in greater detail, the system is perfectly capable of supplying the required experimental data. In the

course of this work though, it was used as an important diagnostic tool. The imposition of regular perturbations to the liquid jet rendered accurate jet velocity information. Also, and perhaps more important, the consistent production of uniform arrays of droplets permitted a detailed examination of the way the droplets (and their vapors) were displaced under the influence of the acoustic field.

The operation of the droplet generator is based on a method suggested by Nicholls, et al[22]. It is shown in Figure 4. The device allows a maximum of four fine liquid streams to be injected simultaneously into the pseudo rocket. This would permit the four liquid jets to be observed at four slightly different stations and hence determine if, and to what extent the individual streams interact with each other. However, for reason of photographic clarity, in this study only one such stream was examined. The other three were blocked off, but can be reopened at a later date.

The droplet generator is attached to the voice coil of a 20 watt speaker. Though the use of a 20 watt audio amplifier and another audio oscillator, the generator can be made to vibrate at any desired frequency. Like all vibrating capillary devices for producing a stream of uniform liquid drops, the operation of this generator is based on Rayleigh's analysis of the instability of capillary jets[1]. By considering a cylindrical liquid jet whose surface is perturbed, Rayleigh has shown, by calculating the change in potential and kinetic energy from the unperturbed condition, that the frequency of maximum instability of the jet is

$$f_c = \frac{u_j}{4.508\, d_j} \qquad (1)$$

where $u_j$ is the jet velocity and $d_j$ the jet diameter. When the jet is mechanically disturbed at such a frequency, droplets of uniform size are formed. However, it has been observed by this writer that a range of frequencies can result in uniform drop sizes. This fortunate situation allows the production of a variety of droplet sizes and spacing without changing the injector needle diameter or the injection velocity. The droplet size will of course depend upon the driving frequency and, as can be shown from the conservation of volume, the initial drop size D (ignoring the vaporization prior to the droplet formation) is related to the initial jet diameter by:

$$\frac{D}{d_j} = \left(\frac{3}{2}\,\frac{\lambda}{d_j}\right)^{1/3} \tag{2}$$

The selection of drop diameter D is not as flexible, however, as is indicated by the above. Schneider[23], has shown that in order to produce a smooth capillary jet a minimum pressure head exists. Below this value the liquid forms a small drop which is attached to the exit surface by the action of surface tension. The drop grows and when it reaches a size such that its weight can overcome the surface tension, it detaches from the surface and falls. Droplets formed in this way are usually very large. If the liquid head is increased above this limiting value a smooth liquid jet of diameter equal to the tube diameter is formed. The minimum velocity of a smooth jet exiting from a capillary tube is dependant on the surface tension, the density of the fluid and the tube diameter. Schneider's analysis shows that

$$\overline{U_m}^2 > \frac{8\sigma}{d_j \rho_\ell} \tag{3}$$

therefore jet velocities below this value cannot be attained. Consequently the driving frequency (Eq. 1) is limited which in turn restricts the droplet size (Eq. 2).

Another consideration with regard to the droplet generator is the terminal velocity of the droplets formed. By equating buoyancy and gravity forces this terminal velocity, when the droplet is falling through a quiescent atmosphere, may be expressed by:

$$V_T = \frac{g D^2 (\rho_f - \rho_a)}{18 \mu_a} \tag{4}$$

where the drag coefficient has been chosen equal to $\frac{24}{Re}$ for laminar flow. Therefore, in order to produce droplets of uniform spacing, the initial droplet velocity must be equal to the terminal velocity. If the initial velocity is less than this value (but higher than that specified by Equation 3) the droplet spacing will increase as the drops proceed through the chamber. If the initial velocity is higher than the terminal velocity, coalescence of the droplets will occur. The curves of Figure 5, which represent the terminal and minimum velocities for two of the liquids studied, show that a minimum jet velocity exists below which the droplet generator (stream generator) cannot function. Apparently therefore, in a stagnant atmosphere, jet length will go from zero at zero injection velocity# to some finite value when the pressure differential is sufficient to impart $u_m$ to the fluid.

Three different size capillary tubes were used in this study; .006", .012" and .024", inside diameter and 0.5 cm long. A photograph of a typical stream of droplets produced by this generator is shown in Figure 6. Here the tube diameter is .012" and the chamber gas is stagnant. The injected fluid is water and the chamber pressure is 0 psig.

---

# That is, the formation of initial large drops, dripping.

It has been previously stated that as well as being capable of producing such an array of droplets, the generator was utilized to measure jet velocity. In general, the technique to procure the experimental data was as follows:

A stable liquid jet was established in a quiescent chamber and its breakup length $L_b$ would be measured. The stream vibrator was then activated at a suitable frequency to produce regularly spaced droplets or thickenings of the solid portion of the jet. The distance between the droplets or thickenings is related to the jet velocity by:

$$u_j = \lambda f$$

where $\lambda$ is the distance between the droplets and $f$ is the frequency of vibration.# Having performed such a measurement, the stream vibrator was deactivated and the steady jet breakup length was again measured. This then gave one point on a curve relating jet breakup in a stagnant atmosphere to jet velocity.

To then examine the effects of acoustic oscillations the chamber was resonated in the first tangential mode. The breakup was again measured and compared to the steady jet behavior. Having done so, the chamber was then permitted to resume a quiescent state. Then by activating the stream vibrator, the jet velocity was again measured. The results from the first velocity measurement and the last measurement were averaged to obtain an accurate value of $u_j$. At no time were both the stream vibrator and the acoustic driver unit (which resonated the chamber) in operation at the same time in the tests described.

---

# To insure a good degree of accuracy, for each jet configuration, several frequencies were imposed and the distance $\lambda$ measured for each case. The computed velocities were then averaged to give the final value of $u_j$.

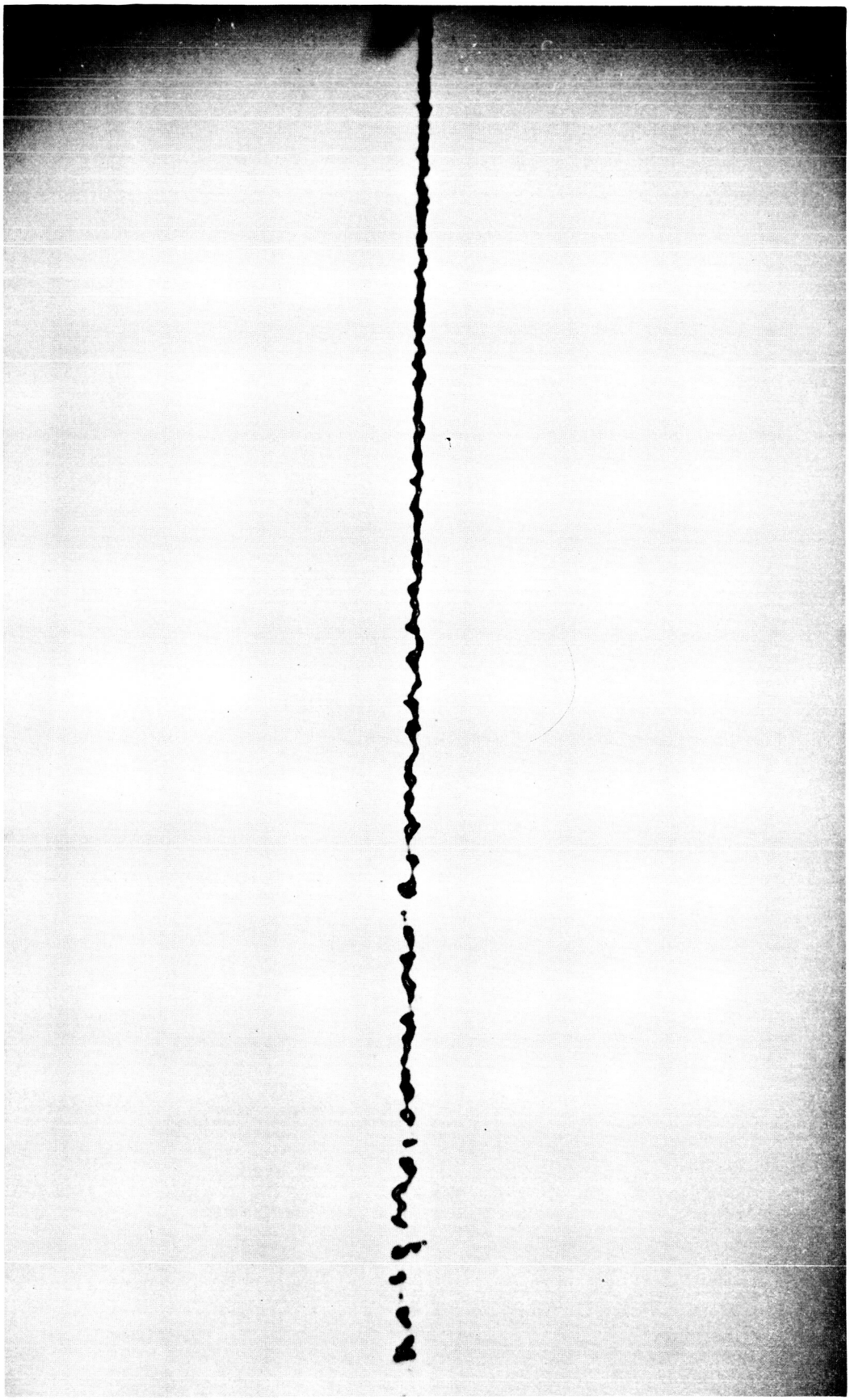

*Turbulent jet breakup - quiescent chamber*

*Figure 9*

JP21-4128-66

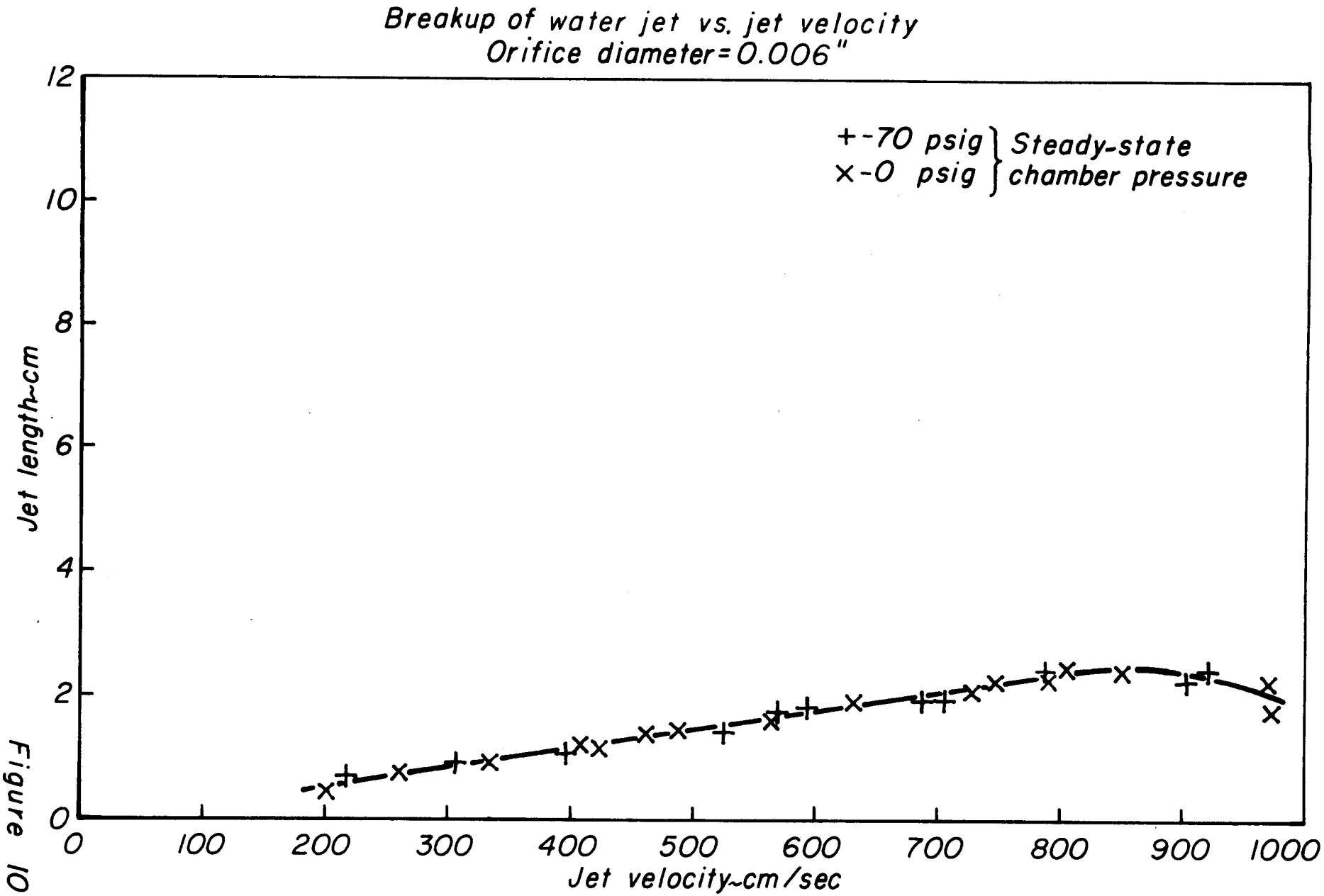


Figure 10

JP21-4129-66

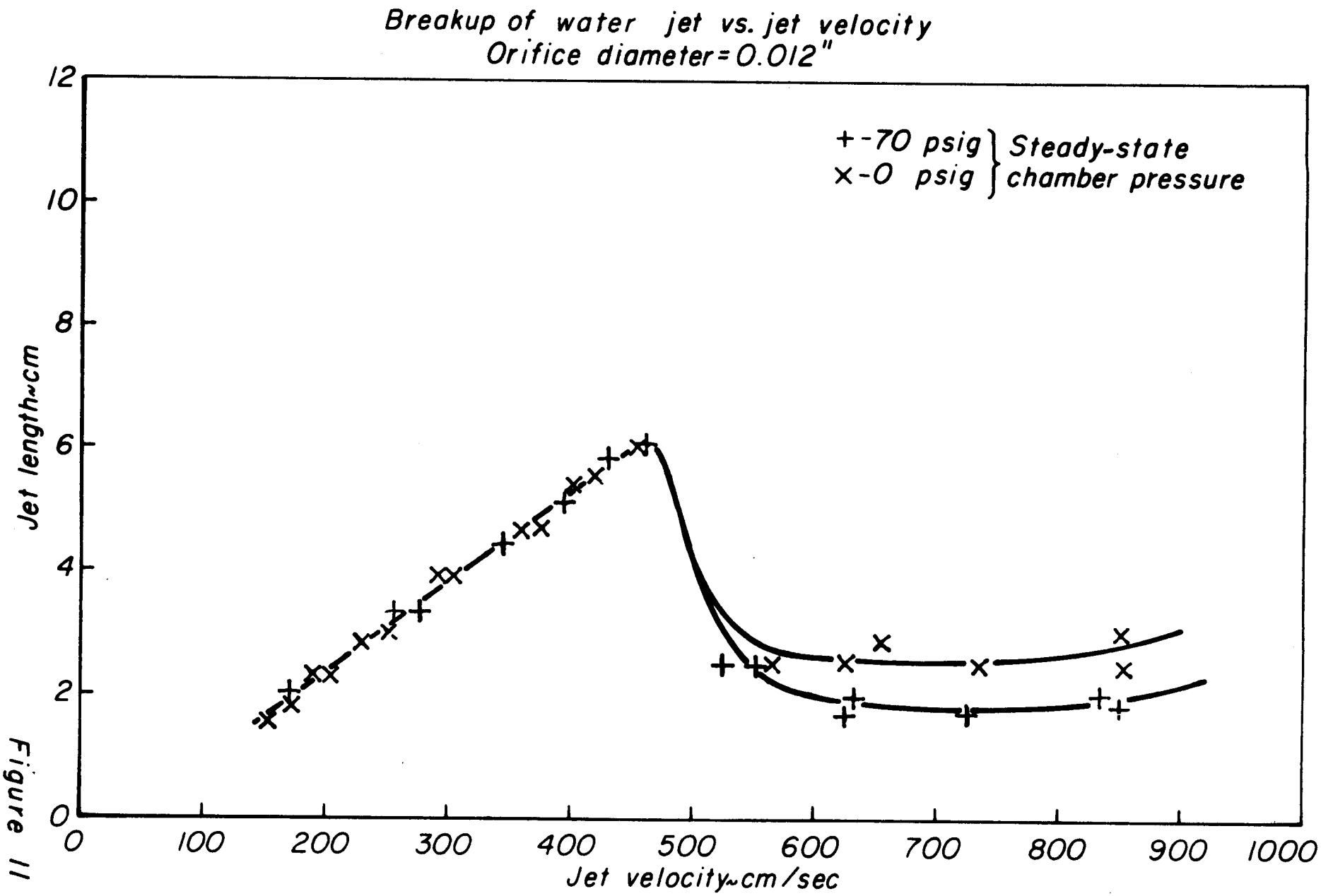


Figure 11

JP21-4130-66

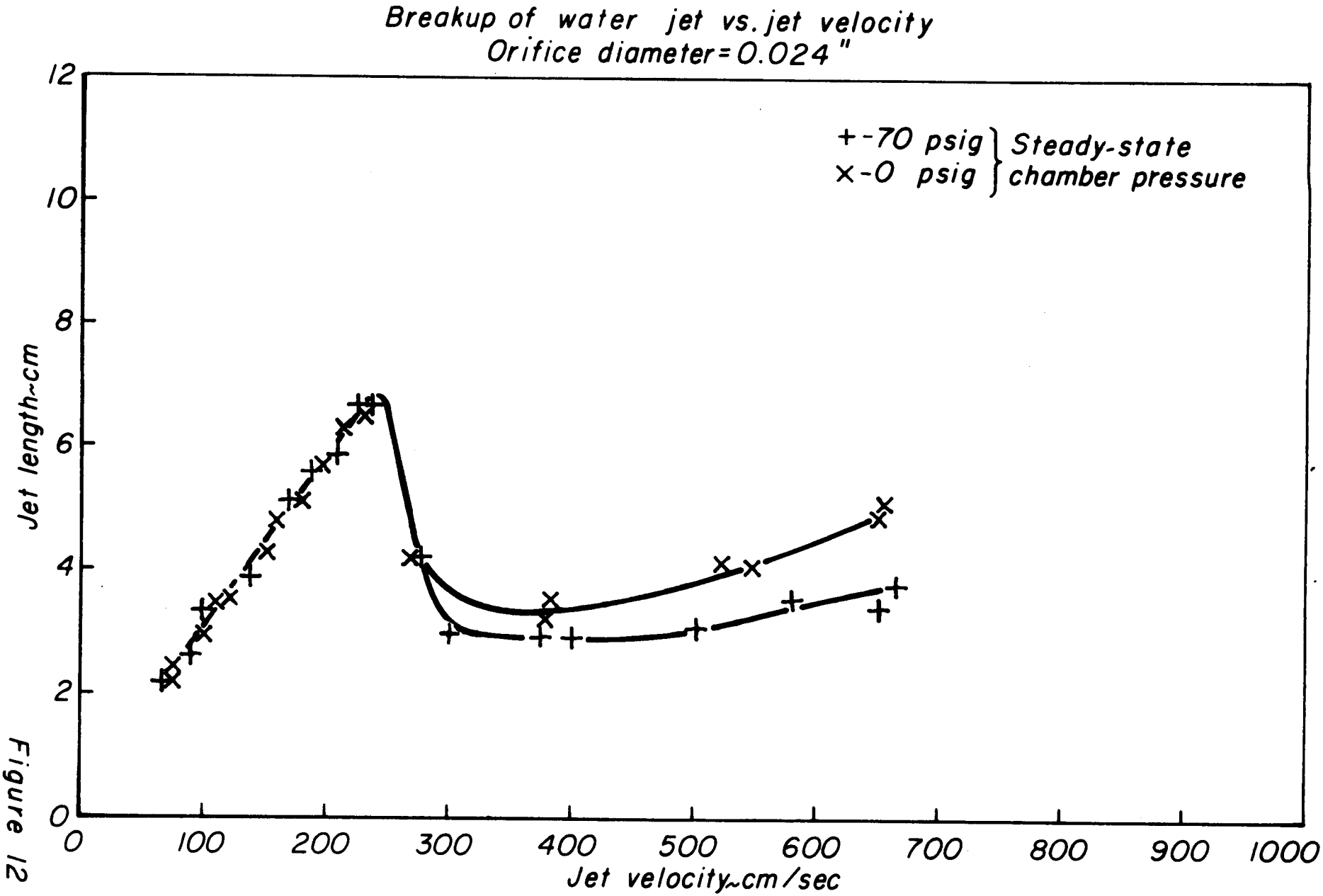


Figure 12

JP21-4131-66

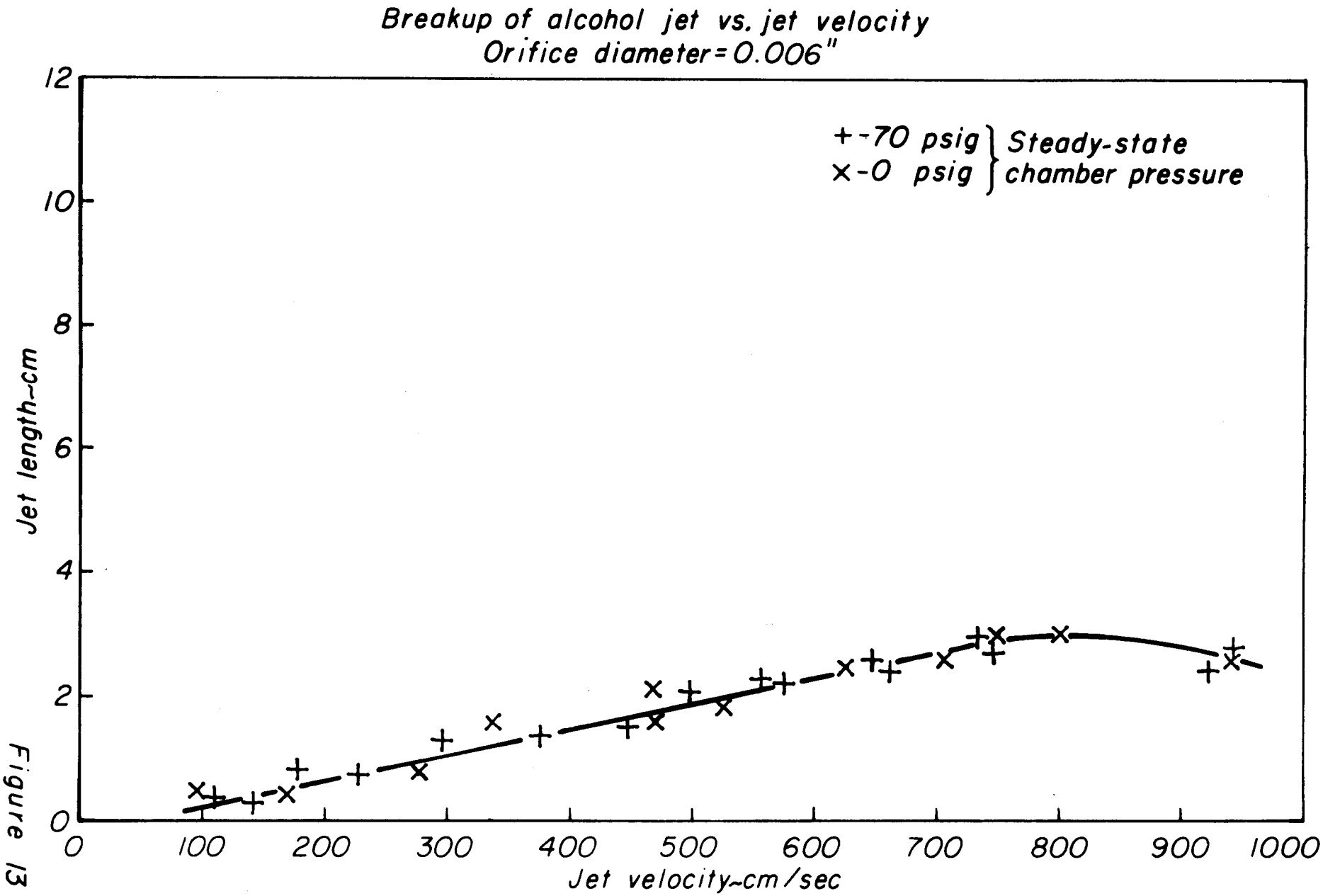


Figure 13

JP 21-4132-66

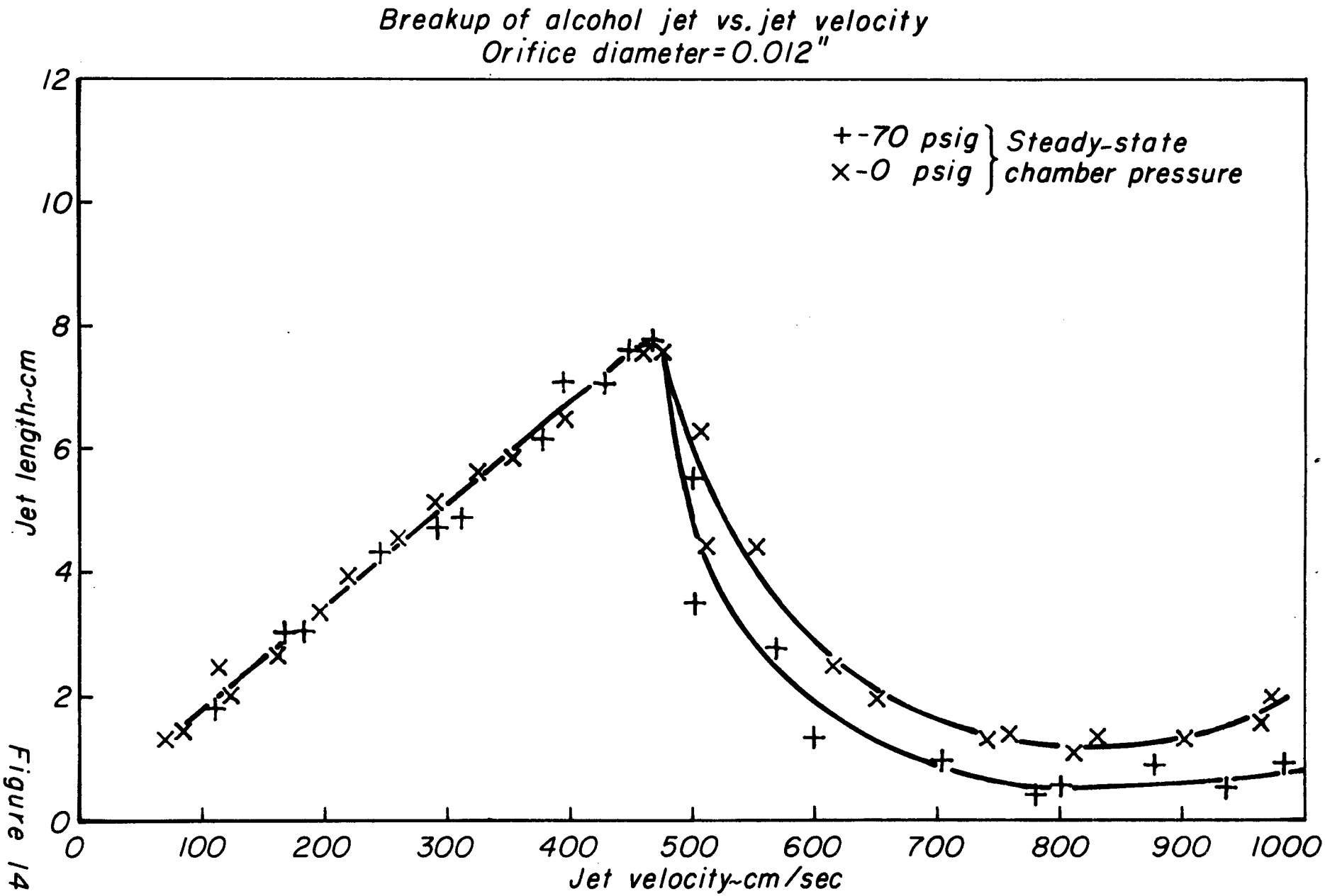


Figure 14

JP21-4133-66

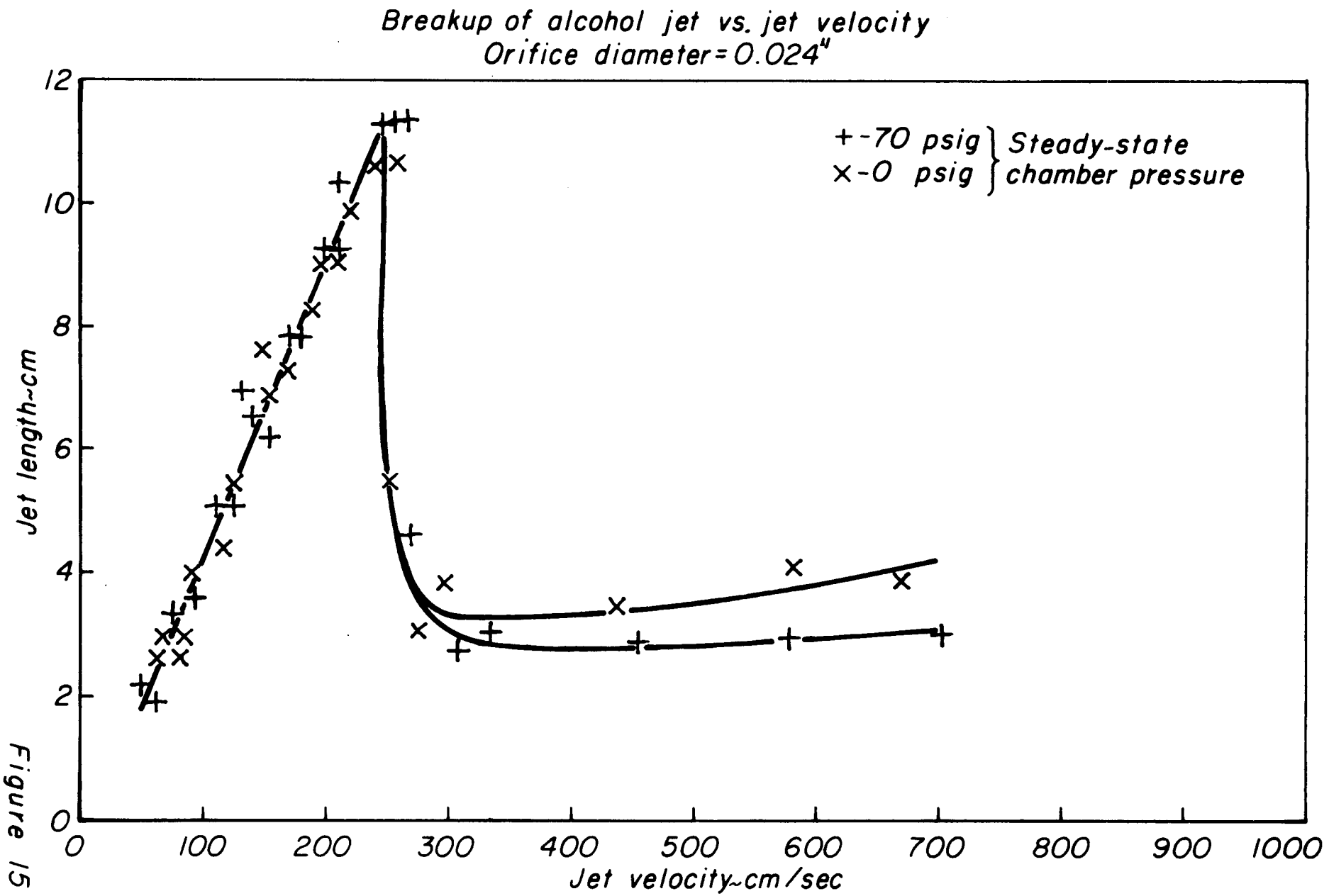


Figure 15

JP21-4134-66

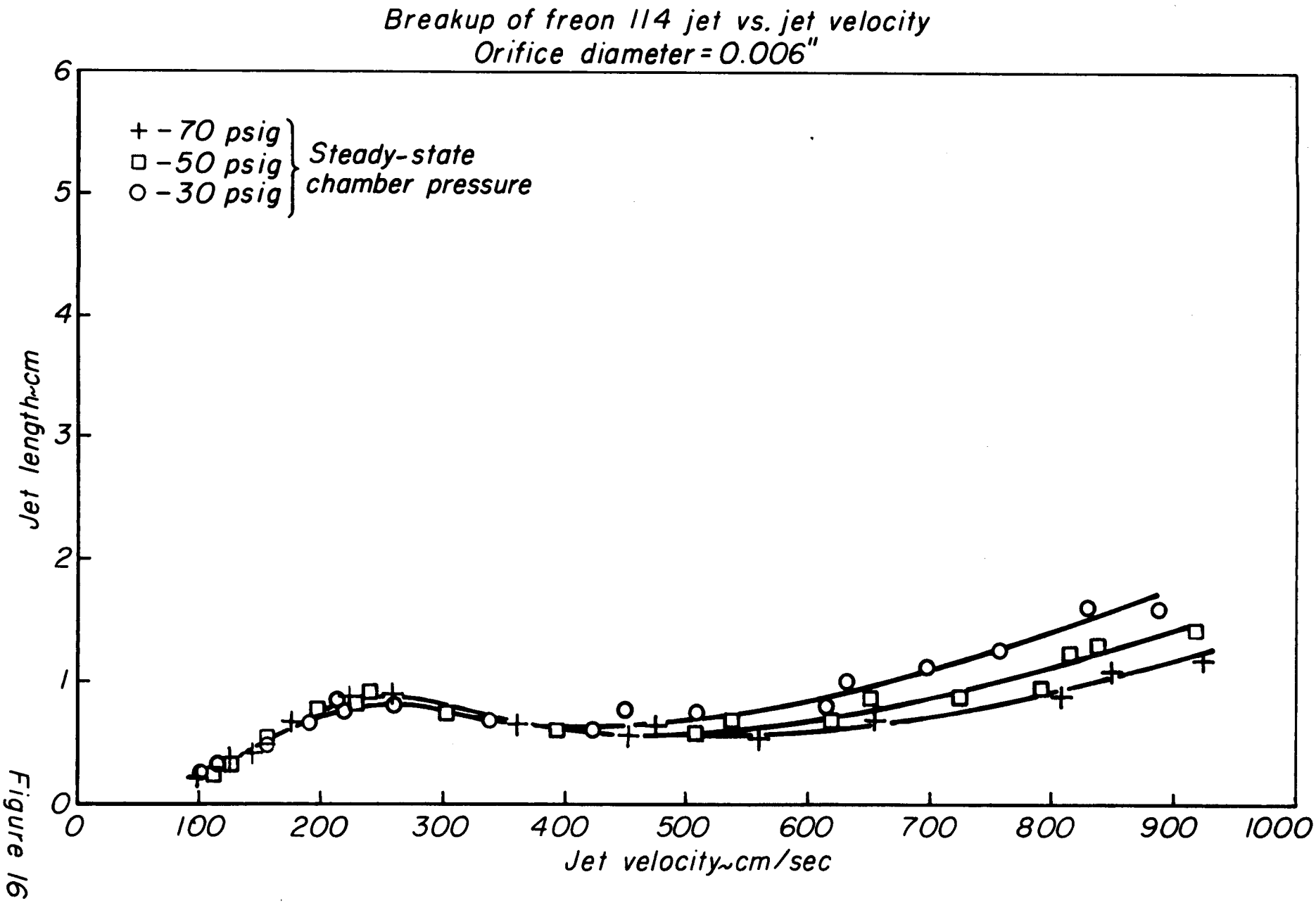


Figure 16

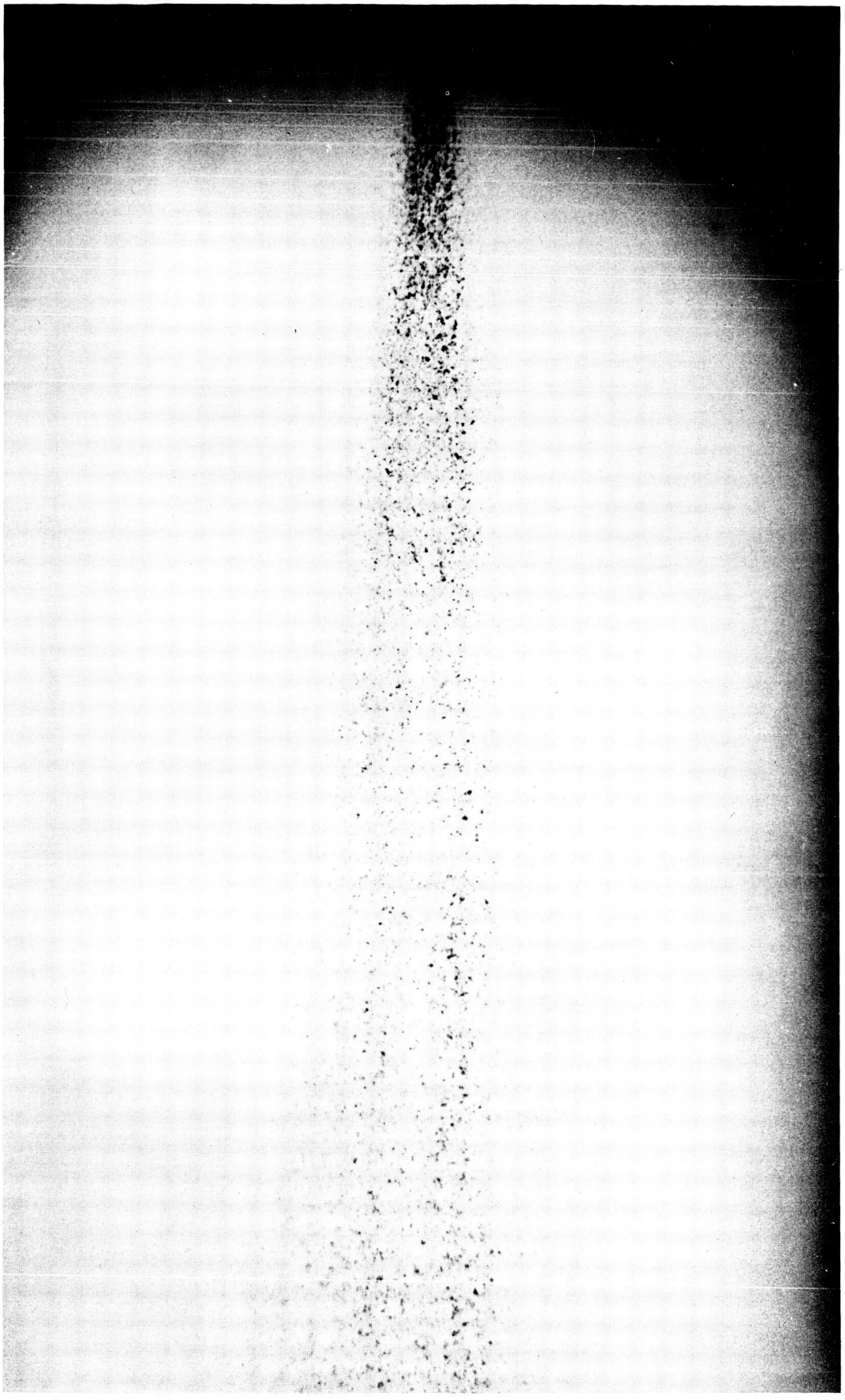

JP21-P32-66

*Jet breakup-chamber pressure below liquid vapor pressure*

*Figure 17*

JP21-4135-66

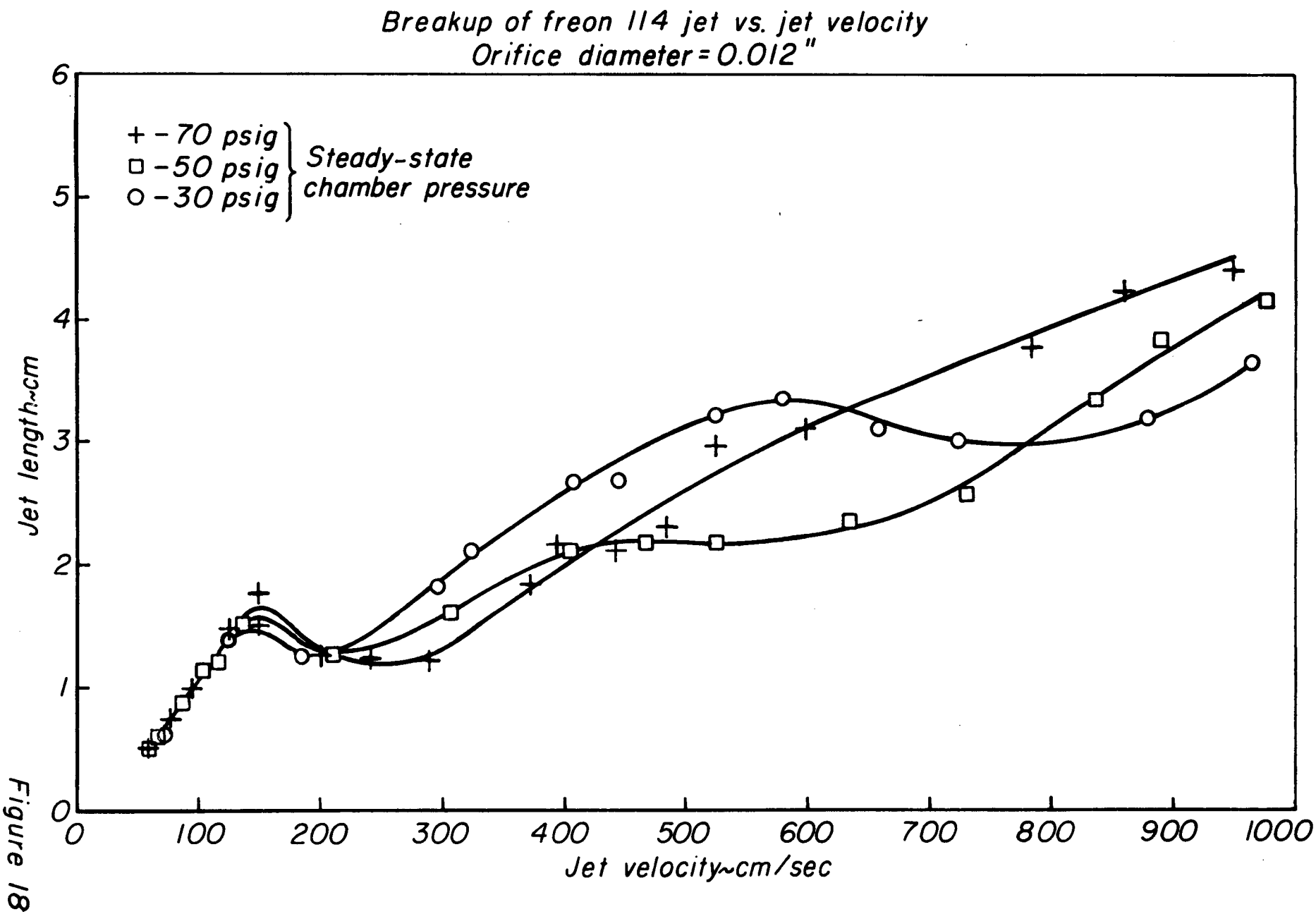


Figure 18

JP 21-4136-66

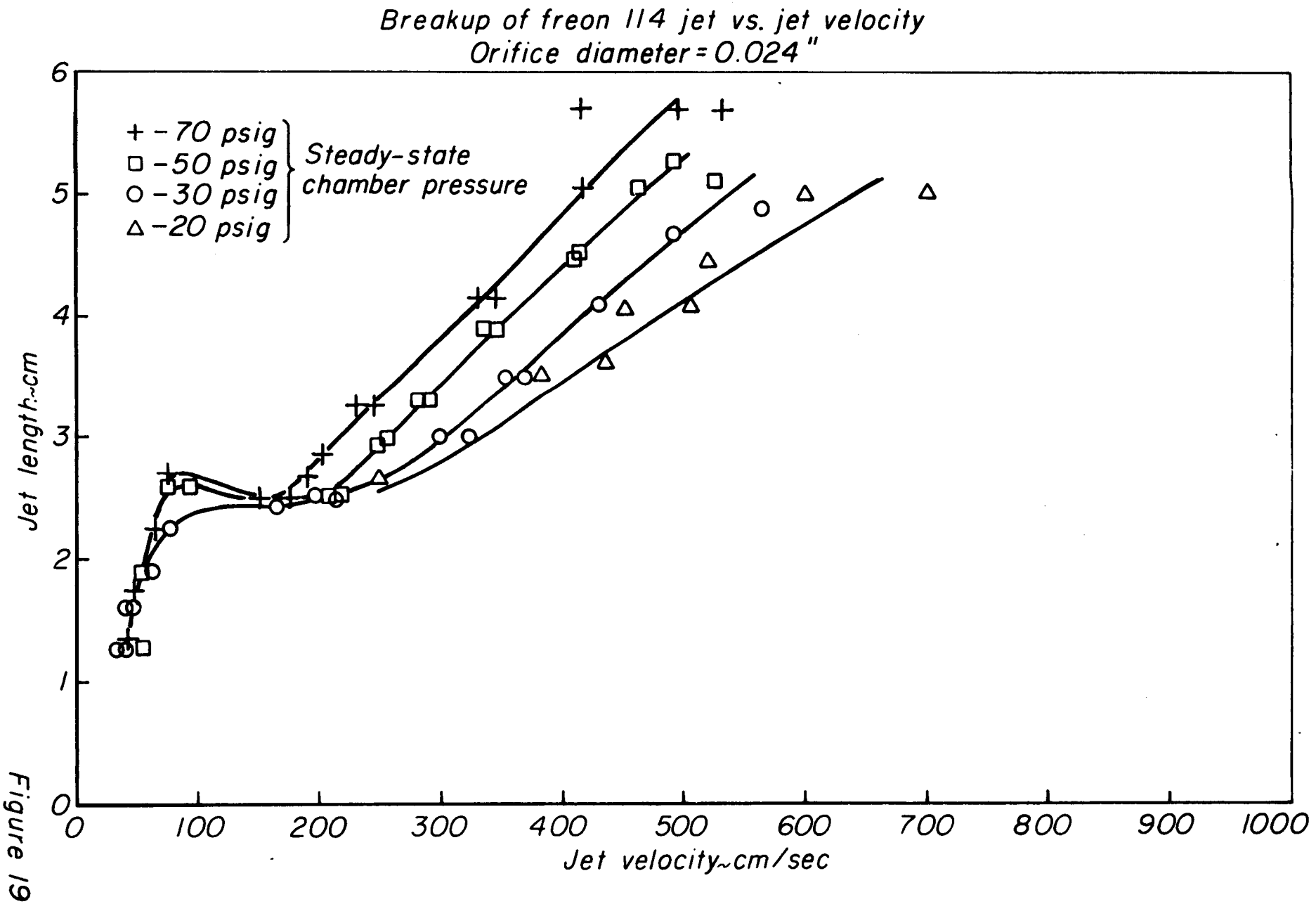


Figure 19

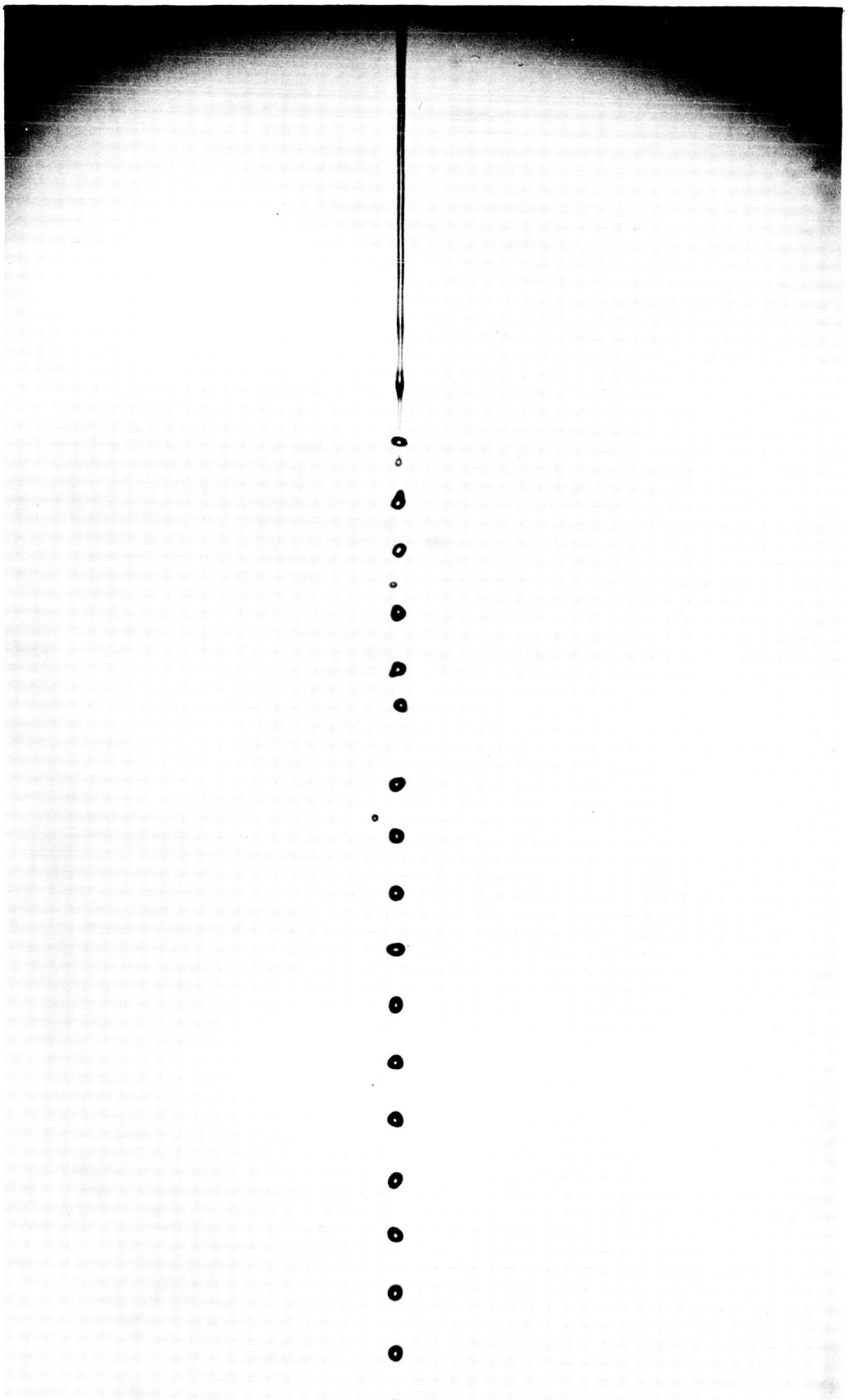

Laminar jet breakup - resonant chamber

Figure 20

JP21-4137-66

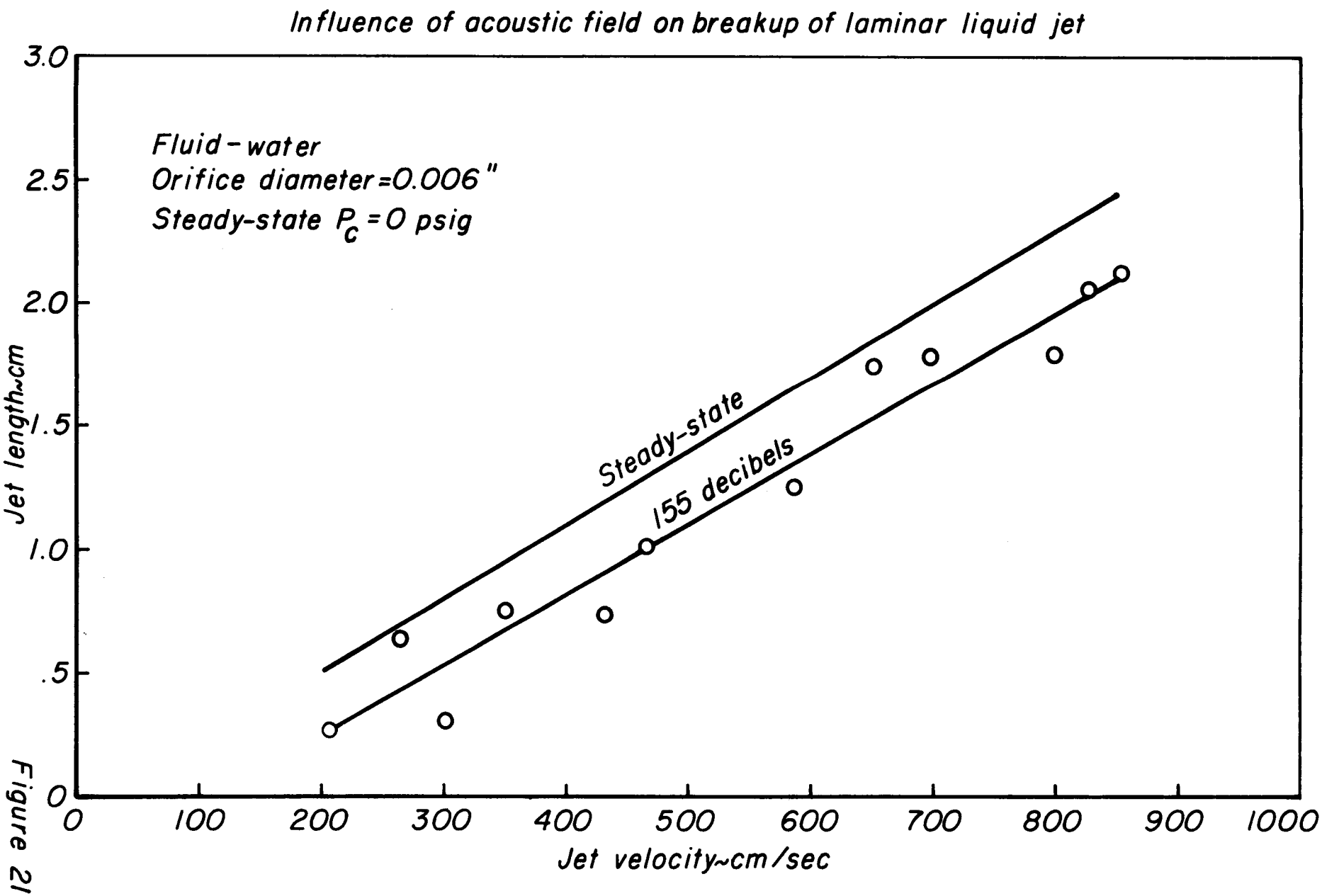


Figure 21

JP 21-4138-66

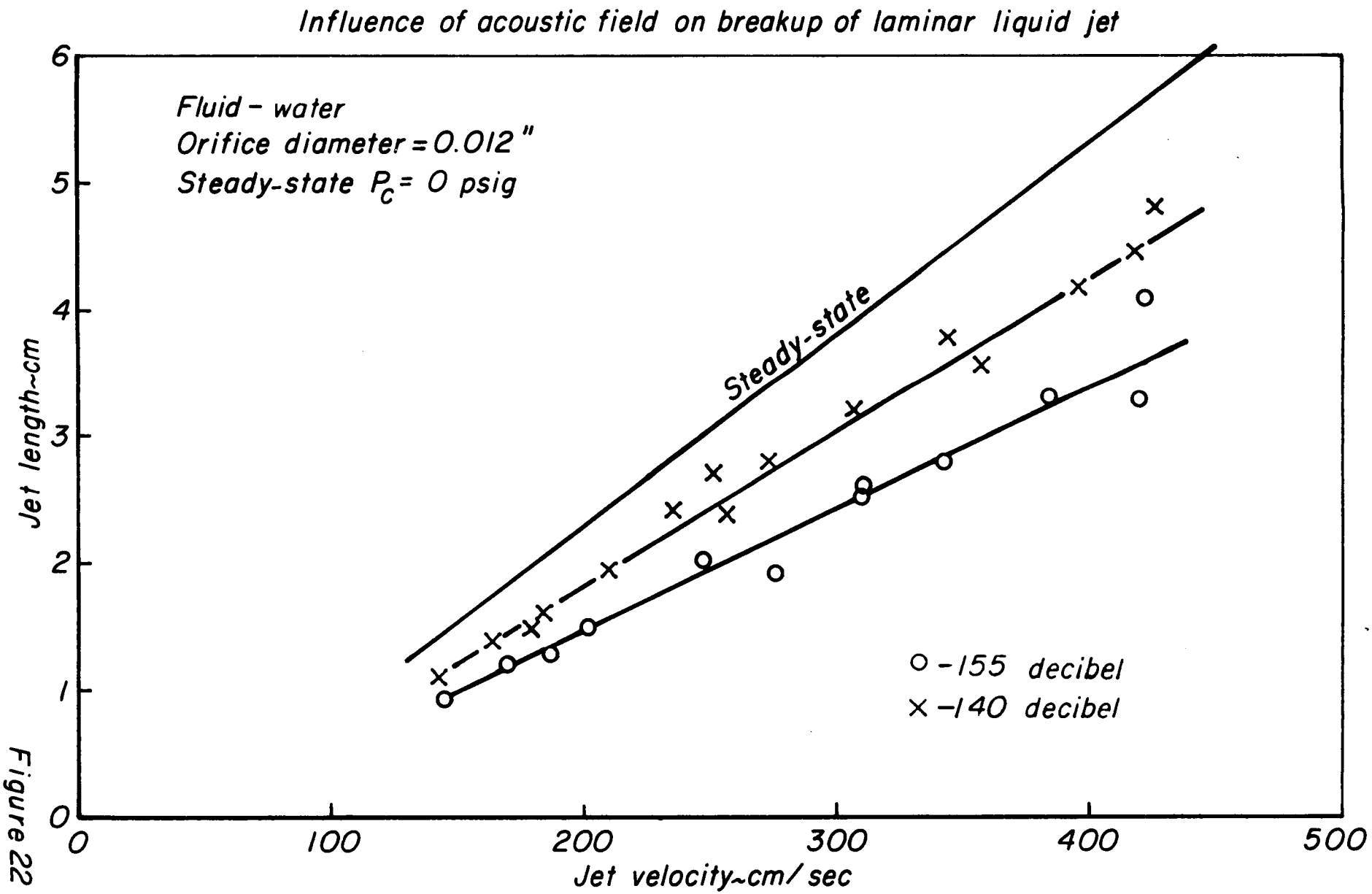


Figure 22

JP21-4140-66

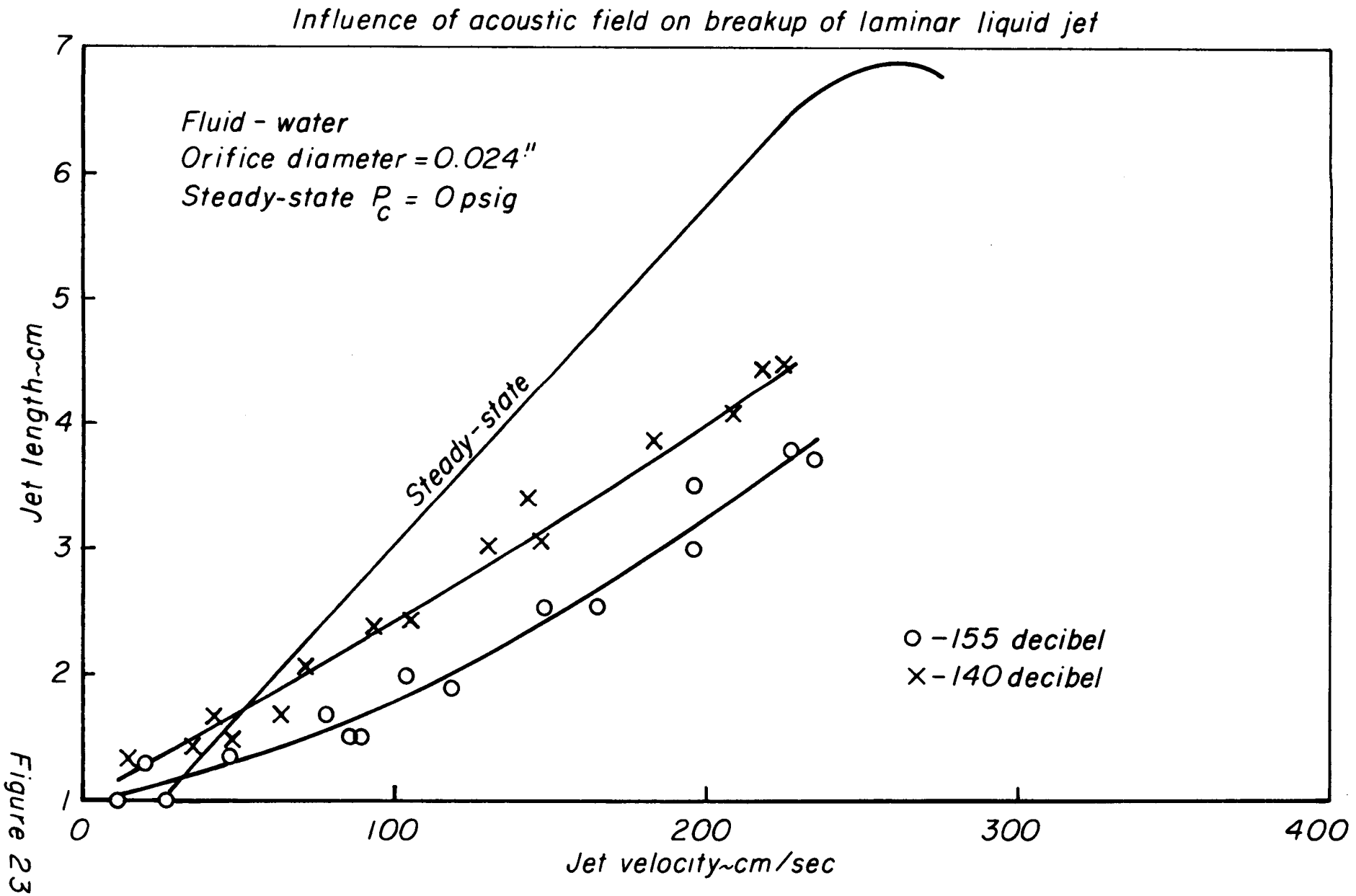


Figure 23

UP21-4141-66

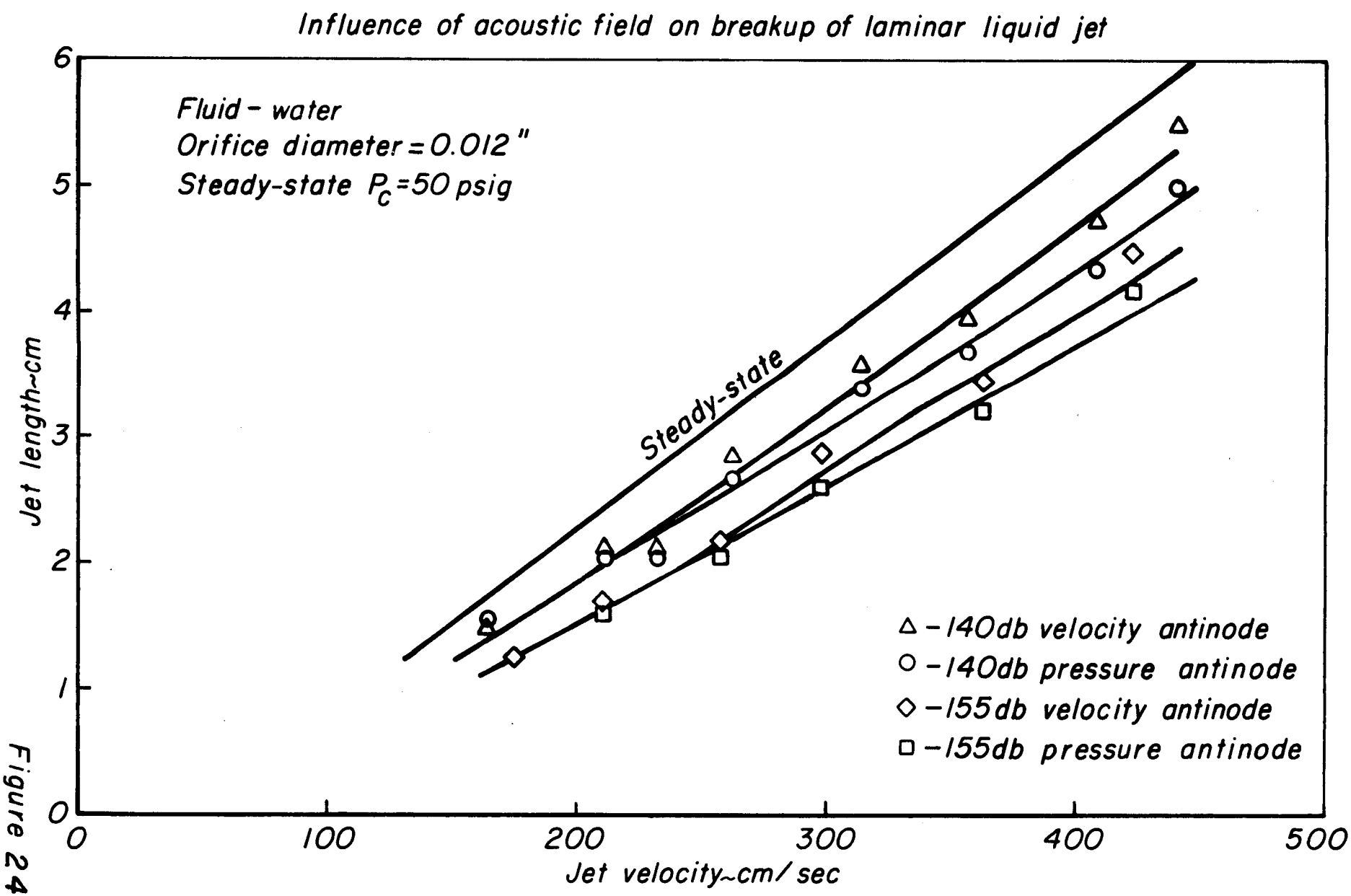


Figure 24

JP21-4142-66

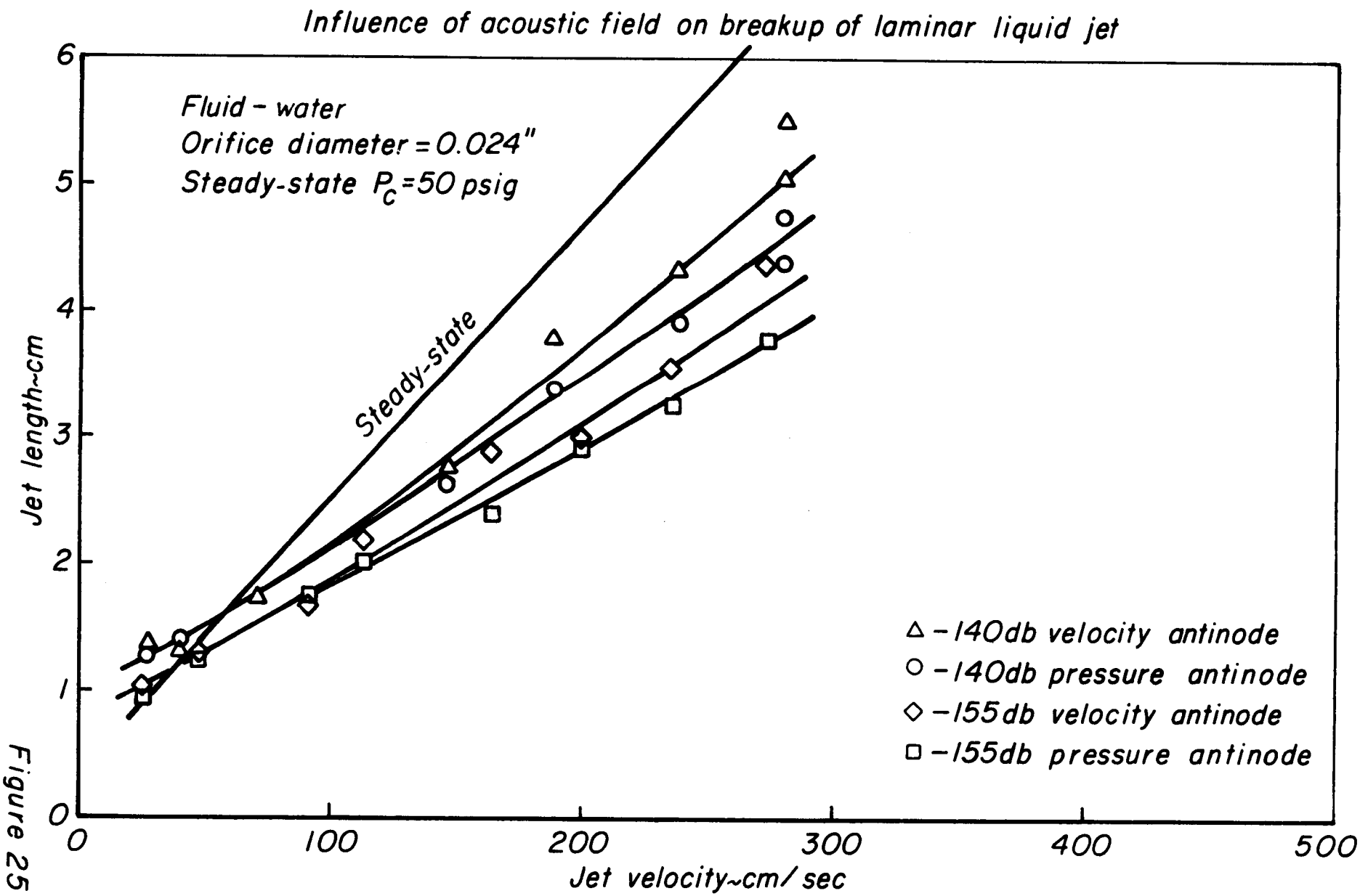


Figure 25

JP21-4143-66

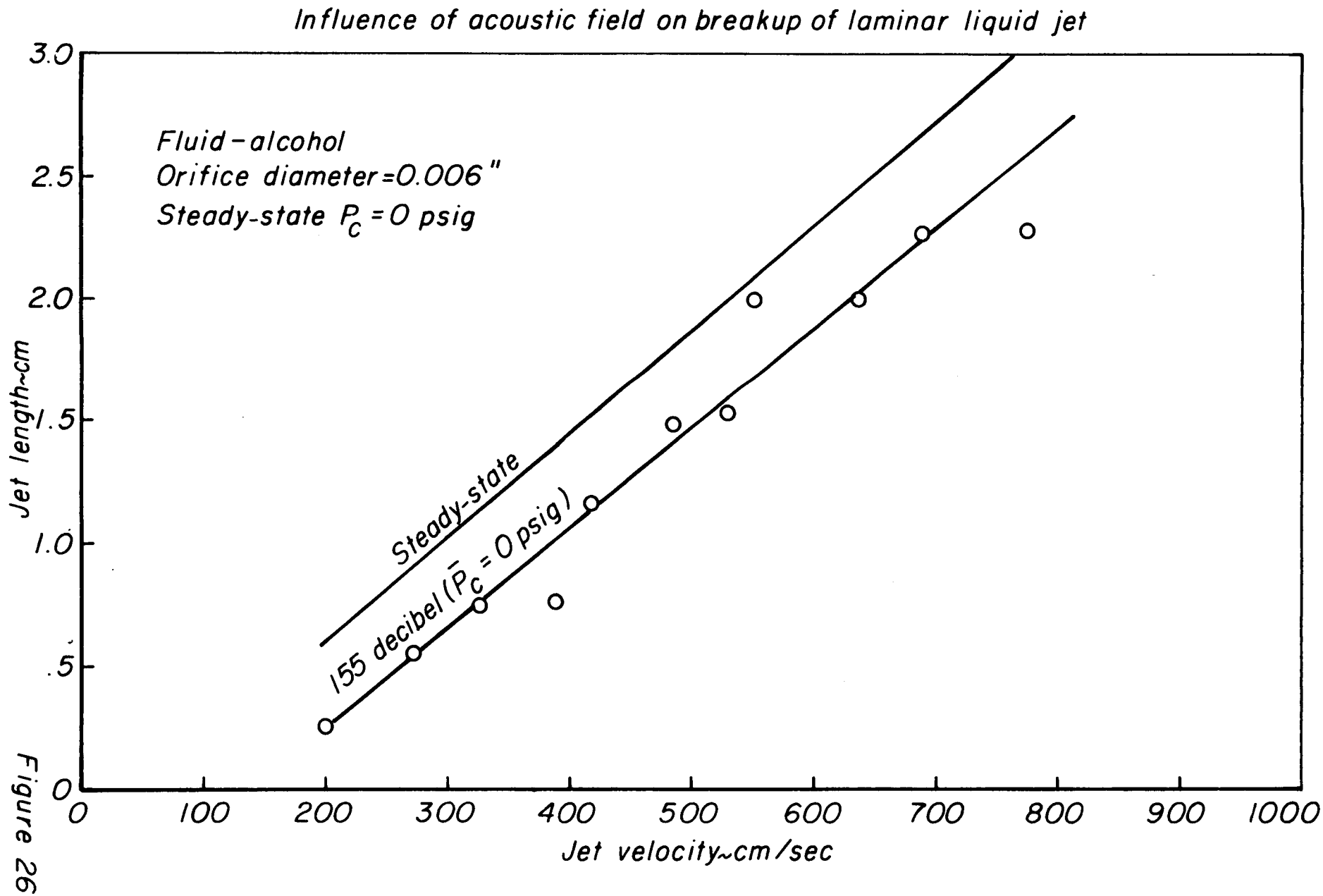


Figure 26

JP21-4144-66

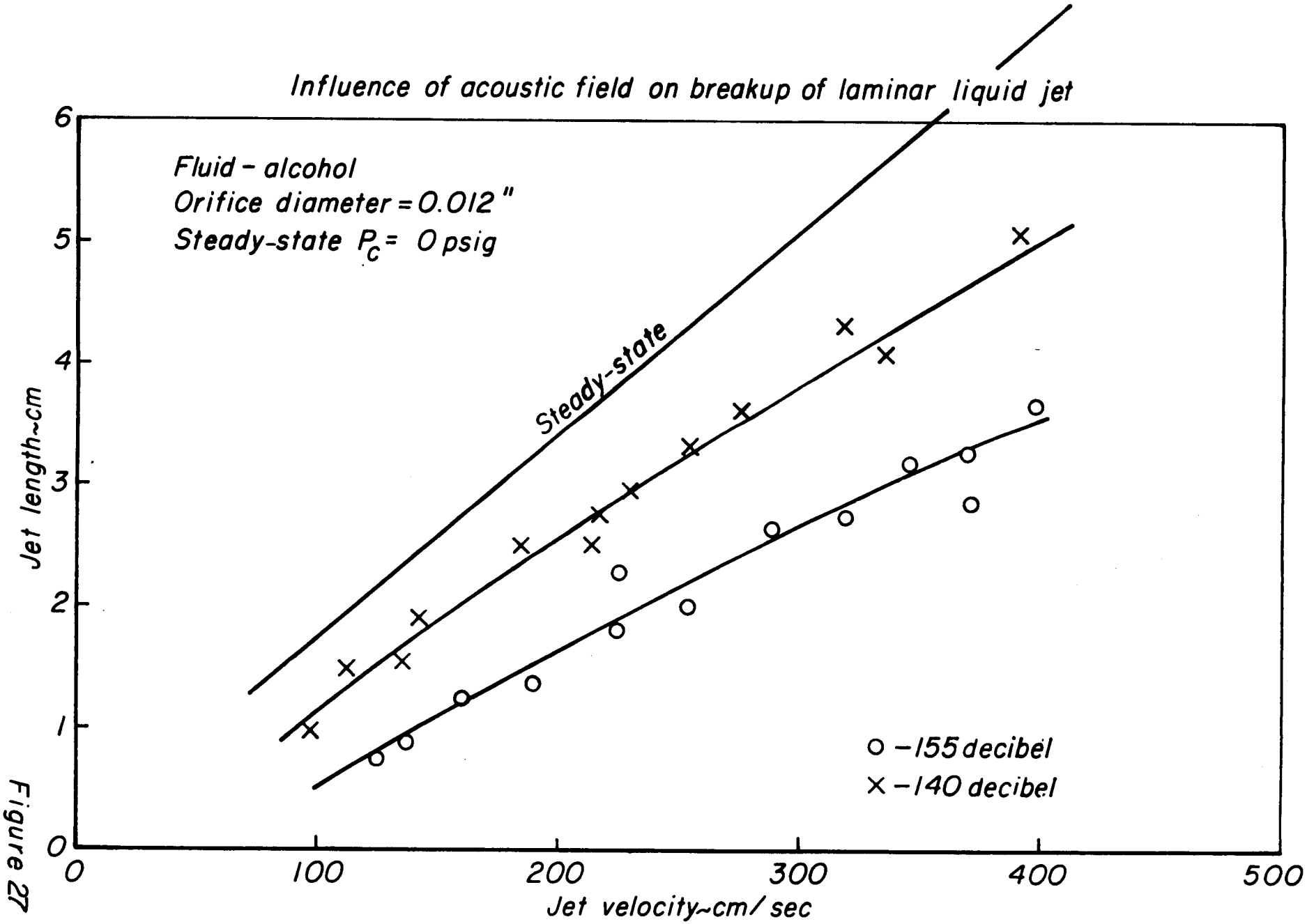


Figure 27

JP 21-4145-66

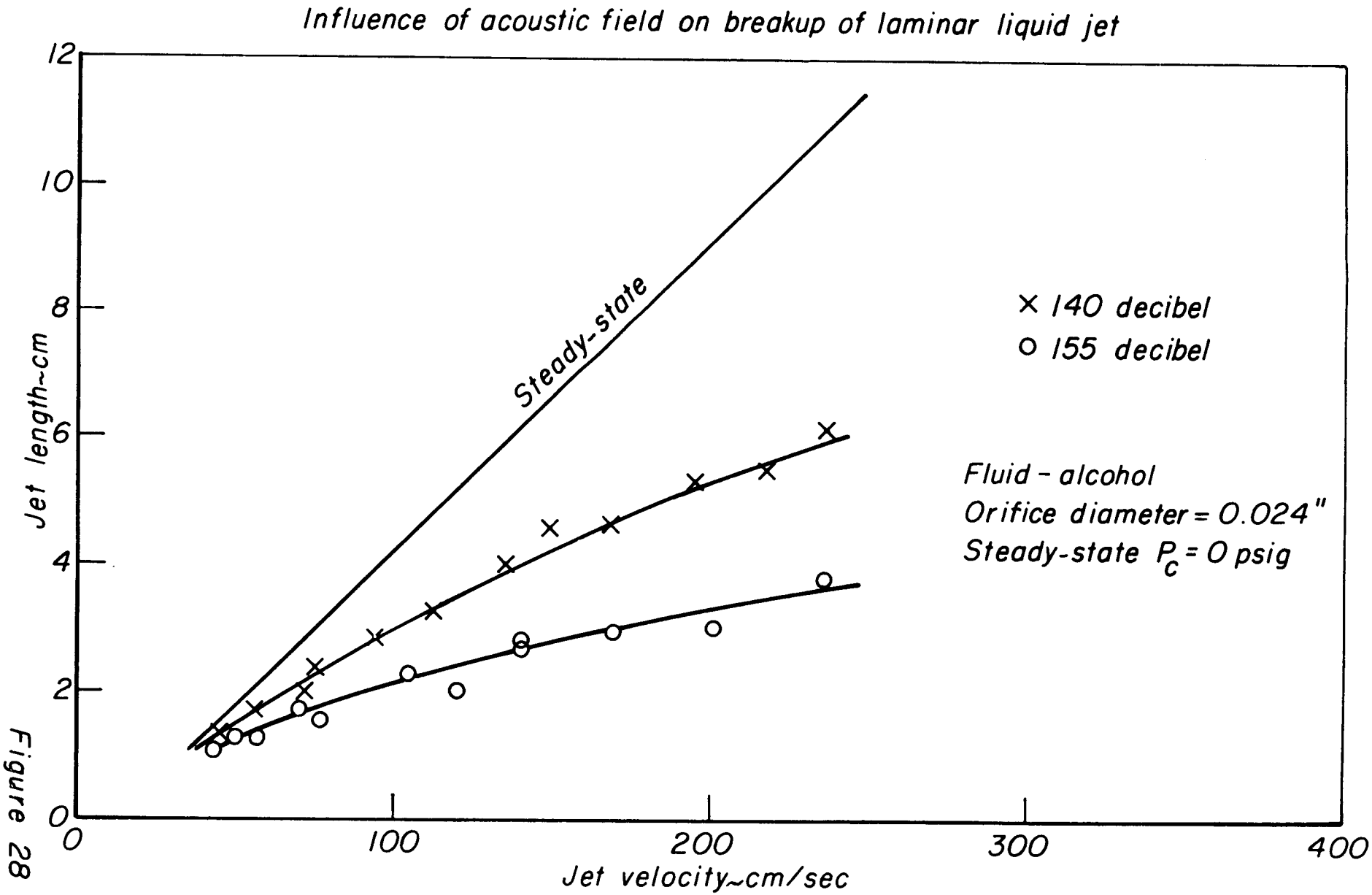


Figure 28

JP21-4146-66

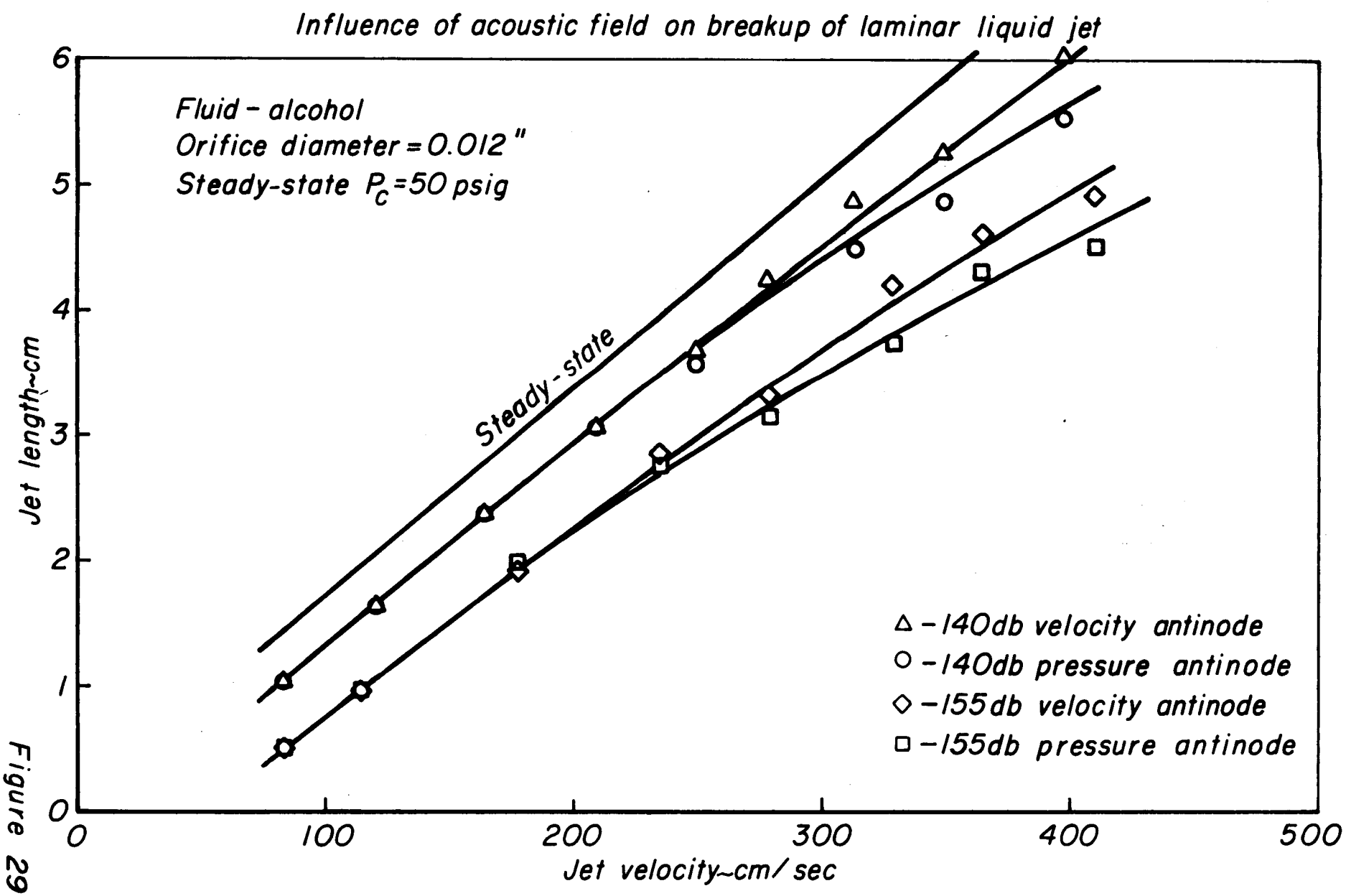


Figure 29

JP21-4147-66

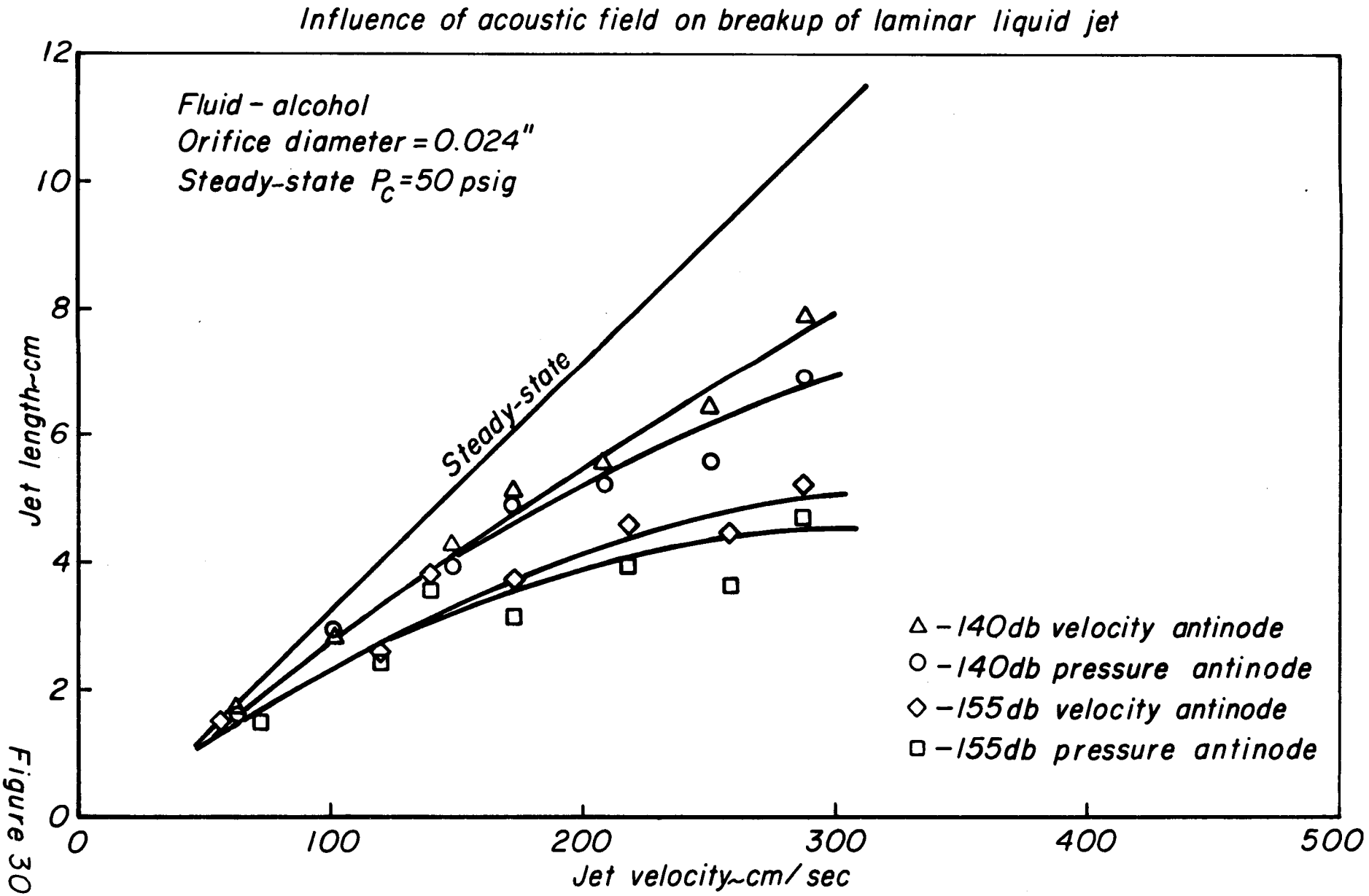


Figure 30

JP21-4139-66

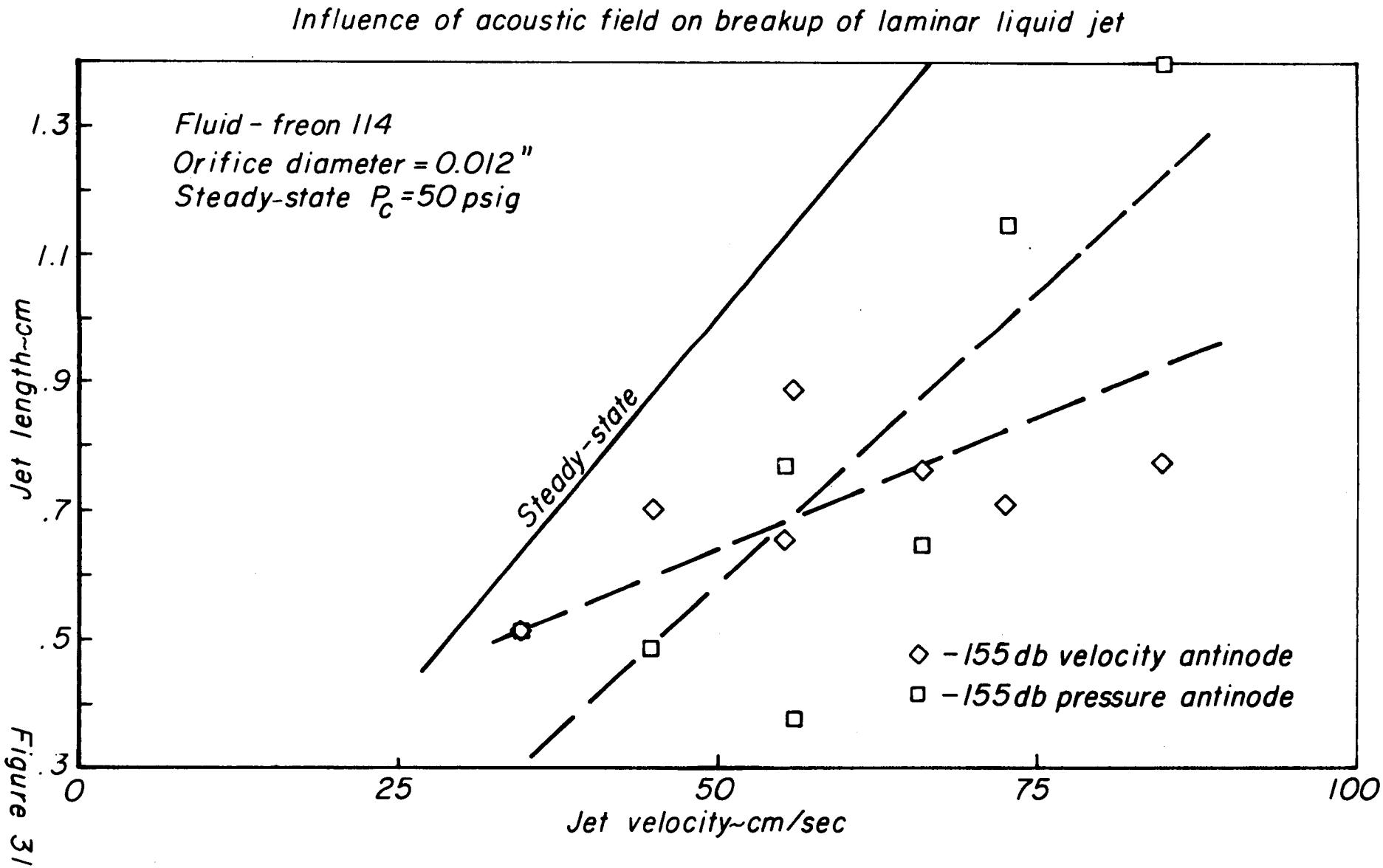


Figure 31

JP 21-4148-66

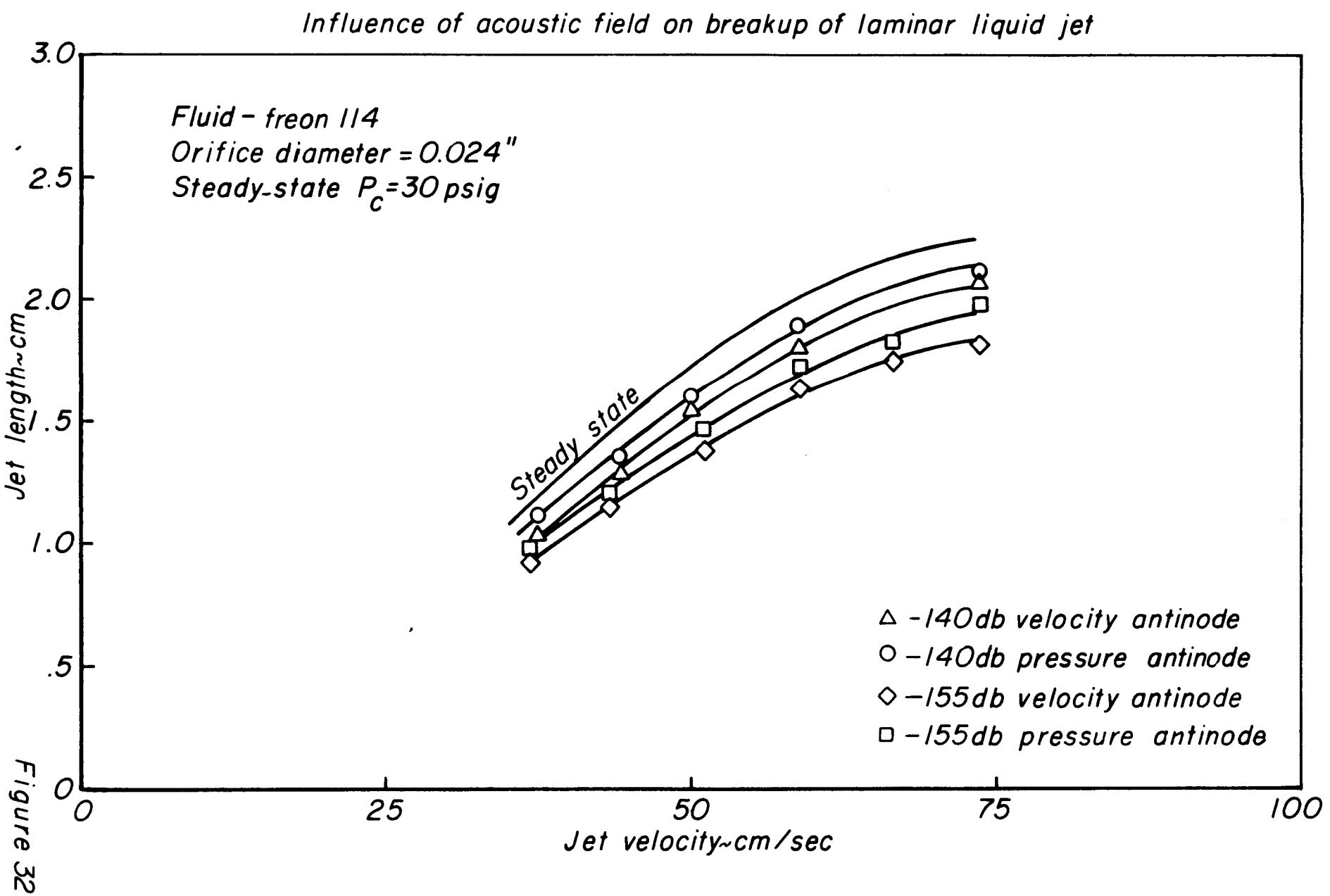


Figure 32

JP21-4149-66

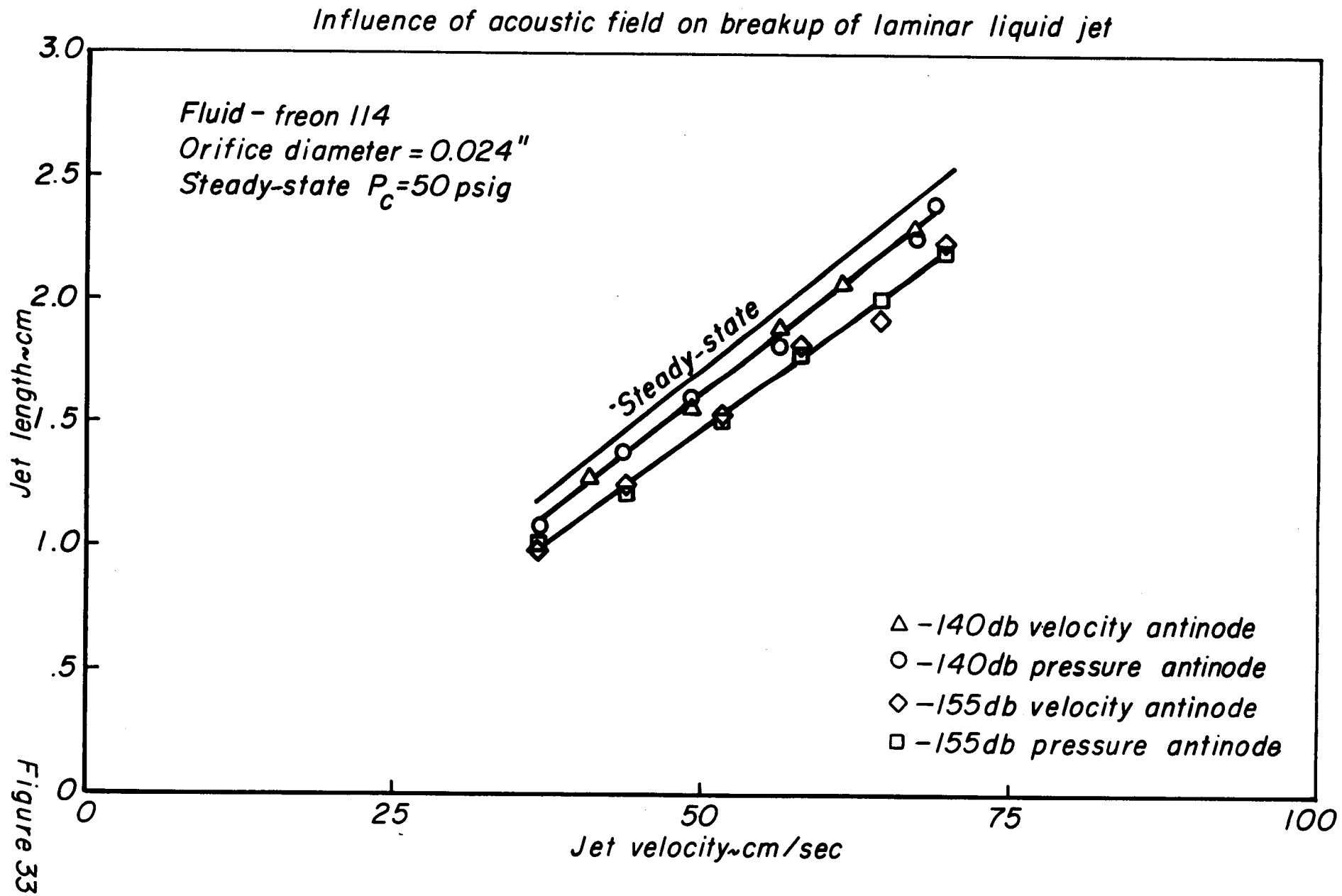


Figure 33

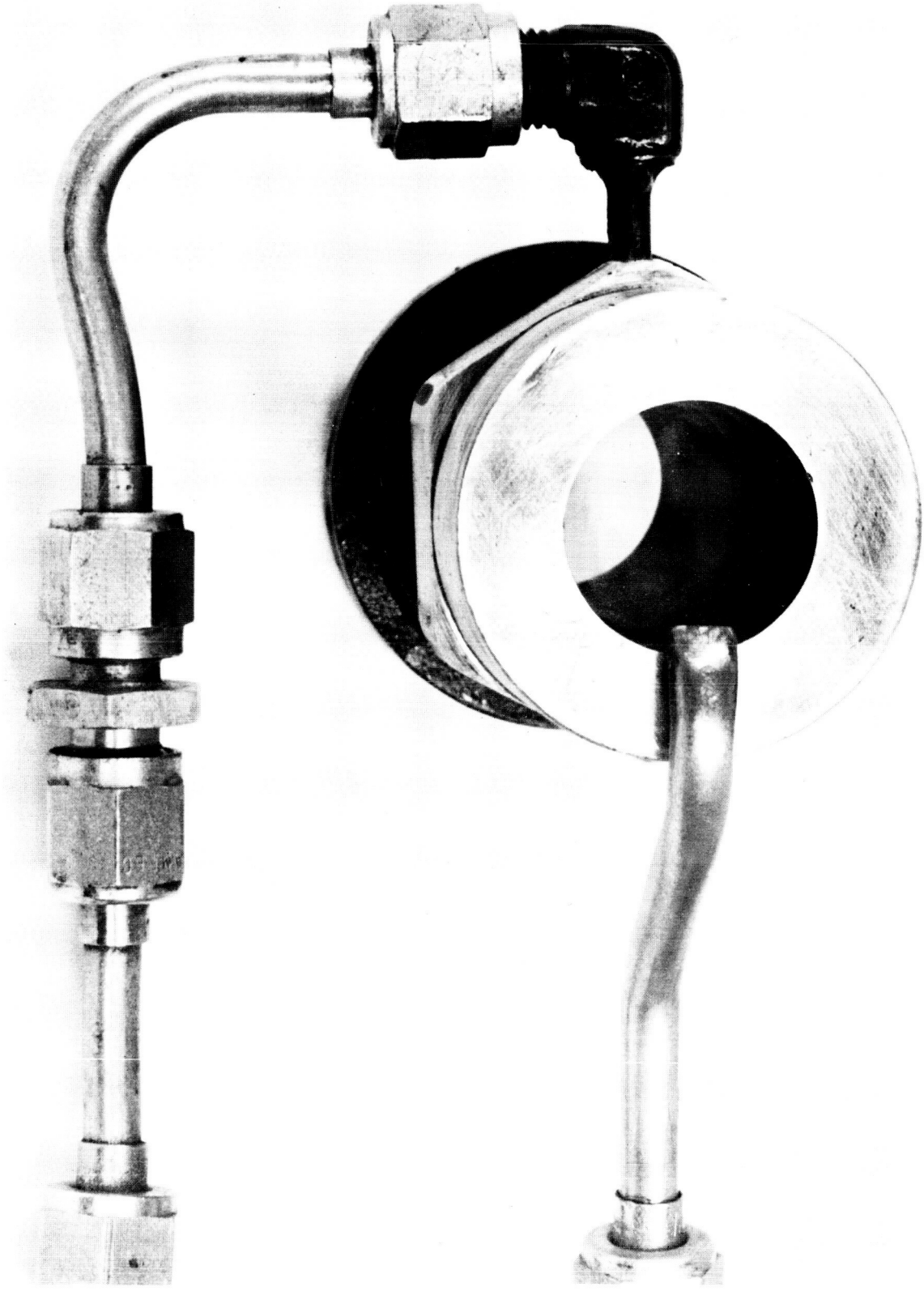

Window assembly

Figure A I

JP21 P44 67

JP 21 P45 67

Figure A2

Modified spud

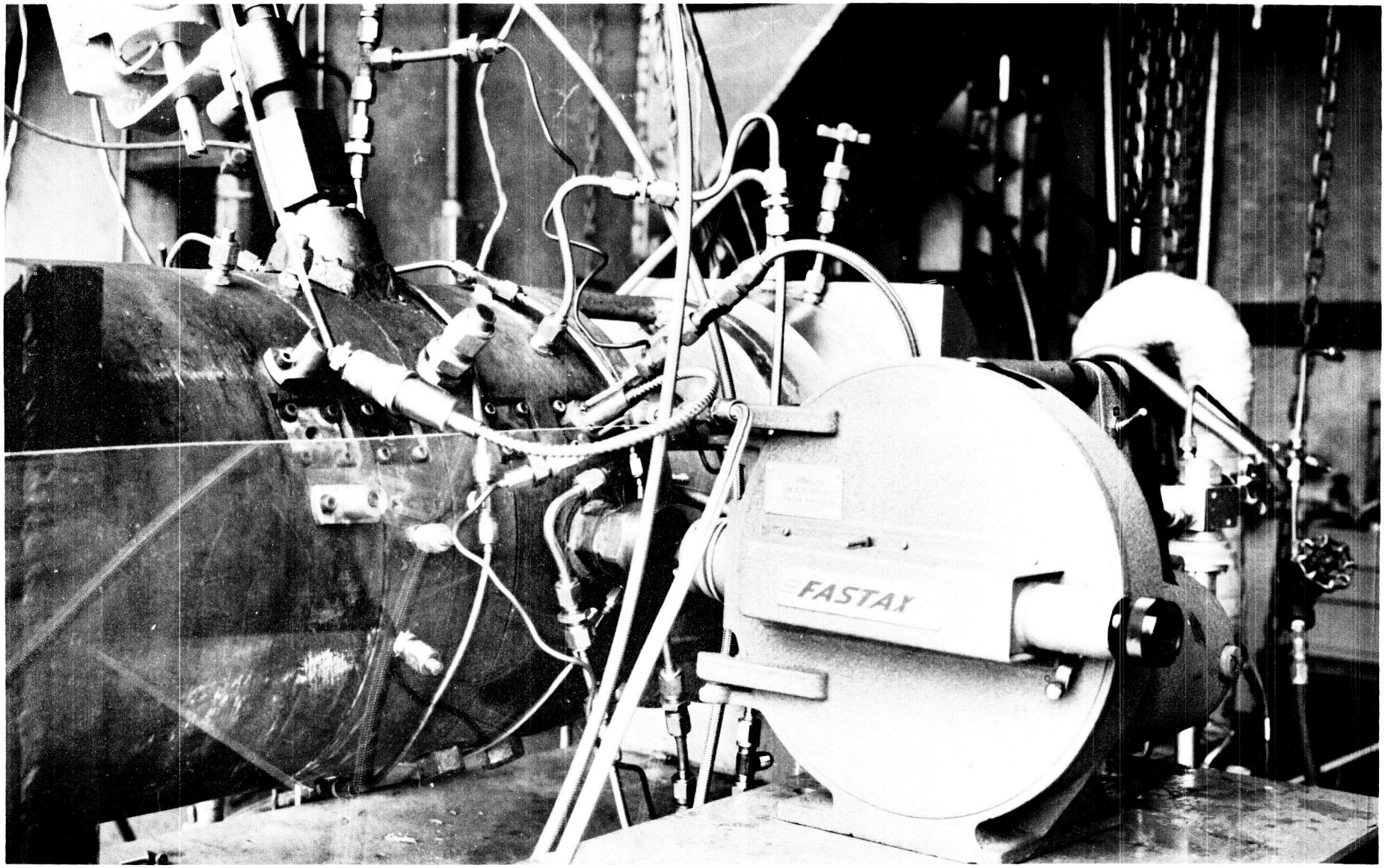


Experimental apparatus (close-up)

Figure A3

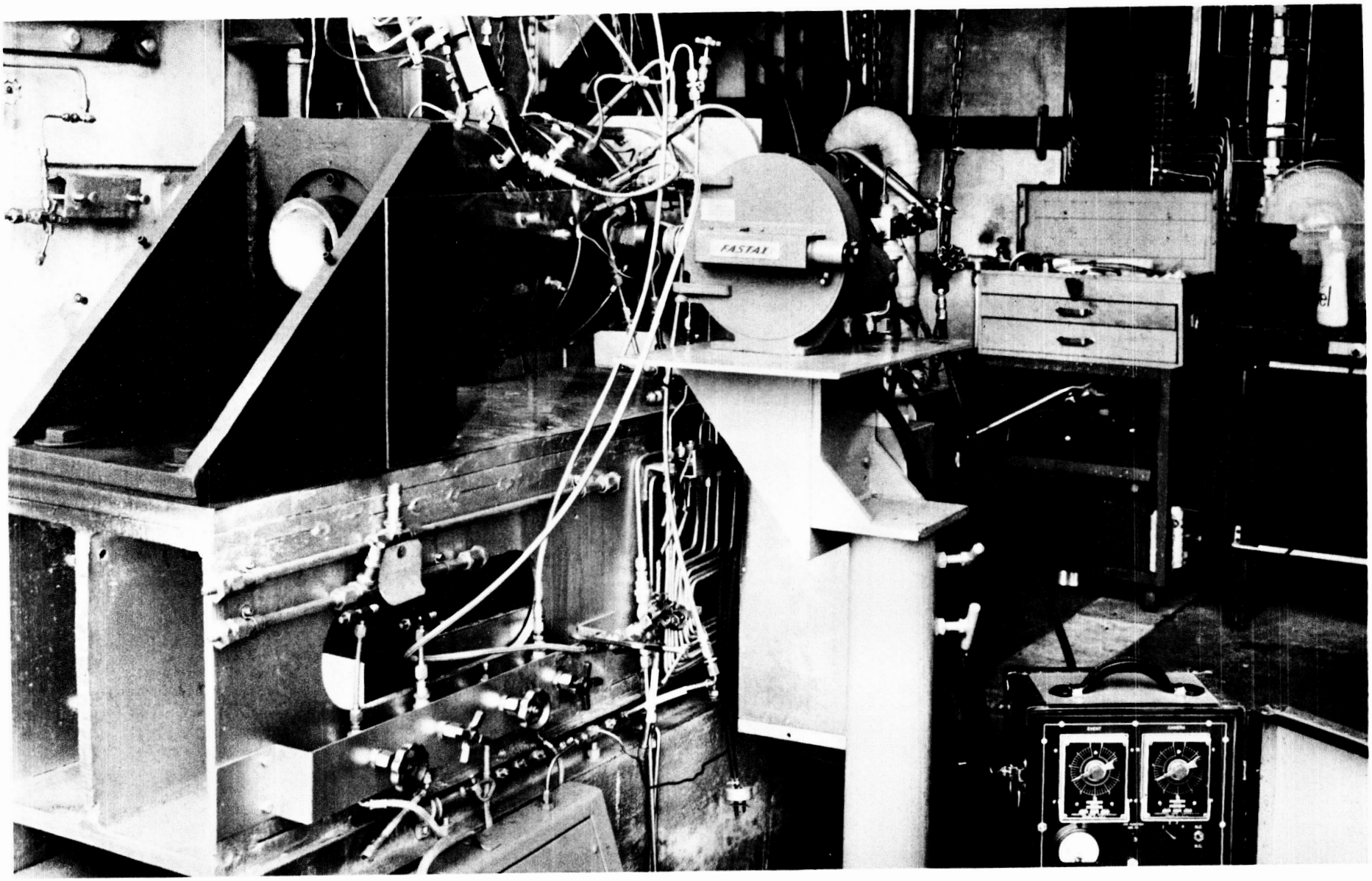


Experimental apparatus (overall view)

Figure A4

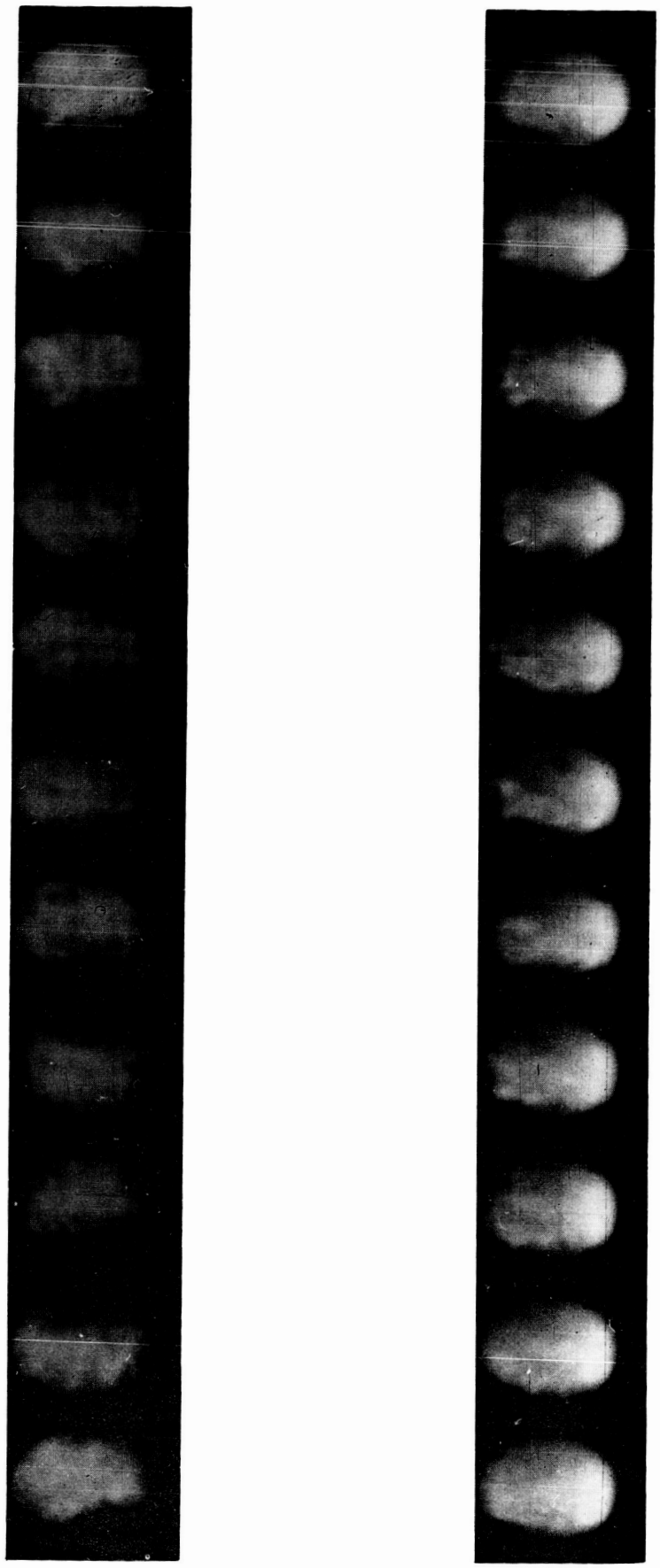

Behavior of seeded fuel in rocket engine

Figure A5

Pressure transducer

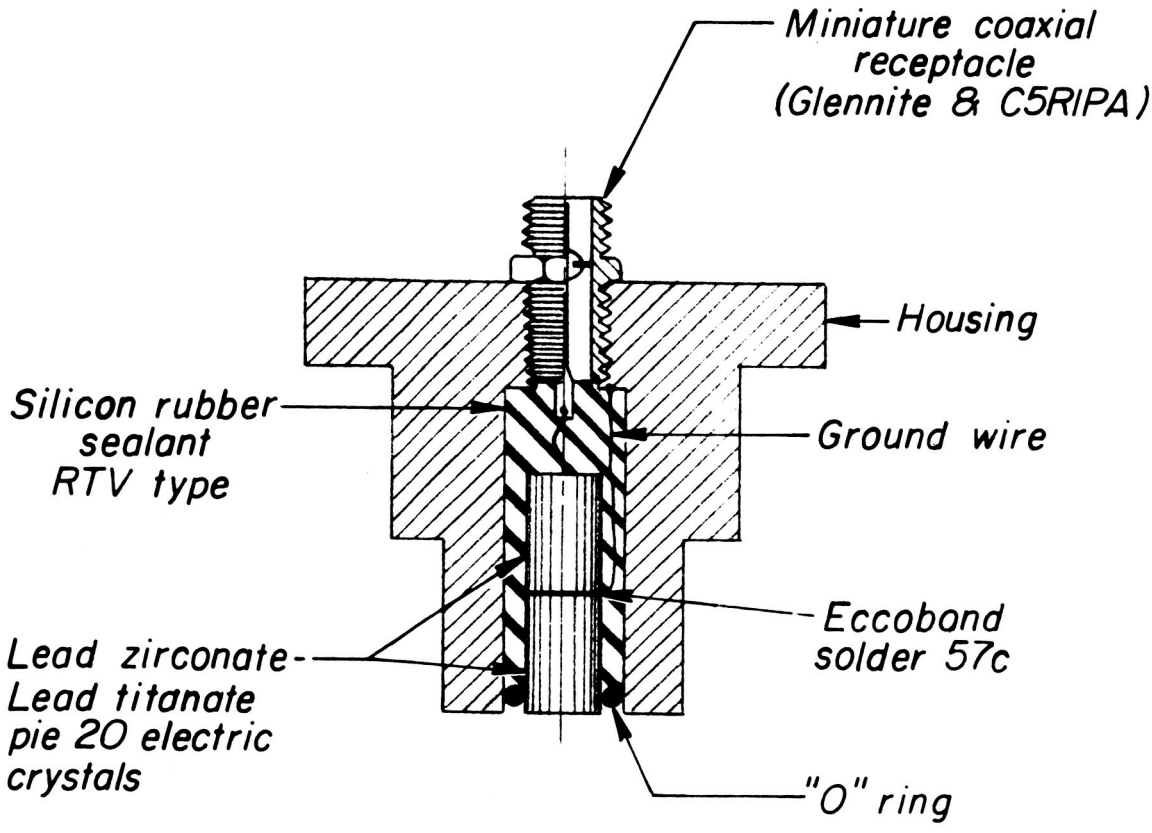


JP21-4/26-66

Figure B1

JP21-4123-66

Calibration curves for lead titanate-lead zirconate pressure transducers.
Last calibration date-Aug.6, 1966

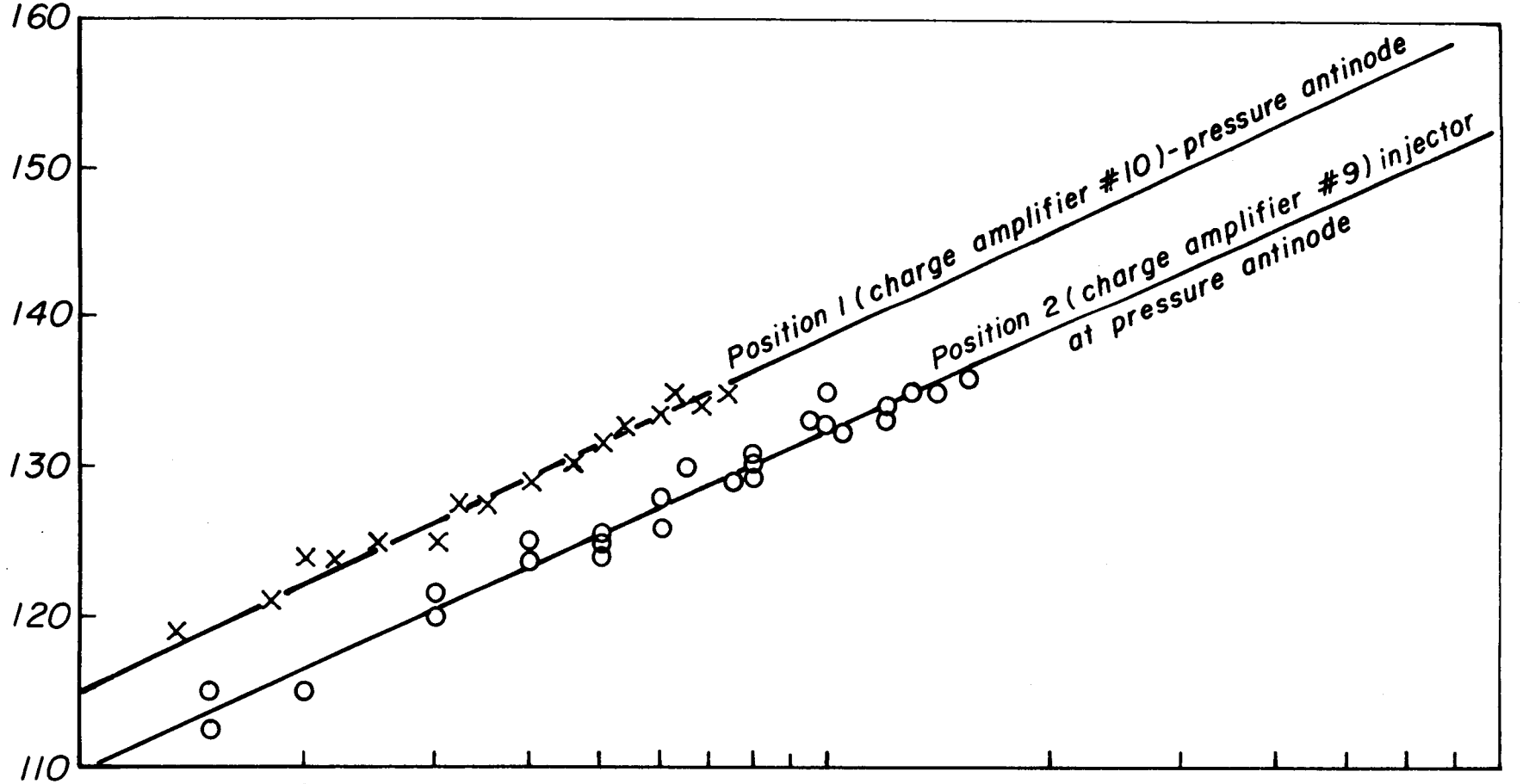


Figure 82

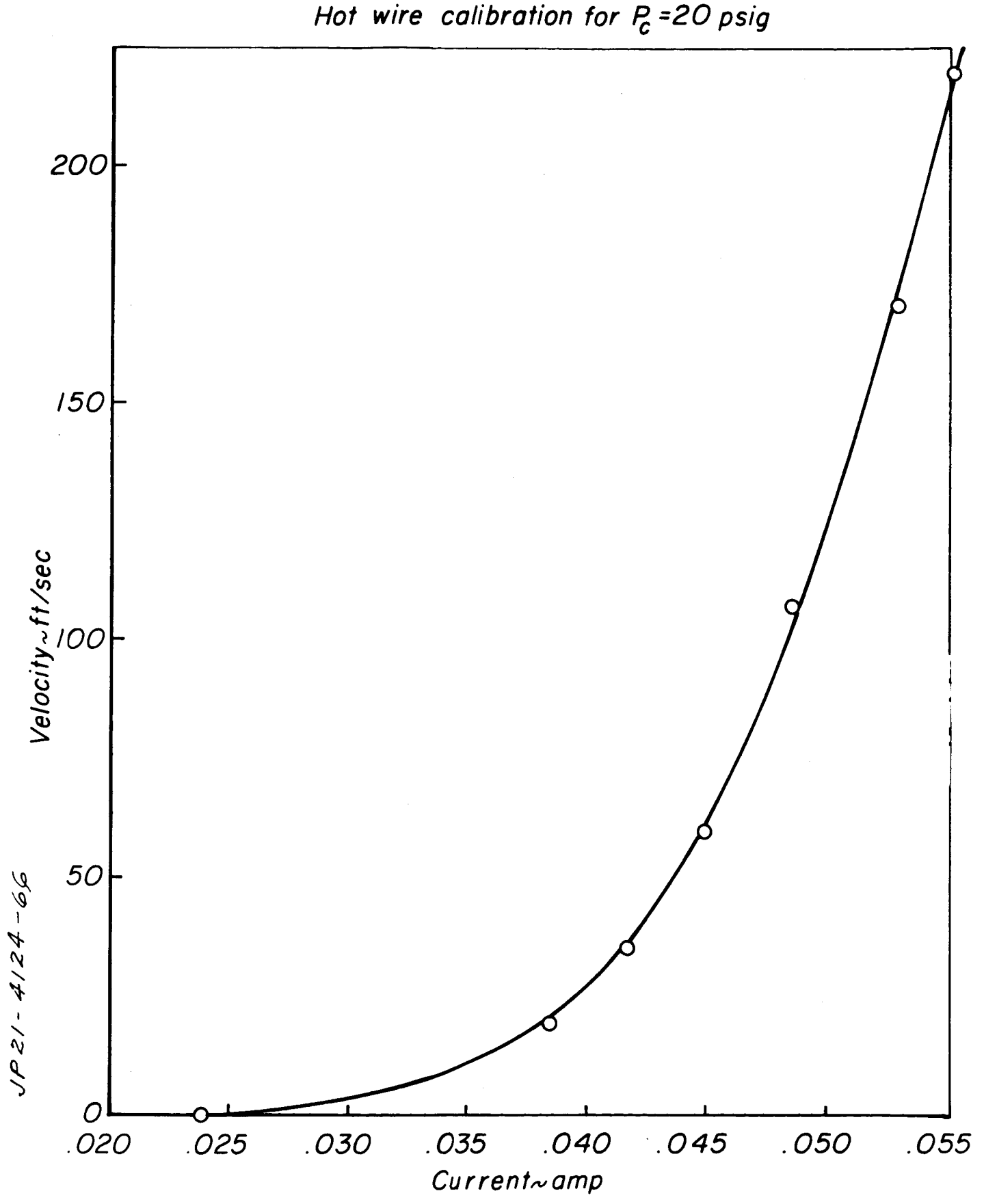
Hot wire calibration for $P_c$ =20 psig
200
150
100
50
0
Velocity~ft/sec
.020
.025
.030
.035
.040
.045
.050
.055
Current~amp
JP21-4124-66

Figure B3a

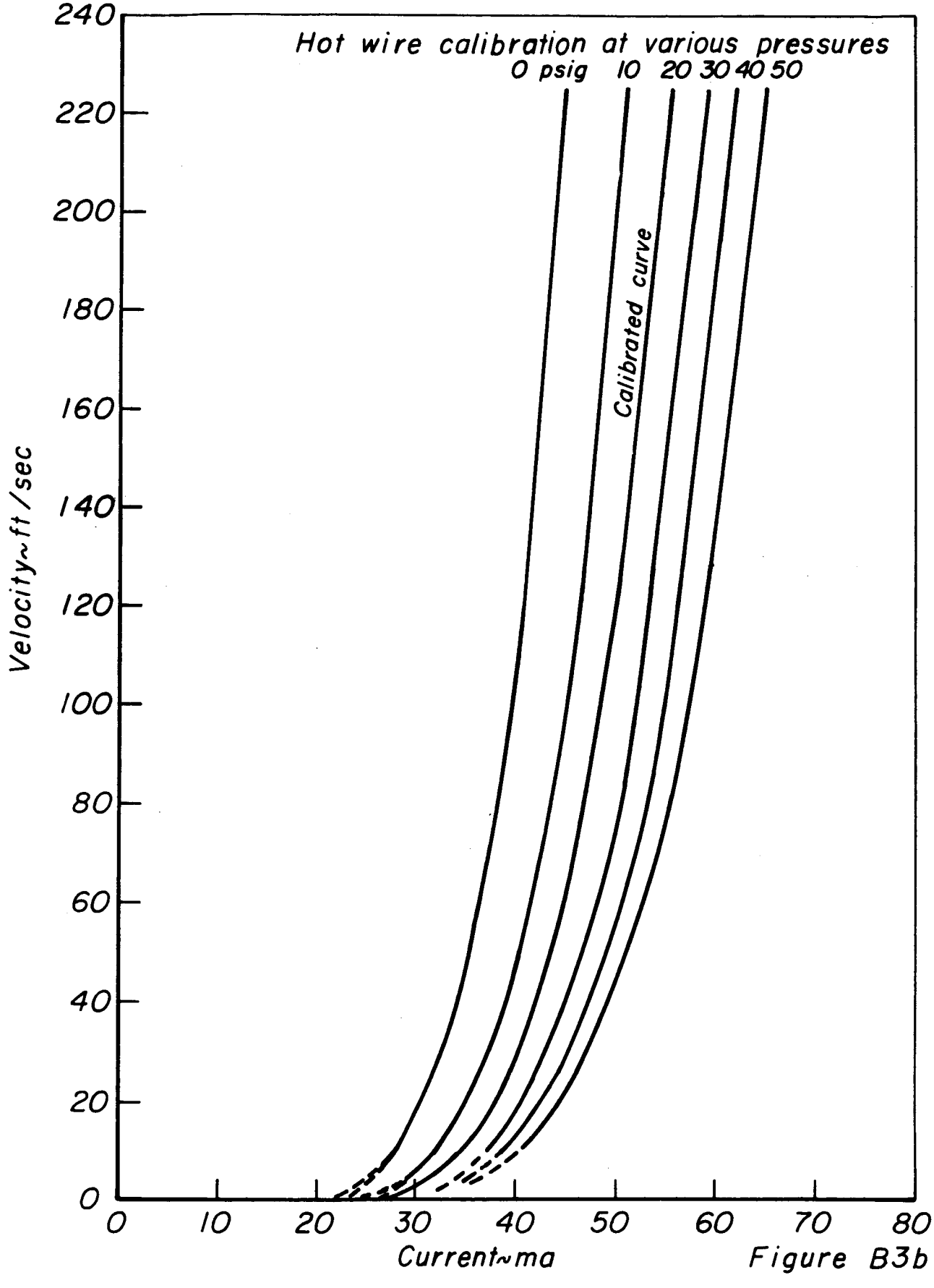


Figure B3b

JP21-4125-66

## DISTRIBUTION FOR THIS REPORT

NASA

NASA Headquarters
Washington, D.C. 20546
Attn: Alfred Gessow
Robert S. Levine RPL (3)
A. O. Tischler RP

NASA
Universal North Building
Connecticut & Florida Avenues
Washington, D.C.
Attn: T.L. Smull, Director
Grants & Space Contracts (10)

NASA Scientific & Technical
Information Facility
P.O. Box 33
College Park, Maryland 20740 (15)

NASA Headquarters
Washington, D.C. 20546
Attn: E.L. Gray, Director
Advanced Manned Missions, MT
Office of Manned Space Flight

Attn: V.L. Johnson, Director
Launch Vehicles & Propulsion, SV
Office of Space Science

Ames Research Center
Moffett Field
California 94035
Attn: Technical Librarian
Designee: Harold Hornby
Mission Analysis Division

Goddard Space Flight Center
Greenbelt, Maryland 20771
Attn: Technical Librarian
Designee: Merland L. Moseson
Code 620

Jet Propulsion Laboratory
California Institute of Technology
4800 Oak Grove Drive
Pasadena, California 91103
Attn: J.H. Rupe

Attn: Technical Librarian
Designee: Henry Burlage, Jr.
Propulsion Div., 38

John F. Kennedy Space Center, NASA
Cocoa Beach, Florida 32931
Attn: Technical Librarian
Designee: Kurt H. Debus

Langley Research Center
Langley Station
Hampton, Virginia 23365
Attn: Technical Librarian
Designee: Floyd L. Thompson, Director

NASA
Lewis Research Center
21000 Brookpark Road
Cleveland, Ohio 44135
Attn: M.F. Heidmann (Technical Monitor)
R.J. Priem
E. Conrad

Attn: Technical Librarian
Designee: A. Silverstein, Director

Manned Spacecraft Center
Houston, Texas 77001
Attn: G. Spencer

Attn: Technical Librarian
Designee: Robert R. Gilruth, Director

Marshall Space Flight Center
R-P&VED
Huntsville, Alabama 35812
Attn: Jerry Thomson
R.J. Richmond

Attn: Technical Librarian
Designee: Hans G. Paul

GOVERNMENT INSTALLATIONS

Headquarters, U.S. Air Force
Washington 25, D.C.
Attn: Technical Librarian
Designee: Col. C.K. Stambaugh
AFRST

Aeronautical Systems Division
Air Force Systems Command
Wright-Patterson Air Force Base
Dayton, Ohio 45433
Attn: Technical Librian
Designee: D.L. Schmidt
Code ASRCNC-2

Air Force Missile Test Center
Patrick Air Force Base
Florida
Attn: Technical Librarian
Designee: L.J. Ullian

Air Force Office of Scientific Research
Propulsion Division
Washington, D.C.
Attn: B.T. Wolfson

Air Force Rocket Propulsion Laboratory
Research & Technology Division
Air Force Systems Command
Edwards, California 93523
Attn: R.R. Weiss, RPRR

Attn: Technical Librarian
Designee: H. Main

Air Force Systems Division
Air Force Unit Post Office
Los Angeles 45, California
Attn: Technical Librarian

ARL (ARC)
Building 450
Wright-Patterson Air Force Base
Dayton, Ohio
Attn: K. Scheller

Arnold Engineering Development Center
Arnold Air Force Station
Tullahoma, Tennessee
Attn: Technical Librarian
Designee: H.K. Doetsch

Department of the Navy
Bureau of Naval Weapons
Washington, D.C.
Attn: Technical Librarian
Designee: J. Kay
RTMS-41

Department of the Navy
Office of Naval Research
Washington, D.C. 20360
Attn: R.O. Jackel

Defense Documentation Center Headquarters
Cameron Station, Building 5
5010 Duke Street
Alexandria, Virginia 22314
Attn: TISIA

Naval Ordnance Station
Research & Development Dept.
Indian Head, Maryland 20640
Attn: Lionel A. Dickinson

Picatinny Arsenal
Dover, New Jersey 07801
Attn: E. Jenkins

Attn: Technical Librarian
Designee: I. Forsten, Chief
Liquid Propulsion Lab.
SMUPA-DL

Redstone Scientific Information
Building 4484
Redstone Arsenal
Huntsville, Alabama
Attn: Technical Librarian

RTNT
Bolling Field
Washington, D.C. 20332
Attn: L. Green, Jr.

U.S. Army Missile Command
Redstone Arsenal
Huntsville
Alabama 35809
Attn: J. Connaughton

Attn: Technical Librarian
Designee: Walter Wharton

U.S. Atomic Energy Commission
Technical Information Services
Box 62
Oak Ridge, Tennessee
Attn: Technical Librarian
Designee: A.P. Huber
Gaseous Diffusion Plant
(ORGDP) P.O. Box P

U.S. Naval Ordnance Test Station
China Lake
California 93557
Attn: E.W. Price

Attn: Technical Librarian
Designee: Code 4562
Chief,
Missile Propulsion Div.

CPIA

Chemical Propulsion Information Agency
Applied Physics Laboratory
The John Hopkins University
8621 Georgia Avenue
Silver Spring, Maryland 20910
Attn: T.W. Christian

Attn: Technical Librarian
Designee: Neil Safeer

INDUSTRY CONTRACTORS

Aerojet-General Corporation
P.O. Box 296
Azusa, California 91703
Attn: Technical Librarian
Designee: L.F. Kohrs

Aerojet-General Corporation
P.O. Box 1947
Sacramento, California 95809
Attn: R.J. Hefner

Attn: Technical Librarian
Bldg. 2015, Dept. 2410
Designee: R. Stiff

Aeronutronic
Philco Corporation
Ford Road
Newport Beach, California 92663
Attn: Technical Librarian
Designee: D.A. Carrison

Aerospace Corporation
P.O. Box 95085
Los Angeles, California 90045
Attn: O.W. Dykema

Attn: Technical Librarian
Designee: John G. Wilder
MS-2293
Propulsion Dept.

Astrosystems International, Inc.
1275 Bloomfield Avenue
Fairfield, New Jersey 07007
Attn: Technical Librarian
Designee: A. Mendenhall

Atlantic Research Corporation
Edsall Road and Shirley Highway
Alexandria, Virginia 22314
Attn: Technical Librarian
Designee: A. Scurlock

Autonetics
Div. of North American Aviation, Inc.
3370 Miraloma Avenue
Anaheim, California 92803
Attn: Dr. Ju Chin Chu

Battelle Memorial Institute
505 King Avenue
Columbus 1, Ohio
Attn: Charles E. Day,
Classified Rept. Librarian

Bell Aerosystems Company
P.O. Box 1
Buffalo 5, New York 14240
Attn: K. Berman
J. Senneff

Attn: Technical Librarian
Designee: W.M. Smith

Boeing Company
P.O. Box 3707
Seattle, Washington 98124
Attn: Technical Librarian
Designee: J.D. Alexander

Bolt, Berenak & Newman, Inc.
Cambridge, Mass.
Attn: Dr. Dyer

Chrysler Corporation
Missile Division
P.O. Box 2628
Detroit, Michigan 48231
Attn: Technical Librarian
Designee: John Gates

Curtiss-Wright Corporation
Wright Aeronautical Division
Wood-Ridge, New Jersey 07075
Attn: Technical Librarian
Designee: G. Kelley

Defense Research Corporation
6300 Hollister Avenue
P.O. Box 3587
Santa Barbara, California 93105
Attn: B. Gray
C.H. Yang

Douglas Aircraft Company
Missile & Space Systems Division
3000 Ocean Park Boulevard
Santa Monica, California 90406
Attn: Technical Librarian
Designee: R.W. Hallet
Advanced Space Tech.

Douglas Aircraft Company
Astropower Laboratory
2121 Paularino
Newport Beach, California 92663
Attn: Technical Librarian
Designee: George Moc
Director, Research

Dynamic Science Corporation
1445 Huntington Drive
South Pasadena, California
Attn: M. Beltran

General Dynamics/Astronautics
Library & Information Services (128-00)
P.O. Box 1128
San Diego, California 92112
Attn: Technical Librarian
Designee: Frank Dore

General Electric Company
Advanced Engine & Technology Dept.
Cincinnati, Ohio 45215
Attn: Technical Librarian
Designee: D. Suichu

General Electric Company
Malta Test Station
Ballstan Spa, New York
Attn: Alfred Graham, Manager
Rocket Engines

General Electric Company
Re-Entry Systems Department
3198 Chestnut Street
Philadelphia, Pennsylvania 19101
Attn: Technical Librarian
Designee: F.E. Schultz

Geophysics Corporation of America
Technical Division
Bedford, Massachusetts
Attn: A.C. Toby

Grumman Aircraft Engineering Corp.
Bethpage
Long Island, New York
Attn: Technical Librarian
Designee: Joseph Gavin

Institute for Defense Analyses
RESD
400 Army-Navy Drive
Arlington, Virginia
Attn: Warren C. Strahle

Ling-Temco-Vought Corporation
Astronautics
P.O. Box 5907
Dallas, Texas 75222
Attn: Technical Librarian
Designee: Warren C. Trent

Arthur D. Little, Inc.
20 Acorn Park
Cambridge, Massachusetts 02140
Attn: E. Karl Bastress
Attn: Technical Librarian

Lockheed Missiles & Space Co.
P.O. Box 504
Sunnyvale, California 94088
Attn: Technical Information Center
Designee: Y.C. Lee

Lockheed Propulsion Company
P.O. Box 111
Redlands, California 91409
Attn: Technical Librarian
Designee: H.L. Thackwell

McDonnell Aircraft Corporation
P.O. Box 516
Municipal Airport
St. Louis, Missouri 63166
Attn: Technical Librarian
Designee: R.A. Herzmark

The Marquardt Corporation
16555 Saticoy Street
Van Nuys, California 91409
Attn: Technical Librarian
Designee: Warren P. Boardman, Jr.

Martin Marietta Corporation
Denver Division
P.O. Box 179
Denver, Colorado 80201
Attn: Technical Librarian
Designee: J.D. Goodlette (A-241)

Multi-Tech. Inc.
Box 4186 No. Annex
San Fernando, California
Attn: F. B. Cramer

Northrup Space Laboratories
3401 West Broadway
Hawthorne, California
Attn: Technical Librarian
Designee: William Howard

Georgia Institute of Technology
Aerospace School
Atlanta 13
Georgia
Attn: Ben T. Zinn

Illinois Institute of Technology
10 W. 35th Street
Chicago, Illinois
Attn: P.T. Torda

The John Hopkins University
Applied Physics Laboratory
8621 Georgia Avenue
Silver Spring, Maryland
Attn: W.G. Berl

Massachusetts Institute of Technology
Cambridge 39
Massachusetts
Attn: T.Y. Toong
Dept. of Mechanical Engineering
Attn: Gail E. Partridge, Librarian
Engineering Projects Laboratory

New York University
Dept. of Chemical Engineering
New York 53, New York
Attn: P.F. Winternitz

Ohio State University
Rocket Research Laboratory
Dept. of Aeronautical & Astronautical Eng.
Columbus 10, Ohio
Attn: Technical Librarian

Polytechnic Institute of Brooklyn
Graduate Center
Route 110
Farmingdale, New York
Attn: V.D. Agosta

Purdue University
School of Mechanical Engineering
Lafayette, Indiana
Attn: J.R. Osborn

Sacramento State College
Engineering Division
60000 J. Street
Sacramento, California 95819
Attn: F.H. Reardon

Sheffield University
Research Laboratories
Harpur Hill
Buxton, Derbyshire
England
Attn: V.J. Ibberson

University of California
Institute of Engineering Research
Berkeley, California
Attn: A.K. Oppenheim

University of Michigan
Aeronautical & Astronautical Eng. Labs.
Aircraft Propulsion Lab.
North Campus
Ann Arbor, Michigan
Attn: J.A. Nicholls

University of Southern California
Dept. of Mechanical Engineering
University Park
Los Angeles, California 90007
Attn: M. Gerstein

University of Wisconsin
Dept. of Mechanical Engineering
1513 University Avenue
Madison, Wisconsin
Attn: P.S. Myers

Yale University
Dept. of Engineering & Applied Science
Mason Laboratory
400 Temple Street
New Haven, Connecticut
Attn: B.T. Chu

Rocket Research Corporation
520 South Portland Street
Seattle, Washington 98108
Attn: Technical Librarian
Designee: Foy McCullough, Jr.

Rocketdyne
Division of North American Aviation
6633 Canoga Avenue
Canoga Park, California 91304
Attn: R. Fontaine
R.B. Lawhead

Attn: Technical Librarian
(Library 586-306)
Designee: E.B. Monteath

Space & Information Systems Division
North American Aviation, Inc.
12214 Lakewood Boulevard
Downey, California 90241
Attn: Technical Librarian
Designee: H. Storms

Rohm & Haas Company
Redstone Arsenal
Huntsville, Alabama
Attn: Librarian

Stanford Research Institute
333 Ravenswood Avenue
Menlo Park, California 94025
Attn: Technical Librarian
Designee: G. Marxman

Thiokol Chemical Corporation
Huntsville Division
Huntsville, Alabama
Attn: Technical Librarian
Designee: John Goodloe

Thiokol Chemical Corporation
Reaction Motors Division
Denville, New Jersey 07832
Attn: D. Mann

Attn: Technical Librarian
Designee: Arthur Sherman

TRW Systems
One Space Park
Redondo Beach, California 90278
Attn: G.W. Elverum
Attn: Donald H. Lee

Attn: Technical Librarian
Designee: Sam J. Van Grouw

United Technology Center
Division of United Aircraft Corporatio
P.O. Box 358
Sunnyvale, California 94088
Attn: R.H. Osborn
Attn: Technical Librarian

Pratt & Whitney Aircraft Company
Division of United Aircraft Corp.
West Palm Beach
Florida
Attn: G. Lewis

Pratt & Whitney Aircraft Company
Division of United Aircraft Corp.
Engineering, Building 1-F
East Hartford, Connecticut
Attn: D.H. Utvik

Research Laboratories
Division of United Aircraft Corp.
400 Main Street
East Hartford, Connecticut 06108
Attn: Technical Librarian
Designee: Erle Martin

Walter Kidde and Company
Aerospace Operations
567 Main Street
Belleville, New Jersey 07109
Attn: Technical Librarian
Designee: R. J. Hanville

Warner-Swasey Company
Control Instrument Division
32-16 Downing Street
Flushing, New York 11354
Attn: R.H. Tourin

UNIVERSITIES

California Institute of Technology
204 Karman Laboratory
Pasadena, California 91109
Attn: Fred E. Culick

Case Institute of Technology
Engineering Division
University Circle
Cleveland, Ohio 44106
Attn: C.R. Klotz

Dartmouth University
Hanover
New Hamshire
Attn: P.D. McCormack

detail later. At this point it is worthwhile to examine in some detail the breakup characteristics of the test fluids.

JET BREAKUP MECHANISMS (STEADY-STATE)

a) Water: Figure 7 shows jet breakup and droplet formation for an injection velocity of 400 cm/sec. The jet is laminar in appearance and any initial disturbances do not become recognizable until near the end of the jet, where they cause it to breakup. This appearance is characteristic at all velocities above the minimum jet velocity $u_m$ and below the velocity at which turbulence begins to set in. These tests (see Figures 10, to 12) have verified earlier studies[3] that in this region the breakup time (jet length divided by jet velocity) remains essentially constant for a given injector diameter. It is also apparent that chamber pressure has no noticeable effect on jet breakup in this region. This is not unexpected because: if the flow is truly laminar, the liquid particles flow in parallel streams inside the orifice, the layer next to the wall having zero velocity which increases in a parabolic manner approaching the tube axis. Since the wall exerts no direct influence on either the periphery or the inside of the jet, the velocity distribution immediately past the orifice will be the same as inside the orifice. Consequently no appreciable velocity difference exists between the gas and the liquid close to the orifice, the skin of the jet being virtually stationary. It is clear that air friction (i.e., air density) cannot assist the disintegration of the jet as long as the liquid velocity distribution drops to zero at the periphery.

As can be seen from Figures 10, 11 and 12, as jet velocity is further increased the disintegration length suddenly decreases. The value

# RESULTS AND CONCLUSIONS

## LIQUIDS TESTED:

The selection of the liquids studied in these tests was dictated primarily by their relative evaporation rates. It was also endeavored to obtain wide differences in their physical properties. This was possible however, only to a limited degree. The liquids chosen for investigation were water, ethyl alcohol and Freon 114. Their physical properties of interest are shown in Table I. They are listed in order of increasing relative evaporation rates, as indicated by their vapor pressures.

TABLE I

PHYSICAL PROPERTIES

| | Water | Alcohol# | Freon 114 |
|---|---|---|---|
| Density - $gm/cm^3$ | 1 | .79 | 1.44 |
| Viscosity - centipoise | 1 | 1.2 | .356 |
| Surface tension - dyne/cm | 70.3 | 23 | 13 |
| Vapor pressure ($25^{\circ}$ C) - mm Hg | 23.7 | 75.2 | 1558 |

Of the four categories of jet breakup specified by Haenlein, this study confines itself primarily with the first three, that is, 1) droplet formation without the aerodynamic influence of the surrounding gas, 2) jet breakup with the aerodynamic influence of the gas, and 3) wave formation due to aerodynamic forces. Representative pictures of these three categories appear in Figures 7, 8 and 9. These categories were always present for all of the steady experimental conditions with water and alcohol but not necessarily so for the rapidly vaporizing Freon. This will be discussed in more

# Solox was used in these tests and the hot firings. Solox consists of approximately 94% ethyl alcohol, 3% water, 1% ethylacetate, 1% methylisobutylketone and 1% gasoline.

of the disintegration length varies greatly in this region and sometimes the jet breaks up simultaneously in several places. Because of the large amount of scatter of the data points, it is not possible to determine what effect the chamber pressure has, however, one would anticipate an acceleration of jet breakup with pressure in this region. It is evident in Figure 8, that the jet possesses surface irregularities in the forms of rotationally symmetric disturbances. The decrease in the disintegration length can perhaps now be attributed to the influence of the surrounding gas since the surface irregularities provide places where air friction can become effective. In addition it must be kept in mind that if the flow in the orifice is turbulent, the orifice wall is bombarded by liquid particles having radial velocity components. As soon as the restraint imposed by the orifice wall ceases, such particles are kept in bounds only by the surface film. This may soon break under the impact of the radial particles and a general disruption will occur. When a jet is turbulent throughout, no air friction is necessary for dispersion. It will breakup even in a vacuum as has been demonstrated by Lee and Spencer.[24] As a result probably both mechanisms, turbulence and air friction, promote jet breakup in this regime.

In Figure 9, the typical wavy characteristic of the jet at higher velocities is shown. In this region jet length increases slowly and breakup time decreases with velocity. In this region the effect of the surrounding gas density becomes evident. Though not an enormous effect, the breakup length is shorter the higher the chamber pressure. This behavior can be attributed to the increased effect of air friction.

For water the following conclusions can be drawn. In the laminar

regime jet length increases with increasing jet velocity, the breakup time remaining essentially constant. Jet length and time to breakup decrease with decreasing orifice diameter. A marked decrease in jet length occurs at the onset of turbulence. Air friction is only effective in the transition and fully-turbulent regions and increased gas density accelerates breakup in the turbulent region.# In the high jet velocity region, jet length increases with velocity but breakup time decreases.

b) Alcohol: In general the breakup of an alcohol jet has the same overall characteristics as water, (Figures 13 to 15), though a few slight differences are evident.

In the laminar region, jet length is slightly larger than that of water for the same tube diameter and jet velocity. This effect can likely be attributed to the higher viscosity of alcohol. The large difference in surface tension does not lead to any large differences in jet behavior. Experiments performed in the past[25] have shown that the decisive influence on jet breakup in this region is indeed viscosity, and surface tension plays only a minor role.

The evaporation process, which will be somewhat more rapid for alcohol than for water, seems to have no effect in this region as is borne out by the fact that chamber pressure again has no apparent effect on the breakup length. At very low pressures, however, (i.e., approaching the vapor pressure of alcohol) an effect may be noticeable.

As the jet velocity is increased above the velocity required to permit turbulence to occur, the sudden decrease of jet length, observed

---

# Also expected in the transition regime where data scatter prohibits a positive statement.

In Figure 16 the behavior of Freon issuing from a 0.006" diameter orifice is shown. In general the curves, at the pressures indicated, have the same overall characteristics as water and alcohol with the following exceptions: In the laminar regime, at a pressure of 30 psig a slight, but noticeable, decrease in the maximum jet length is observed. Since, until now, pressure has had no influence on breakup in this region, this effect must be solely due to the evaporation process. Qualitatively this effect can be described as follows. It has been observed that jet length decreases with decreasing jet diameter. If vaporization of the solid portion of the jet can reduce its diameter appreciably prior to breakup, then this observation would be expected. Also it is noticed that maximum jet length in this region is much less than that for alcohol or water. This can be explained because of the very low viscosity of Freon. The velocity at which maximum laminar jet length occurs is much lower than the former liquids because, due to the high density and low viscosity, turbulence occurs at a much lower velocity. (In all cases turbulence sets in at a Reynolds number (based on jet diameter) of about 1500).

The characteristic dip in the breakup curve when turbulence occurs is again noted here. The effect however is not so severe as it was for the former liquids since jet length is so small in the preceding region.

As jet velocity is increased into the fully-turbulent regime the jet length increases slowly with velocity. It stays quite small though at all the velocities studied. As was the case with alcohol, this can be attributed to the low surface tension. In this region the effect of pressure is to decrease the jet length because of increased air friction. For a diameter this small, and the accuracy of the experimental results, no effect of the

with water, occurs. This decrease becomes more and more gradual as orifice diameter is decreased. This trend was observed only to a limited extent, since at the smallest tube size, splashing on the windows accompanying the erratic jet behavior resulted in difficulty in obtaining experimental data. The remarks pertaining to the disintegration mechanisms in this region are the same as those for water.

As velocity is increased further, the breakup length increases slowly, perhaps more slowly than in the case of water. A discussion of the predominant mechanisms in this region have been given in the former section for water, and would apply here. The less rapid rise of the curve in the turbulent region may be attributed to alcohol's lower surface tension; that is, the surface film which restrains the fluid particles with radial velocity components is less effective and hence breakup is accomplished more readily. This may also explain why generally in the turbulent region breakup length of an alcohol jet is less than a similar water jet. As was the case also with water, the effect of gas density is evident in this region. The increased air friction at higher pressures causes a decrease in jet length. The fact that the evaporation process is retarded at the higher pressures does not have any apparent effect. This is most likely because the evaporation rates at all of the pressures studied[#] are not sufficiently great to have any influence.

c) Freon 114: Because of the somewhat complex nature of the jet breakup curves of Freon it is best to discuss each of Figures 16, 17 and 18 separately.

---

[#] In the tests with all fluids, jet breakup was examined at every 10 psi increment between 0 and 70 psig. Only those that showed significant differences have been included in this report.

evaporation process can be detected until the chamber pressure is reduced below 30 psig (the vapor pressure of Freon 114 at 75°F is 29 psig). At this pressure and below the liquid immediately forms a widely dispersed array of droplets and ligaments. This effect is illustrated in Figure 17. The predominant mechanism for this type of disintegration is that the large quantities of vapor being produced throughout the jet as the liquid boils, causes a violent eruption of the liquid core. This very efficient breakup mechanism could very well occur in an actual rocket engine, (for example, restart in space or high altitude where the chamber pressure would be very low or even under sea level conditions for the cryogenics).

In Figure 18 the behavior of the Freon jet issuing from a 0.012" diameter orifice is shown. Initially the trend is the same as all the former cases discussed. Jet length increases in a linear fashion and breakup time remains essentially constant. At a jet velocity of about 125 cm/sec the effect of the vaporization process is again exhibited. The lower the chamber pressure the lower the maximum jet length. Here the distinction is a little more clear than in Figure 16, however, it must be kept in mind that throughout the entire transition region the determination of jet length depends largely on the judgment of the observer, and consequently between 125 cm/sec and about 200 cm/sec the exact behavior of the jet is questionable.

From about 210 cm/sec to 400 cm/sec the behavior of the liquid jet is much the same as that of all preceding liquid jets. At a given velocity the lower the chamber pressure the longer the jet length. Hence if the evaporation process has any influence on jet breakup, the effect is secondary

and air friction is the controlling mechanism. As velocity is further increased the breakup process proceeds in a somewhat unusual manner. In the range of jet velocities between 400 and 700 cm/sec both evaporation and air friction appear to play significant roles. The 70 psig curve (that of slowest evaporation) is not seriously affected and jet length increases with velocity in a fashion similar to water or alcohol. The 50 psig curve, though, tends to flatten out between 450 and 600 cm/sec and then increases again. The length of the most rapidly vaporizing jet, the 30 psig curve, continues to increase under the apparent controlling influence of air friction to a velocity of about 600 cm/sec then a slight decrease occurs as jet velocity is further increased. It must be assumed that the evaporation rate, now greatly enhanced by the high jet velocity and large surface area of the turbulent stream, is beginning to overtake air friction as the controlling breakup factor. The jet length at velocities higher than 800 cm/sec begins again to increase with velocity. Above 800 cm/sec the relationship between jet length and chamber pressure is the opposite to that of former observations. The higher the pressure the longer the jet prior to breakup.

Air friction and turbulence, it may be stated, are the main factors which bring about the final disruption of the jet in this region but here the evaporation process has a decisive parametric influence and could possibly be regarded as a physical property of the fluid (analogous to viscosity and surface tension) which is significantly different at various chamber pressures. At low pressures (30 psig) the evaporation process is so rapid that jet breakup is permitted to occur much sooner even though the effect of air

friction is small and hence is conducive to longer jet lengths. As gas density is increased to 50 psig, jet length increases primarily because vaporization is retarded. The added effect of friction is not sufficient to overcome this behavior. A further increase of chamber pressure to 70 psig again results in a longer solid jet. The same remark applies here as was made about conditions at 50 psig. One can hypothesize that if gas density were to continue to increase the evaporation process would be sufficiently retarded that air friction would again become controlling and for a given jet velocity in this region, a further increase in pressure would result in a shorter jet.

The manner by which a 0.024" diameter Freon jet breaks up is shown in Figure 19. Again the familiar trend at low injection velocities is noted. Jet length increases linearly with velocity, the breakup time remaining essentially constant. The curves for 70, 50 and 30 psig all exhibit a form similar to those of water and alcohol. The significant difference being in their relationship to one another.

The maximum length of the laminar jet length for a chamber pressure of 70 psig is approximately 2.7 centimeters and occurs at a velocity of about 75 cm/sec. As velocity is increased jet length is shortened somewhat until at a velocity of 160 cm/sec jet length begins again to increase. Within the accuracy of the experimental observations, the relationship between jet length and jet velocity is essentially linear in the turbulent range.

The curve depicting jet length versus velocity for a chamber pressure of 50 psig behaves in much the same manner but the maximum laminar jet

length is only 2.6 centimeters. This slight decrease can be attributed to the increased vaporization rate at 50 psig and the subsequent reduction of stream diameter. In the transition region a slight decrease in jet length again occurs. Between 150 and 200 cm/sec the curve seems to flatten out somewhat. In this region turbulence, air friction and evaporation are all assisting jet breakup. As jet velocity is increased above 200 cm/sec jet length increases again in a linear fashion. In the turbulent region though, the value of the jet length is always less with decreasing chamber pressure. As was the case with the 0.012" diameter orifice this can only be explained by giving conisderation to the evaporation process. At all velocities in the turbulent regime the increased evaporation rate at 50 psig is more than sufficient to overcome the reduction in air friction. The 'cross-over' region where evaporation begins to become a significant factor does not occur in the turbulent region as it did in the 0.012" diameter case. Where it does occur is not clear. It may be in the erratic transition range or it in fact may not occur at all. That is, at all velocities the vaporization rates may have a stronger influence of jet breakup than turbulence or air friction.

The curve which was established at a chamber pressure of 30 psig, exhibits the same tendencies as the former two in the turbulent region and presumably the reasoning to describe the behavior at 50 psig would be applicable at 30 psig. In the low velocity region it is noted that a departure in the linear behavior of the curve occurs as jet velocity is increased. Due to the rapid evaporation of the fluid from the jet, the decrease in the diameter of the jet prior to breakup causes it to disrupt at a significantly shorter length. This behavior has been noted before but only,

with any accuracy, at maximum jet length.

To further elucidate the trend with pressure, the breakup was examined at a chamber pressure of 20 psi. At low velocities gasification of the fluid in the lines made any observations impossible. As jet velocity was increased to 300 cm/sec this effect became less severe and although erratic jet behavior occurred, it was possible to establish jet length and velocity when vapor bubbles were not present. At even higher velocities it was possible to produce a stable turbulent jet which was not disrupted by vapor bubbles. (So long as the total pressure in the droplet generator reservoir was above the vapor pressure of the fluid, gasification did not take place in the reservoir.) The results of the test at this pressure, though subject to a good deal of scatter, seem to substantiate the behavior at higher pressures.

Again one might presume that if chamber pressure was increased to such an extent that evaporation was greatly retarded then, for the same jet velocity, a further increase in pressure would result in a shorter turbulent jet because of the increased effect of air friction.

## EFFECT OF ACOUSTIC OSCILLATIONS ON JET BREAKUP

The character of a liquid jet subjected to acoustic oscillations is shown in Figure 20. The observations pertaining to this portion of the study are shown in Figures 21 to 33.

1. Acoustic oscillations have a measurable effect only in the laminar capillary jet region. With all the fluids tested, under a variety of imposed steady and oscillatory pressure levels, no significant effect was noted in the transition or turbulent regions.

2. Due to the complex nature of jet breakup under oscillatory conditions and because in several cases generalized trends were not observed, the specific influence of the evaporation of a given liquid cannot be isolated, and consequently it has not been possible to completely categorize the effects of the individual parameters which affect breakup. These parameters include, jet diameter, jet velocity, steady-state pressure level, acoustic velocity and pressure oscillations (i.e., the location of jet with respect to the nodal line of the standing mode and the influence of the spinning mode), fluid viscosity, density, and surface tension, and the vaporization process itself.

3. Like any disturbance applied to a liquid jet (e.g., dirt in the orifice, imperfect roundness of orifice), sonic oscillations generally accelerate jet breakup in the laminar regime. The disturbances, which are manifested as protrusions or depressions on the jet surface, eventually lead to the disintegration of the jet. The perturbations may be applied in the form of gas velocity or gas pressure oscillations and the efficiency of each depends on the nature of the experimental environment.

4. Generally, for a given jet velocity, sonic oscillations are more efficient in causing jet breakup when the jet diameter is large.

5. The higher the acoustic field intensity, the more severe is the effect of the oscillations.

6. The manner by which breakup occurs under oscillatory conditions appears to be affected, to a certain extent, in accordance with Rayleigh's theory of instability of liquid jets. That is, for a given disturbance of a specific frequency (resonant chamber frequency), and a given jet velocity, the effect of jet diameter is somewhat erratic and suggests that preferred combinations of velocity, diameter and frequency exist (see "Experimental Apparatus", Equation 1, page 18). The effect however is not so well bounded as Equation 1 suggests and there are several reasons. 1) It has been observed with the vibrating droplet generator, that for a given jet velocity and diameter, a range of frequencies will cause the jet to be unstable. 2) Rayleigh's analysis confines itself to a situation where breakup results from the imposition of infinitestimal initial disturbances. In this experiment the disturbances are finite and are present along the entire length of the jet. 3) Rayleigh's analysis is restricted to a nonviscous fluid with zero velocity, a situation which obviously is not present here.

In Figure 21, is shown the influence of the acoustic field on the breakup of a 0.006" diameter water jet. The effect it will be noticed is extremely small and because of the short jet length is subject to much scatter. Whether the mode be spinning or standing had no measurable effect. The inefficiency of the sonic oscillations can in part be explained by considering Rayleigh's criterion. For this jet, and the velocities encountered,

the frequency of maximum instability varies from 4,500 cycles/sec to 20,000 cycles/sec. The frequency of the transverse mode in the chamber is, as has been previously stated, approximately 880 cycles/sec. Figure 21 has been obtained for a chamber pressure of 0 psig. At higher pressures the same characteristic jet behavior was noted.

Figure 22 illustrates the behavior of a water jet 0.012" in diameter at a chamber pressure of 0 psig. Again no significant difference was observed whether the jet was at a pressure antinode, a velocity antinode or subjected to the spinning mode. Consequently, it must be assumed that, within the experimental accuracy, pressure oscillations or velocity oscillations are both about as effective, the mechanisms however are different. When subject to pressure oscillations alone, the liquid is subjected to a periodic variation in flow rate. This, it has been observed, produces regular thickenings in the jet, due to coalescence of the faster fluid particles with the slower. The presence of these surface imperfections promotes the condition which would have come about by viscous and surface tension forces alone, hence breakup is more readily accomplished. Unlike the pressure oscillations, the transverse gas motion,which occurs at the pressure node, does not produce a flow variation but by aerodynamic forces causes an oscillatory transverse motion of the liquid jet. This cyclic lateral displacement again produces surface irregularities on the jet and again promotes jet breakup. In addition to the aerodynamic drag on the jet, convective evaporation occurs which reduces the jet diameter. In the case of water the vaporization process would be relatively slow since its vapor pressure is so low.

Figure 23 depicts the behavior of a 0.024" diameter water jet.

Again, between the disturbing forces; pressure oscillations, velocity oscillations or both (spinning mode), no difference in breakup length was evident. Of course, jet length is affected, regardless of the mechanism, when the sonic oscillations are present.* However, at very low velocities (approaching the minimum jet velocity) an anomaly occurs. Jet length, it will be noted, is larger when sonic oscillations are present. At very low acoustic levels no appreciable change is found. As sound intensity is increased to 140 db, jet length increases. A further increase in sound level produces a shortening of the jet, but in all cases the length of the solid portion of the jet is greater than when no acoustic field is present. This behavior has been observed by other members of the research staff, but as yet there is no plausible explanation. As jet velocity is increased the jet behaves in much the same manner as in the two former cases.

To ascertain whether chamber pressure had any direct influence on jet breakup, the former three tests were repeated at 50 psig. In the 0.006" diameter case no measurable difference from 0 psig was noted. The 0.012" and 0.024" diameter jet (Figures 24 and 25), however, showed slight deviations from the atmospheric case. First, the acoustic oscillations are generally not quite as effective at the higher chamber pressure and second, pressure oscillations are more effective than velocity oscillations in breaking up the jet. Also it was observed that the spinning mode was of essentially the same effectiveness as the standing mode with the injector at the pressure antinode. The decreased effectiveness of the acoustic particle velocity can be explained simply by considering the isentropic relationship between pressure and particle velocity. In the equation

$$\frac{\Delta V}{a_o} = \frac{\gamma \Delta P}{\bar{P}}$$

* The question of droplet displacement in an unstable combustor is discussed in Appendix C.

$\Delta V$ is the amplitude of the oscillatory velocity, $a_0$ the steady-state speed of sound, $\gamma$ the ratio of specific heats, $\Delta P$ the amplitude of the oscillatory pressure and $\bar{P}$ is the steady-state pressure. Since $\Delta P$ was held constant and $\bar{P}$ was increased by a factor of 4.4, a corresponding decrease in acoustic velocity occurred. The reduction in velocity causes a reduction in the aerodynamic drag which leads to smaller lateral jet oscillations. It is well to mention here that with the spinning tangential mode, unidirectional streaming was detected. However this seemed to have little effect on jet breakup. In Clark's model[11] liquid jet breakup is accomplished solely by the action of a unidirectional transverse gas motion. Breakup was brought about by the transverse spreading of the jet and the subsequent reduction to zero of the jet cross section. In the present experiment no such transverse spreading of the jet was detected. The jet Weber numbers are much lower than in Clark's case though, and the streaming velocity was not very severe ($\simeq$ 8-10 feet sec).

The effect of acoustic oscillations on the breakup of an alcohol jet was also examined and the results appear in Figures 26 to 30. In general the characteristics are the same as for water. The negligible effect for a jet diameter of 0.006" is noted in Figure 26. In Figure 27 the behavior of a 0.012" diameter jet is illustrated. Breakup is accelerated by the acoustic field; the higher the field intensity the larger the effect. The anomalous increase of jet length at low velocities which was observed for water was not noted here. The velocity at which this occurred for water could not be obtained with alcohol. For both the 0.012" case and the 0.024" case, the sonic oscillations appear to be more effective (i.e., a

greater fractional change in jet length) in disrupting the jet. Possibly this can be attributed to the lower surface tension of alcohol. Due to the lower resistance of the jet skin, the surface irregularities can be more easily applied to the liquid jet.

To examine the influence of chamber pressure on the breakup of an alcohol jet, the former tests were repeated at a chamber pressure of 50 psig. The results appear in Figures 29 and 30. The behavior is virtually identical to the behavior of water. Again it is noticed that pressure oscillations are more effective than velocity oscillations in bringing about jet breakup.

To this point in the study, the influence which the evaporation process has on breakup under oscillatory conditions has not been ascertained. In order to clarify this matter, the same tests were performed using the rapidly vaporizing Freon 114. It was not possible, of course, to establish a laminar Freon jet at 0 psig and the fluid was examined at 30 and 50 psig.

Under all possible oscillatory conditions, no measurable change could be detected for the 0.006" diameter jet. This is due primarily to the extremely small jet length that exists under steady conditions which leads to large inaccuracies in the measurement of jet length. The 0.012" diameter jet is subject to the same inaccuracies and the resultant scatter is evidenced in Figure 31. Obviously no significant remarks can be made here. In Figure 32, however, a reasonably accurate trend has been observed. First of all, the effect of the acoustic intensity is similar to those cases studied earlier. The higher the intensity, the shorter becomes the jet length.

Secondly, the influence of velocity oscillations is more pronounced than with water and alcohol. At 50 psig the velocity oscillations are just as effective in producing jet breakup as are the pressure oscillations, and at 30 psig the velocity oscillations appear more effective than pressure oscillations. This behavior must be attributed to the fact that the Freon is evaporating. The pressure oscillations produce the same periodic flow variations that occur with all liquids[#] and the velocity oscillations cause cyclic lateral displacement of the liquid jet. In addition, the velocity oscillations cause convective evaporation of the fluid. This effect is more pronounced at the lower chamber pressure because the amplitude of the velocity oscillations is higher and the steady-state evaporation rate, because of the reduced saturation temperature of the fluid, is greater. When subjected to the spinning mode the jet breaks up in the same manner as it does with the most effective portion of the standing mode. That is, if for the standing mode, pressure oscillations are most effective, the jet will react to the spinning mode as it does to the standing mode pressure oscillations. Similarly, it has been observed, that the spinning mode is as efficient as velocity oscillations when such oscillations are more effective than pressure oscillations.

The combined effect of vaporization and acoustic oscillations, admittedly, is not very severe and the importance of these observations is questionable. However the specific effect of the vaporization process has been observed, if only to a limited extent.

---

[#] A very small cyclic change in the evaporation rate can also be expected due to the oscillating chamber pressure and the subsequent oscillations in the droplet saturation temperature. This effect, it would be anticipated, would be very small.

test conditions permit rapid fluid vaporization. Under other circumstances (i.e., high chamber pressure) where evaporation is retarded, the jet behaves in a normal manner. Consider, however, what might happen at a very high chamber pressure in an actual rocket engine. Friction would obviously become extremely effective, but the evaporation rate of the fluid would also be very high. This is due to the extremely high heat transfer rates and the fact that the latent heat of vaporization approaches zero. In addition, surface tension, apparently an important parameter in the turbulent regime, becomes very small, and in fact is zero at the critical point of the fluid. One would hence deduce that under these circumstances, jet breakup would be remarkably fast. One must again, however, be wary of such an extrapolation since there is no guarantee that under such conditions another yet unconsidered parameter, may be important. For example, and this is conjecture, since both gas and liquid are of comparable density the entire problem may reduce essentially to one of turbulent mixing. Or perhaps, even though surface tension is small, the jet may retain a reasonably stable configuration until, due almost primarily to evaporation, the jet diameter is reduced to zero. Here the assumption is made that the rate of mass removal is greater than the rate at which normal surface irregularities propagate through the liquid jet. In which case the viscosity of the fluid which governs the rate of this propagation, and the level of turbulence (in the liquid and the gas) which determines the magnitude of the initial disturbances become important factors. In any case, it is difficult to predict with any accuracy the magnitude of the effect that fluid evaporation will have.

In this experiment the effect of acoustic oscillations on jet breakup has been examined with the intent of elucidating jet behavior in an unstable

## DISCUSSION

In the foregoing study, attention has been focused on the parametric influence of fluid vaporization on the breakup of a liquid jet. The inclusion of this parameter to the already long (and apparently incomplete) list of parameters has not lead to any empirical relationship which describes its influence. It is apparent though that vaporization could invalidate some of the already crude similarity relationships which have been presented. In other words, the behavior of the jet can deviate from that expected from a fluid with similar breakup properties (i.e., viscosity, surface tension, jet velocity, etc.) because other properties (i.e., latent heat of evaporation, thermal conductivity, fluid vapor pressure, etc.) can become important. Therefore the unusual behavior which has been observed has been attributed to this general characteristic of the fluid (i.e. vaporization) without any attempt being made to analytically describe the behavior. For example, the deviations in the laminar jet behavior noted in Figure 19, have been attributed to the reduction of the solid portion of the jet prior to breakup. However, one cannot exclude the possibility that perhaps the unusual behavior may, at least partially, be due to the unusual properties of the atmosphere surrounding the jet. That is, because of radial diffusion of heat and mass, the physical characteristics of the immediately surrounding gas are drastically different than if the fluid were not evaporating. Consequently, due to uncertainties of this nature one must be wary of extrapolation to regions far removed from those of this experiment.

Consider now the behavior of a vaporizing jet in the turbulent regime. This study has shown that indeed the evaporation process can play a significant role in determining the steady-state rate of jet breakup when

combustor. Both evaporating and essentially non-evaporating fluids have been studied. When the liquid evaporates slowly, it has been found that velocity and pressure oscillations act primarily as small disturbances which, in the laminar regime, accelerate jet breakup. The perturbations are so small though, that in the turbulent regime surface irregularities due to turbulence are far more important than acoustic effects. In fact, the acoustic levels attainable with this apparatus, produced no noticeable improvement in jet breakup in the turbulent regime.

In these tests two acoustic levels were examined; 140 decibel and 155 decibel (i.e., .002 dyne/$cm^2$). These correspond to peak to peak oscillations of 0.08 psi and 0.47 psi. At atmospheric pressure, these represent non-dimensional pressure amplitudes of 0.0055 and 0.032 respectively. The writer would be very reluctant to suggest that the behavior of a jet in an unstable combustor of say, 32 psi peak to peak pressure oscillations and a mean pressure of 1000 psi, could be adequately described by the results of these tests. But the experiments do point out the implications which arise from acoustic oscillations and how their presence effects jet breakup. The tests have, for example, suggested that periodic oscillations in the chamber could only be effective in the turbulent regime if the amplitude and frequency of the oscillations produced irregularities in the jet of equal or greater magnitude than those produced by turbulence alone. Also the study has shown the importance of whether the disturbances in the vicinity of the jet be pressure or velocity oscillations. It has been observed that at a low mean pressure, velocity and pressure oscillations are equally effective in promoting jet breakup, at least over the range of acoustic levels examined here. One could not predict that this would be the case since the mechanisms which

promote breakup are different in each case. In the presence of only pressure oscillations jet breakup is accelerated due to surface imperfections imposed on the jet due to the oscillatory flow rate of the liquid. In the presence of just velocity oscillations, jet breakup is accelerated due to surface imperfections brought about by the cyclic lateral deflections of the jet. At higher chamber pressures, pressure oscillations appear more effective in disrupting the jet than do velocity oscillations but both are less effective than at the lower mean pressure level. This response of the jet suggests that the breakup length $L_b$ is a function of the non-dimensional pressure level $\frac{\Delta P}{\overline{P}}$. The functions are apparently different at a velocity antinode and a pressure antinode.

Consider the behavior of a jet situated at the pressure antinode of a transverse acoustic field. The variation in fluid flow rate is proportional to the absolute value of the oscillatory component of chamber pressure (i.e., $\Delta m \sim \Delta P$). The imposition of surface irregularities is a function of the oscillatory flow rate and consequently the acceleration of jet breakup is a function of $\Delta P$. This is a contradiction of the experimental results which have shown breakup to be less effective at a higher $\overline{P}$ even though $\Delta P$ was unchanged. Therefore at a pressure antinode the increased efficiency of jet breakup seems to be a function of $\frac{\Delta P}{\overline{P}}$ and the absolute value of $\Delta P$.

Consider now the behavior of a jet situated at the pressure node of a transverse acoustic field. Assuming the lateral motion of the jet due to aerodynamic forces is small, the magnitude of these deflections would be proportional to $\rho \Delta V^2$, where $\rho$ is the steady-state gas density and $\Delta V$ is the amplitude of the oscillatory gas motion. The experiments have

shown that an increase in $\bar{P}$ decreases the efficiency of the acoustic velocity oscillations even though $\Delta P$ was unchanged. This seems logical since an increase in $\bar{P}$, though it produces an increase in $\rho$, decreases the amplitude of the oscillatory velocity $\Delta V$. However, since $\Delta V$ is squared the result is to decrease $\rho \Delta V^2$ (e.g., doubling $\bar{P}$, reduces $\rho \Delta V^2$ by a factor of two assuming $\Delta P$ is not changed and the steady-state speed of sound $a_0$ is constant). This is assuming the gas obeys a law of the form

$$\frac{\Delta V}{a_0} \sim \frac{\Delta P}{\bar{P}}$$

This relationship is derived from the wave equation for isentropic flow. However it can easily be seen that jet behavior in the presence of velocity oscillations cannot be specified as a function of $\frac{\Delta P}{\bar{P}}$ only. The ratio $\frac{\Delta P}{\bar{P}}$ specifies the magnitude of $\Delta V$ but unless the absolute value of $\Delta P$ is known, the gas density $\rho$ cannot be evaluated. Therefore the behavior of a liquid jet in the vicinity of a pressure node is a function of $\frac{\Delta P}{\bar{P}}$ and $\Delta P$. This is not the same functional relationship that describes jet behavior at a pressure antinode though the same parameters, $\frac{\Delta P}{\bar{P}}$ and $\Delta P$, are governing.

It is apparent therefore that the behavior of a non-evaporating jet in an oscillatory environment is very complex in nature. This experiment has not provided an adequate description of this behavior in regions far removed from the confines of this study. However, it is now possible, at least qualitatively, to anticipate when some parameters are more important than others.

As an additional complication to the above issue, the effect of fluid evaporation under oscillatory conditions has been examined to determine

how the presence of the parameter influences the jet behavior. In general, its influence is to modify the response of the jet to velocity oscillations. That is, in addition to aerodynamic effects, the gas velocity oscillations produce convective removal of mass from the jet, resulting in a continual decrease in jet diameter. This effect, it has been observed, further promotes jet breakup. In a realistic unstable combustor with large velocity amplitude oscillations, if the fluid is susceptible to convective evaporation, the effect discussed above may become more important than the effects of aerodynamic forces. When this occurs is again very dependent on the particular situation in question.

In conclusion, due to the exploratory nature of this study, it is not possible to conclusively state the behavior of a liquid jet for any given situation. However, given a specific case it is possible to estimate the order of magnitude of the effects due to pressure and velocity oscillations and fluid vaporization.

## CONCLUDING REMARKS

The results of this study show that vaporization of the liquid and acoustic oscillations do promote jet breakup. Unfortunately it has not been possible to empirically describe either effect in terms of the physical properties of the fluid and its environment. Consequently accurate jet breakup data for fluids other than those tested and at conditions other than those encountered in the study cannot be obtained. The experiment however, does suggest the implications which arise from fluid vaporization and acoustic oscillations and hence gives an indication of when a specific parameter becomes more important than another.

# APPENDIX A

## PHOTOGRAPHIC INVESTIGATION OF PROPELLANT BEHAVIOR NEAR THE INJECTOR FACE OF AN ACTUAL ROCKET MOTOR

The transverse motion of gases and liquids in a rocket combustion chamber has long been regarded as an important parameter in the initiation and control of transverse combustion instability (27, 28 and 29). To qualify some of the limitations imposed on the pseudo rocket and especially to indicate to what extent unidirectional motion exists in an unstable (1T spinning mode) rocket engine[#], a high speed motion picture study of the processes occurring near the injector face of the nine-inch diameter transverse rocket hardware was performed. In order that further work may be done in this area and that further improvements may be made to the experimental technique, there follows a brief description of the development of the project to its existing state.

A quartz window, one inch in diameter and half an inch thick, was mounted approximately one and a half inches from the injector face. The window and injector were aligned such that the spray from the closest injector element passed through the center of the viewing area. The window, recessed several inches from the chamber wall to avoid direct contact with the propellants, was fitted with a nitrogen purge system and it was necessary to have the gas impinge on both the inner and outer face of the window to prevent frosting or fogging. It was also helpful to preheat the incoming gas by passing it through a heat exchanging water jacket. To prevent

---

[#] A second order streaming in the direction of the wave travel has been predicted by Sirignano[30] and a viscous boundary layer streaming opposite to the direction of wave travel has been predicted by Maslen and Moore[26]. Either of these effects could have a pronounced influence on the nature of the combustion process if they were of significant magnitude.

any severe disturbances arising from the nitrogen gas flow into the combustion chamber, its velocity was kept limited to a few feet per second by an upstream sonic orifice. The window assembly is shown in Figure A-1.

A twelve spud like-on-like impinging injector assembly was utilized in the initial tests. The spuds were aligned such that the narrowest portion of the spray was observed through the window; that is, the spray fans were aligned radially.[27]

To take the pictures a Wollensak WF3 Fastax camera and Dupont 913A rapid reversal film (ASA #125) were used. In the initial tests, it was found that the field of view was far too small to make statements about the flow characteristics. Individual burning fuel droplets or groups of droplets could be distinguished but their exact origin and direction of travel could not be determined.

To increase the field of view the spud nearest the window was blocked off while the diametric spud was photographed. This permitted the spray to be observed over a greater portion of its length. Photographically this did produce an improvement, however, with the one spud blocked it was virtually impossible to produce a 1 T spinning mode. The preference was the 1 T standing mode. To rectify this problem a sixteen spud injector was installed. It was felt that the blocking of one of sixteen spuds would have a less pronounced effect than the blocking of one of twelve spuds. This in fact proved to be true and 1 T spinning modes (amplitude of approximately 100 psi) could again be established. To further increase the field of view the window port was shortened to approximately 2", and again a slight improvement in photographic quality was noted.

At the framing rates used in these tests (approximately 3000 frames per second), it appeared that a better exposure would be favorable. In this regard Kodak Tri-X negative film (ASA #250) was substituted for the Dupont 931A. With this film it was possible to attain greater clarity. The next problem to overcome was lack of contrast, the prime difficulty being that the subject (the burning spray fan) was of the same color and intensity as its environment. To make the spray fan of interest stand out from its surroundings, an auxiliary feed system was constructed that would supply the fuel to only the injector element of interest. (The other spuds were fed by the regular feed system.) Prior to running the motor, the auxiliary fuel tank was filled with a saturated solution of ethyl alcohol and sodium salicylate ($2HOC_6H_4CO_2Na$). A valve switching arrangement was installed so that at any specified time, the fuel to the spud of interest could be changed from pure alcohol to the seeded fuel. Using a first order 5892 angstrom, interference filter between the window and the camera lens, allowed the film to be exposed only to the sodium D line radiation accompanying the combustion of the seeded fuel. It was also found that the use of a polarizing filter eliminated a lot of undesirable reflections from the combustion chamber walls and the inside of the window port. With this technique far better contrast was attained and the burning, seeded fuel could easily be distinquished from its surroundings, however, further improvements were still necessary before conclusive statements about gas motion could be made.

As previously stated, the use of the seeded fuel greatly increased the contrast, but it was now evident that the size of the burning fuel spray relative to the window (and hence the camera frame) was

too large. Because the boundaries of the spray were not visible any remarks about transverse motion would have been premature. A black and white grid painted (with high temperature paint) on the inside of the chamber in the vicinity of the spud was of no help since it became coated with an aluminum oxide film after ignition. (Ignition is accomplished by introducing hypergolic triethylalumina into an oxygen environment.) To alleviate this difficulty, the spud was modified so that the seeded fuel was introduced through a 1/16" diameter tube. The modified spud is shown in Figure A-2.

With the motor operating in a stable manner, the tracer stream was readily observed as it passed from the injector along the chamber through the approximately two and a half inch long field of view. When pulsed and instability occurred, however, a good deal of the detail was lost. The intensified gas phase mixing, the apparent increased burning rate (as deduced from the large increase in radiant intensity), and the oscillatory gas motion associated with the tangential mode again made conclusive observations difficult.

A further attempt to improve the situation was made by using color film (Kodak Ektachrome ER type B). Since the film was sensitive to the blue (alcohol-oxygen reaction) and yellow (sodium D line radiation), the interference filter was removed. The polarizing filter, however, was left in position. Also, because aperture masks (to decrease exposure time) were not available and because a) better stopping of the motion was desirable and b) without the interference filter much more light was available to the film, the framing rate was increased to a maximum of 7000 frames per second. This was done with a Wollensak Goose unit. (Camera voltage set to 220 volts.)

In the course of testing with the tracer stream it was necessary to know whether the stream itself influenced the velocity environment. An analysis of such tests, i.e., identical test conditions with and without the tracer stream, was reported in Reference 31 and concluded that the stream had no effect.

The existing experimental apparatus is shown in Figures A-3 and A-4. A plexiglas shield in front of the camera was installed to prevent serious damage to the camera should the window fail. Also, during operation the camera was shrouded in a rubberized cape to insure no water, fuel, etc., touched it if a leak should have occurred.

Several frames of the last roll of film have been reproduced (in a very unorthodox fashion) in Figure A-5. The true color film has been used to make the color print, but of course the true colors are not reproduced. This is not important since the only thing that is desirable is the distinction between the seeded fuel and its background. In Figure A-5a, the combustion gases from the tracer stream (the dark striations) are easily seen on the orange colored background. The combustion gases move in fairly well defined regions travelling through the chamber toward the nozzle. No severe turbulent mixing is evident. In Figure A-5b is a series of pictures from the same roll of the tracer stream after the chamber has been pulsed into 1 T spinning combustion instability. The details are not quite as clear here as in the original, however it is immediately apparent that gas phase (and possibly liquid phase) mixing is greatly enhanced. It is also possible to detect the oscillatory transverse gas motion. Apparently there is no severe unidirectional transverse motion for the conditions of this test. (Steady-state

chamber pressure of 300 psi and oscillatory pressure of 100 psi peak-to-peak). The latter observation though could be made with more assuredness if further refinements were made to the system. Those refinements might include: 1) A smaller diameter, low velocity tracer stream. This would prevent rapid stream breakup and hence confine the stream to a smaller area. 2) The addition of another window opposite the existing one. This would allow the use of back lighting and therefore permit the observation of the liquid and not just the combustion products of the stream. 3) A drum or strip camera of constant framing rate. Its use would enable the operator to make better use of the "stroboscope" effect, (i.e., setting the framing rate slightly different than the frequency of the chamber oscillations). 4) The use of aperture masks to reduce the exposure time and further stop the motion. This would permit far better frame-to-frame detail examinations. 5) A camera shield which is more transparent than the existing plexiglas. The plexiglas to a lesser extent has the same effect as fogging of the window. 6) A larger window mounted closer to the injector face allowing improved observation of the tracer stream immediately upon entering as well as subsequent behavior in the chamber.

# APPENDIX B

## EXPERIMENTAL PROCEDURE

In order that further work may be done with this equipment or that the results herein may be verified or extended, the following experimental procedure is given:

1. Install droplet generator of appropriate orifice diameter. Insure that "O" ring seal is properly seated.

2. With chamber pressure regulator, set chamber pressure to desired level. Check to insure that, the lines from the chamber to the horns are installed. If not, severe damage to the speaker diaphragms will result.

3. With Freon tank pressure regulator set appropriate tank pressure. Insure that Freon prop valve and hand valve downstream from prop valve is closed.

4. Switch on power supply to 20 watt amplifier and allow several minutes to warm up. Switch on audio oscillator which drives droplet generator keeping the gain at zero.

5. To make observations of jet behavior in laminar and transition ranges place strobotac behind one window of chamber. Place ground glass screen between strobotac and window. Turn strobotac on at an intermediate flashing rate.

6. Open chamber pressure prop valve and allow chamber pressure to stablize.

7. Open Freon prop valve.

8. Adjust the jet velocity with the small hand valve upstream of the injector. Visual observations of jet character and breakup length can now be made.

9. Adjust generator oscillator gain and frequency such that when viewed with strobotac, jet assumes a stable configuration. As well as regularly spaced equal size droplets, a regular thickening of the solid jet will occur at several places on the jet. Knowing the frequency at which the perturbations are applied, the distance between successive thickenings (or droplets) is indicative of the jet (or droplet) velocity.

10. When making observations in the turbulent region, the value of the jet length is best established by taking a spark photograph, since visual observations require too much judgement on the part of the operator and results in insufficient accuracy.

11. When taking spark photographs the following procedure should be followed:

a) Switch on trigger delay circuit.

b) Switch on power supply to spark source. Leave gain at zero and shorting rod in place.

c) Place photoflood lamp behind chamber window with ground glass screen in place.

d) Focus camera on injector needle. Allow laminar jet to flow from needle and re-focus camera on jet over its entire length. Remove photoflood lamp.

e) Close camera shutter. Insert film holder and film in camera. For polaroid type 52 film a lens aperature of f-1 is required. When using polaroid type 57 film use f-11. Kodak Royal Pan requires f-1.

f) Remove shorting rod from spark power supply. Set voltage to 11KV. Check occasionally as voltage tends to wander.

g) Establish turbulent jet with hand valve.

h) Extinguish room lights. Open shutter with bulb and activate spark through triggering circuit.

i) Remove film, reload camera, drive droplet generator at predetermined frequency and amplitude and take another photograph or observe the regular perturbations on the jet via the strobotac.

12. Close hand valve and Freon prop valve.

13. Reduce Freon tank pressure and chamber flush chamber with nitrogen after each run.

14. Shut down spark power supply being sure to replace shorting rod.

15. To study jet behavior under the influence of an acoustic field, first switch on oscilloscope, Kistler charge amplifiers, audio oscillator, phase shifting network, the two 100 watt power amplifiers, and the hot wire amplifier.

NOTE: Prior to operating, insure the amplifiers are balanced. Also, it is advisable to calibrate both audio oscillators used in this experiment. Over a long period of time the frequency of the output signal has a tendency to shift somewhat. This calibration is best performed on the digital counter in the recording room.

16. Prior to operating jet, establish a low (130db) acoustic field in the chamber. Adjust frequency of oscillator to produce maximum output (i.e., resonance) from pressure transducers and/or hot wire anemometer (monitor signals on scope).

17. Observing wave forms on scope, adjust the phase shifting network to produce the desired mode (i.e., standing with pressure node

at injector ($0^{o}$ phase difference) standing with velocity mode at injector ($180^{o}$ phase difference) or spinning mode (phasing signals to horns $90^{o}$ or $270^{o}$ apart). Note that the dial indicator of the phase shifter is not accurate and phasing of the signals is best accomplished by observing the pressure and velocity wave forms at the same angular position in the chamber. (As an alternative, the signals from the two pressure transducers which are $135^{o}$ apart, can be monitored).

18. Reduce oscillator gain to zero. Established liquid jet. Set-up desired acoustic level and observe (visually or photographically) the jet behavior.

19. When studying liquids other than Freon the auxiliary tank is installed in place of the Freon tank, but the same regulators and valves are used.

NOTE: A schematic drawing of the lead titanate - lead zirconate pressure transducer, the transducer calibration curves, and the hot wire calibration curves are shown in Figures B-1, B-2, and B-3, respectively.

# APPENDIX C

## DROPLET DISPLACEMENT STUDY IN AN UNSTABLE COMBUSTOR

It has been observed that the behavior of a laminar liquid jet, when injected into a resonant acoustic cavity, behaves somewhat differently than a jet injected into a quiescent environment. This study, though prompted by these observations, does not try to explain this behavior but, by considering a hypothetical unstable rocket engine, permits one to predict the spatial arrangement of droplets that have issued from an oxidizer of fuel injector. When the constraints and assumptions herein are compiled with, it is possible to determine oxidizer or fuel density profiles at any location in the unstable combustor, and, to perhaps deduce under what circumstances amplification or decay of the oscillations will occur. Further examination could perhaps lead to feasible explanations of "preferred spin direction" and/or "triggering".

The theory begins with the idealized propellant feed system shown below. The equation of motion of the fluid in the supply lines is

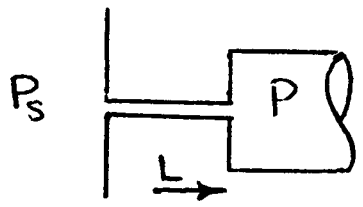


$$\frac{dU}{dt} + U\frac{dU}{dx} = -\frac{1}{\rho_\ell}\frac{dP}{dx} \tag{1}$$

If $U$ and $P$ are perturbed such that

$$U = a(x)\bar{U} + b(x)U'$$
$$P = c(x)\bar{P} + d(x)P' \tag{2}$$

where $U' < \bar{U}$ and $P' < \bar{P}$

and $a(x)$ = axial variation of steady-state velocity

$b(x)$ = axial variation of oscillatory velocity

$c(x)$ = axial variation of line pressure

$d(x)$ = axial variation of oscillatory pressure

$a(0) = b(0) = d(0) = 0;\ c(0) = \frac{P_s}{\bar{P}}$

$a(L) = b(L) = c(L) = d(L) = 1$

then when (2) is substituted into (1), separation yields the lowest order result as a differential equation which is readily integrated to yield

$$\bar{U} = \sqrt{\frac{2(P_s - \bar{P})}{\rho_\ell}} \tag{3}$$

This is the familiar steady-state relation involving fluid velocity and the pressure drop between the supply and the combustion chamber.

Now separating terms of $0(U')$, we obtain

$$b\frac{dU'}{dt} + \frac{d}{dx}\frac{(2ab\bar{U}U')}{2} = -\frac{1}{\rho_\ell}\frac{d(dP')}{dx} \tag{4}$$

By considering the continuity equation for incompressible flow through the line,

$$\rho_\ell A_e(\bar{U} + U') = \rho_\ell A\,(a(x)\,\bar{U} + b(x)U')$$

where $A_e$ is the area of the duct at its exit and $A$ is some other area between $0$ and $L$. Rearranging the above and equating terms of equal magnitude leads to

$$\frac{A_e}{A}\bar{U} = a(x)\bar{U} \qquad \text{or} \qquad \frac{A_e}{A} = a(x)$$

$$\frac{A_e}{A}U' = b(x)U' \qquad \text{or} \qquad \frac{A_e}{A} = b(x)$$

Therefore $a(x) = b(x)$, and hence (4) reduces to

$$a(x)\frac{dU'}{dt} + \bar{U}U'\frac{d(a(x))^2}{dx} = -\frac{1}{\rho_\ell}\frac{d(d(x)P')}{dx}$$

Integrating from 0 to L gives

$$\frac{dU'}{dt} + \frac{\bar{U}U'}{\int_0^L a(x)dx} = -\frac{P'}{\rho_\ell \int_0^L a(x)dx} \tag{5}$$

Recall now that $a(x)$ represents the variation of steady-state velocity along the feed line. Since for inviscid flow (as has been assumed in writing Equation (1)) there can be no velocity gradient in a constant area duct, all the acceleration of the fluid must take place within the supply tank. Miesse[12] has shown that for hyperbolic stream lines converging at the tank exit the integral $\int_0^L a(x)dx = L + \frac{b}{3}$ applies, where $b$ is the distance from the tank exit to the position in the tank of zero fluid velocity.

Therefore (5) may be written (for $\frac{b}{3} \ll L$)

$$\frac{dU'}{dt} + \frac{\bar{U}U'}{L} = -\frac{P'}{\rho_\ell L} \tag{6}$$

In this equation $L$ represents the approximate length of the propellant feed line from the injector to where the propellant velocity is zero (i.e., where $P = P_s$). With the spuds used in the 1000 lb. thrust engine at Princeton, and with an injection velocity of 100 feet per second, the fluid velocity is less than 20 feet per second approximately one inch before entering the combustion chamber. For a nominal chamber pressure of 300 psi, this means that a short distance from the injector exit the line pressure is about $0.98\ P_s$. As an approximation therefore, it may be possible to regard the position in the feed line just prior to the final acceleration of the fluid as the location of the propellant supply.

With regard to $P'$ we shall consider here that the chamber is experiencing the first tangential spinning mode of combustion instability. The well known[26] solution for $P'$ is

$$P' = -\epsilon \bar{P} \gamma \cos(\omega t + \theta) J_1(\alpha) \tag{7}$$

where $\epsilon$ is an amplitude parameter proportional to $\frac{P'}{\bar{P}}$. Using the above, Equation (6) may be written as

$$\frac{dU'}{dt} + \frac{\bar{U}U'}{L} = \frac{\epsilon \bar{P}}{\rho_\ell L} \gamma J_1(\alpha) \cos(\omega t + \theta) \tag{8}$$

To solve (7) let

$$U' = A\sin(\omega t + \theta) + B\cos(\omega t + \theta)$$

Substituting into (7) and equating coefficients leads to

$$A = \frac{\omega L \epsilon \bar{P} \gamma J_1(\alpha)}{\omega^2 L^2 + \bar{U}^2} \quad ; \quad B = \frac{\epsilon \overline{PU} \gamma J_1(\alpha)}{\omega^2 L^2 + \bar{U}^2}$$

Therefore, it is readily found that

$$U' = \frac{\epsilon \bar{P} \gamma J_1(\alpha)}{\rho_\ell (\omega^2 L^2 + \bar{U}^2)^{\frac{1}{2}}} \cos(\omega t + \theta - \phi) \tag{9}$$

where

$$\phi = \tan^{-1} \frac{\omega L}{\bar{U}}$$

When the fluid of mass $m = \bar{m} + m'$ is introduced into the chamber, it is immediately subjected to the oscillatory transverse gas flow If the assumption is made that immediately upon exiting the orifice, the fluid is shattered into small spherical droplets (a reasonable approximation

for impinging injectors), the transverse motion of these droplets can be described by the following equation:

$$m_d \frac{dV_d}{dt} + \text{drag} = 0 \tag{10}$$

Here the effects of gravity have been ignored. For a spherical droplets of diameter $d$, (10) can be rewritten as:

$$\frac{1}{6}\pi d^3 \rho_\ell \frac{dV_d}{dt} - \frac{\pi}{8} C \rho_g \Delta V^2 d^2 = 0 \tag{11}$$

where $C$ is the drag coefficient and $\Delta V$ is the relative transverse velocity between the droplet and surrounding gas. If the assumption is made that $C \sim \frac{1}{Re}$ (this is a good assumption for laminar and semi-turbulent flow around the droplet, but is somewhat in error if fully developed turbulence is present) then Equation (1) can be rewritten as:

$$\frac{dV_d}{dt} + 18 \frac{\mu_g}{\rho_\ell d^2} Vd(t) = 18 \frac{\mu_g}{\rho_\ell d^2} V_g(t) \tag{12}$$

where the drag coefficient $C$ has been chosen equal to $\frac{24}{Re}$ (Stokes flow), and $\Delta V = V_g(t) - V_d(t)$ .

In this equation $V_g$, $V_d$, and $d$ are all functions of time. The explicit time dependance of the droplet diameter under oscillatory conditions is not available, although with certain simplyfying assumptions it may be possible to solve (12). In any case it is instructive to analyze the problem keeping $d$ constant (i.e., assuming the droplet does not evaporate to any great extent nor does it become distorted under the effects of the gas flow).

Under these conditions (12) may be expressed by

$$\frac{dV_d}{dt} + \psi V_d = \psi V_g \tag{13}$$

where $$\psi = \frac{18}{d^2}\frac{g}{}$$

In a spinning transverse acoustic field the gas velocity has both a radial and tangential component. Consideration will be given here only to the tangential component so that the tangential component of $V_d$ may be calculated. The well-known solution for the tangential gas velocity for the first spinning mode is:

$$V_g = \epsilon \cos(\omega t + \theta) a_0 \frac{J_1(\alpha)}{\alpha}$$

Therefore (13) becomes

$$\frac{dV}{dt} + \psi V_d = \epsilon \psi \frac{J_1(\alpha)}{\alpha} a_0 \cos(\omega t + \theta) \tag{13a}$$

where $a_0$ is the steady-state speed of sound in the chamber.

The form of (13) is identical to that of (8) but here the homogeneous portion of the solution must be considered. The solution of (13a) is:

$$V_d = \frac{a_0 J_1(\alpha)\psi}{\alpha(\omega^2+\psi^2)^{\frac{1}{2}}} \cos(\omega t + \theta - \tan^{-1}\frac{\omega}{\psi}) + Ae^{-\psi t} \tag{14}$$

where A is a constant of integration.

If the approximation is made that directly after impingement the droplets all move only in the axial direction the following boundary condition can be applied: At the instant that a particular droplet is

injected, $t = \hat{t}$, its transverse velocity $V_d(\hat{t})$ is zero.* Therefore A is determined and (14) becomes

$$V_d = \frac{\epsilon a_0 J_1(\alpha)\psi}{\alpha(\omega^2+\psi^2)^{\frac{1}{2}}} \cos(\omega t+\theta-\xi) - e^{-\psi(t-\hat{t})}\cos(\omega\hat{t}+\theta-\xi) \quad (15)$$

where $a_0$ and $\omega$ express the chamber conditions, $\frac{J_1(\alpha)}{\alpha}$ expresses the radial dependance, and $\psi$ the physical properties of the droplet and its environment. The inertial phase lag $\xi = \tan^{-1}\frac{\omega}{\psi}$.

The transverse droplet velocity as expressed by (15) may be written as:

$$V_d = V_{dm}\left[\cos(\omega t+\theta-\xi) - e^{-\psi(t-\hat{t})}\cos(\omega\hat{t}+\theta-\xi)\right] \quad (16)$$

where $V_{dm}$ is the amplitude of the oscillatory droplet velocity.

The equation that describes the transverse displacement is obtained by integrating (16)

$$S_d = \frac{V_{dm}}{\omega}\sin(\omega t+\theta-\xi) + \frac{V_{dm}}{\psi} e^{-\psi(t-\hat{t})}\cos(\omega t+\theta-\xi)+K \quad (17)$$

where $K$ is a constant of integration.

Applying the boundary condition that $S_d = 0$ when $t = \hat{t}$ leads to

$$S_d = \frac{V_{dm}}{\omega}\left[\sin(\omega t+\theta-\xi) - \sin(\omega\hat{t}+\theta-\xi)\right] + \frac{V_{dm}}{\psi}\left[(e^{-\psi(t-\hat{t})}-1)\cos(\omega\hat{t}+\theta-\xi)\right] \quad (18)$$

---

* Actually any reasonable spray velocity distribution could be used as an initial condition. The above approximation serves as a simplification in that it avoids the introduction of another independent variable and permits the evaluation of droplet behavior at a fixed value of $\theta$. This approximation will be valid so long as the lateral movement of droplets is not great.

Consider now the axial displacement of a given droplet along the chamber axis. The initial velocity (i.e., $t = t$) is, according to Equation (9),

$$U_{di} = \bar{U} + \epsilon \frac{\gamma \bar{P} J_1(\alpha)}{\rho_\ell (\omega^2 L^2 + \bar{U}^2)^{\frac{1}{2}}} \cos(\omega \hat{t} + \theta - \phi) \tag{19}$$

This axial velocity will be attenuated as the droplet moves through the chamber due to the drag effect of the combustion chamber gases. For a general case the axial velocity distribution of the gas cannot be known; but an approximate model can be used. A good approximation for large engines is that the axial gas velocity is linear with distance from the injector face to the nozzle region; that is, $U_g = mx + B$. The equation of motion in the axial direction therefore becomes:

$$\frac{dU_d}{dt} + \psi U_d = \psi (mx + B) \tag{20}$$

Since this equation is valid for all $x$ and since by definition $U_d = \frac{dx}{dt}$, Equation (20) may be written as

$$\frac{d^2x}{dt^2} + \psi \frac{dx}{dt} - \psi mx = \psi B \tag{21}$$

This is a linear, second order inhomogeneous equation, the solution of which is of the form

$$x = C_1 e^{pt} + C_2 e^{qt} - \frac{B}{m} \tag{22}$$

where $C_1$ and $C_2$ are constants whose values are determined from the initial conditions and $p$ and $q$ are the roots of the differential equation. Using standard techniques it can be shown that these roots are

$$\frac{-\psi \pm \sqrt{\psi^2 + 4m\psi}}{2}$$

Letting $p = \frac{-\psi - \sqrt{\psi^2 + 4m\psi}}{2}$ and $q = \frac{-\psi + \sqrt{\psi^2 + 4m\psi}}{2}$

Application of the initial conditions $x(t) = 0$ and $\frac{dx}{dt}(t) = U_{di}$

leads to the following results

$$C_1 = \frac{Bq - mU_{di}}{m(q-p)} e^{-p\hat{t}}$$

and

$$C_2 = -\frac{Bp - mU_{di}}{m(q-p)} e^{-q\hat{t}}$$

Therefore (22) becomes

$$x_d = \left\{ \frac{B}{m} \cosh \frac{\sqrt{\psi^2+4m\psi}}{2}(t-\hat{t}) + \frac{B\psi+2mU_{di}}{m\sqrt{\psi^2+4m\psi}} \sinh \frac{\sqrt{\psi^2+4m\psi}}{2}(t-\hat{t}) \right\} e^{-\frac{\psi}{2}(t-\hat{t})} - \frac{B}{m} \quad (23)$$

With Equations (23) and (18), it is possible within the limits discussed herein, to determine at any time $t$, the lateral and axial co-ordinates of a droplet injected at time $t$. $U_{di}$ is given by Equation (19) and $V_{dm}$ is given by

$$V_{dm} = \frac{\epsilon a_0 J_1(\alpha)\psi}{\alpha(\omega^2+\psi^2)^{\frac{1}{2}}}$$

Obviously the foregoing analysis could be extended to include radial displacement effects. Also one might wish to examine the effects of the standing mode and to this end a similar approach could be used. Indeed the discussion could be easily modified to include modes other than the first.

To continue, the following data reduction procedure is suggested.

1. Select an arbitrary angular position $\theta$ , and radial position $\alpha$ .

2. Also select an arbitary time $t$ .

3. Select reasonable values for $\omega$ , and $\Psi$ , B and m . Retain the ability to allow these parameters to vary over a substantial range.

4. After selecting a series of values of $\hat{t}$ , calculate $s_d$ and $x_d$ . The values of $\hat{t}$ chosen will be based on a realistic frequency of droplet production. This frequency may or may not be regarded as a function of the frequency of instability .

5. After performing the above, there will result an instantaneous array depicting the location of all the droplets injected during the time $t - \hat{t}_1$. (The subscript 1 refers to the first droplet injected during the specified time interval.)

6. Examine similar arrays at different $r$ and $\theta$ (i.e. different injector locations). This may give some insight into how streams of fuel and oxidizer interact with each other.

7. Allow $t$ to vary over several cycles and, at each increment of time, produced these droplet arrays. This will permit one to examine how the aforementioned interactions change with time.

8. Determine the axial distance between successive droplets. This does not necessarily mean, determine $x_d(\hat{t}_2) - x_d(\hat{t}_1)$, $x_d(\hat{t}_3) - x_d(\hat{t}_2)$, etc., since 'looping' can occur (see next page). This looping is responsible for the familiar "Klystron Effect".

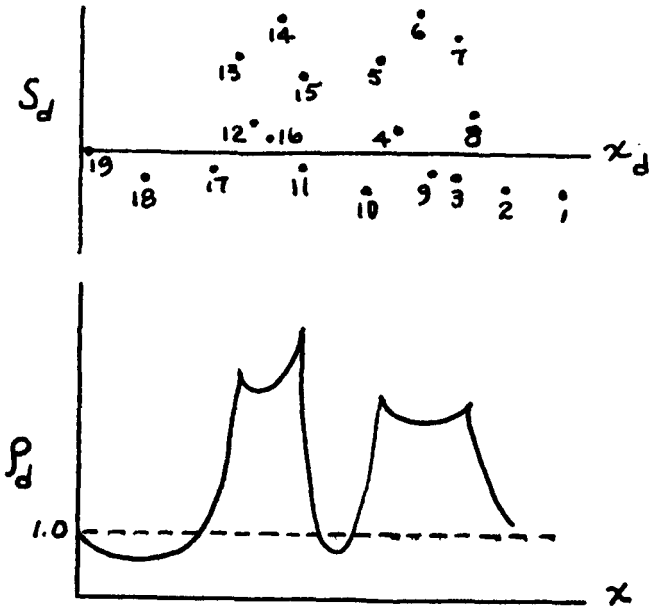


Hypothetical instantaneous droplet array and corresponding droplet density profile illustrating the "Klystron" dual peak effect. In this example maximum density is

$$\frac{\bar{U}}{\omega_d \left[ x_d(\hat{t}_{11}) - x_d(\hat{t}_{15}) \right]}$$

Since the droplets are distinct, separate units and the flow field is non-homogeneous, a droplet density cannot be specified at any one particular location. However, one can discuss the average droplet density variation within a small increment. By tabulating the reciprocal of the aforementioned distance and multiplying by the initial average distance between droplets (i.e. $\frac{\bar{U}}{\omega_d}$ where $\omega_d$ is the frequency of droplet production), one will obtain instantaneous average droplet density profiles. The production of these profiles at various $t$ will allow one to examine how these density waves move through the chamber.

NOMENCLATURE

$a_0$ - Steady-state speed of sound

B - Axial combustion chamber gas velocity at injector

C - Drag coefficient

d - Diameter

$J_1$ - First order Bessel Function

L - Effective length of propellant feed line

m - Slope of axial combustion chamber gas velocity along the chamber

$m_d$ - Mass of droplet

P - Pressure

r - Radial co-ordinate

Re - Reynold's number

s - Transverse displacement

t - Time

$\hat{t}$ - Time of droplet injection

U - Axial velocity

V - Transverse velocity

x - Axial co-ordinate

$\alpha$ - Non-dimensional radial co-ordinate = $\frac{r\omega}{a_0}$

$\gamma$ - Ratio of specific heats

$\epsilon$ - Amplitude parameter

$\theta$ - Angular co-ordinate

$\phi$ - $\tan^{-1} \frac{\omega L}{\bar{U}}$ (defined after (9))

$\xi$ - $\tan^{-1} \frac{\omega}{\psi}$ (defined after (15))

$\rho$ - density

$\psi$ - $\frac{18\mu_g}{\rho_\ell d^2}$ (defined after (13))

$\omega$ - Frequency of oscillation

$\omega_d$ - Frequency of droplet production

SUBSCRIPTS

s - Supply

$\ell$ - Liquid

d - Droplet

g - Gas

m - Maximum

i - Initial

SUPERSCRIPTS

$\bar{}$ - Denotes steady-state

' - Denotes perturbed quantity

REFERENCES

1. Rayleigh, J. W. S., "Instability of Jets", Proc. London Math Soc., Vol. 10, pg. 4 (1878).

2. Castleman Jr., R. A., "The Mechanism of the Atomization of Liquids", National Bureau Standards Journal Research, Vol. 6, pg. 369 (1931).

3. Haenlin, A., "Disintegration of a Liquid Jet", NACA TM 659, February 1932.

4. Priem, R. J., "Breakup of Water Drops and Sprays with a Shock Wave", Jet Propulsion, Vol 27, No. 10, pg. 1084, October 1957.

5. Lane, W. R.,"Shatter of Drops in Streams of Air", Industrial and Eng. Chem., Vol. 43, No. 6, pg. 1312, June 1951.

6. Gordon, G. D., "Mechanism and Speed of Breakup of Drops", Journal Applied Phys., Vol. 30, No 11, pg. 1759, November 1959.

7. Morrell, G., "Critical Conditions for Drop and Jet Shattering", NASA TN D-677, February 1961.

8. Morrell, G., "Breakup of Liquid Jets by Transverse Shocks", Eighth Symposium (International) on Combustion, Williams & Wilkins Co., Baltimore, pg. 1059 (1962).

9. Morrell, G., "Rate of Liquid Jet Breakup by a Transverse Shock Wave", NASA TN D-1728, May 1963.

10. Morrell, G. and Provinelli, F. P., "Breakup of Various Liquid Jets by Shock Waves and Applications to Resonant Combustion", NASA TN D-1728, May 1963.

11. Clark, B. J., "Breakup of a Liquid Jet in a Transverse Flow of Gas", NASA TN D-2424, August 1964.

12. Meisse, C. C., "Effect of Ambient Pressure Oscillations on the Disintegration and Dispersion of a Liquid Jets", Jet Propulsion, Vol. 25, No. 10, pg. 525, October 1955.

13. Reba, I., and Brøsilow, C., "Combustion Instability: Liquid Stream and Droplet Behavior", Part III "The Response of Liquid Jets to Large Amplitude Sonic Oscillations", Aeronautical Research Laboratories WADC TR 59-720, September 1960.

14. Heidmann, M. F., "Oxygen Jet Behavior During Combustion Instability in a Two-Dimensional Combustor", NASA TN D-2725, March 1965.

15. Heidmann, M. F., "Oscillatory Combustion of a Liquid Jet with Gaseous Hydrogen", NASA TN D-2753, March 1963.

16. Rossman, T. G., "A High Speed and High Resolution Photographic Technique for the Observation of Propellant Injected into a Firing Combustion Chamber", Bell Aircraft Corp., Report No. 8007-981-008, May 1959.

17. Rossman, T. G., Eulner, R. N. and Wood, L. M., "Photographic Investigation of Propellant Stream Behavior in a Firing Rocket Engine", Bell Aerosystems, Report No. 9136-95001, June 1966.

18. Ingebo, R. D., "Atomization of Ethynol Jets in a Combustor with Oscillatory Combustion Gas Flow", NASA TN D-3513, July 1966.

19. Dityakin, I. F. and Yagodkin, V. I., "Effect of Periodic Oscillations of Velocity and Density of a Medium on Disintegration of Liquid Jets", Translation of "Vliyanie Periodickeskikh Kolibanii skorosti i plotnosti sredy na rospad zhidkikh struy", Akad. Nauck SSSR, Otdil. Tekh. Nauk No. 4, pg. 115-220 (1957), NASA TT F-63, April 1961.

20. Gartner, E. M., "An Investigation of Vapor Displacement Effects Under Simulated Rocket Chamber Conditions", Master of Science in Engineering Thesis, Princeton University, July 1965.

21. "A Solution for Rocket Combustion Instability", Pratt & Whitney Aircraft, PNA FR-904B, January 26, 1965.

22. Nicholl, J. A. Dabora, E. K. and Ragland, K. W., "A Study of Two Phase Detonation as it Relates to Rocket Motor Combustion Instability", NASA CR-272, August 1965.

23. Schneider, J. M. and Hendricks, C. D., "Source of Uniform-Sized Liquid Drops", Review of Science Inst., Vol. 35, pg. 1349, November 1964.

24. Lee, D. W. and Spencer, R. C., "Photomicrographic Studies of Fuel Sprays", NACA Report No. 454, 1933.

25. Schweitzer, P. H., "Mechanism of Disintegration of Liquid Jets", Journal of Applied Physics, Vol. 8, pg. 513, 1937.

26. Moore, F. K., and Maslen, S. H., "On Strong Transverse Waves Without Shocks in a Circular Cylinder", Journal of Aeronautical Sciences, Vol. 23, No. 6, pg. 583, 1956.

27. Reardon, F. H., Crocco, L., and Harrje, D. T., "Velocity Effects in Transverse Mode Liquid Propellant Rocket Combustion Instability", AIAA Journal, Vol. 2, No. 9, pg. 1631, Sept. 1964.

28. Heidmann, M. F., and Feiler, C. E., "Evaluation of Velocity Effects on Transverse Combustion Instability", NASA TN D-3406, April 1966.

29. Beltran, M.R., Breen, B.P., Hoffman, R.J., Kosvic, T.C., Sanders, C.F., and Wright, R.O., "Analysis of Liquid Rocket Engine Combustion Instability", Air Force Rocket Propulsion Lab. Research and Technology Division, Air Force Systems Command, Technical Report AFRPL-TR-65-254, January 1966.

30. Crocco, L., Harrje, D.T., and Sirignano, W.A., "Nonlinear Aspects of Combustion Instability in Liquid Propellant Rocket Motors", Fifth Yearly Progress Report, Report No. 553-e, May 31, 1965.

31. Crocco, L., Harrje, D.T., and Sirignano, W.A., "Nonlinear Aspects of Combustion Instability in Liquid Propellant Rocket Motors", Sixth Yearly Progress Report, Report No. 553-f, 1 June 1966.

32. Popov, M., "Model Experiments on Atomization of Liquids", NASA-TT-F-65, July 1961.

33. Ohnesorge, W., "Die Bildung von Tropfen an Düsen und die Auflosüna Flüssiger Strahlen", Z. Angew Mata und Mech., Vol. 16, pg. 355, 1936.

## LIST OF FIGURES

FIGURE

INFLUENCE OF ACOUSTIC FIELD ON BREAKUP OF A LAMINAR LIQUID JET

FIGURE

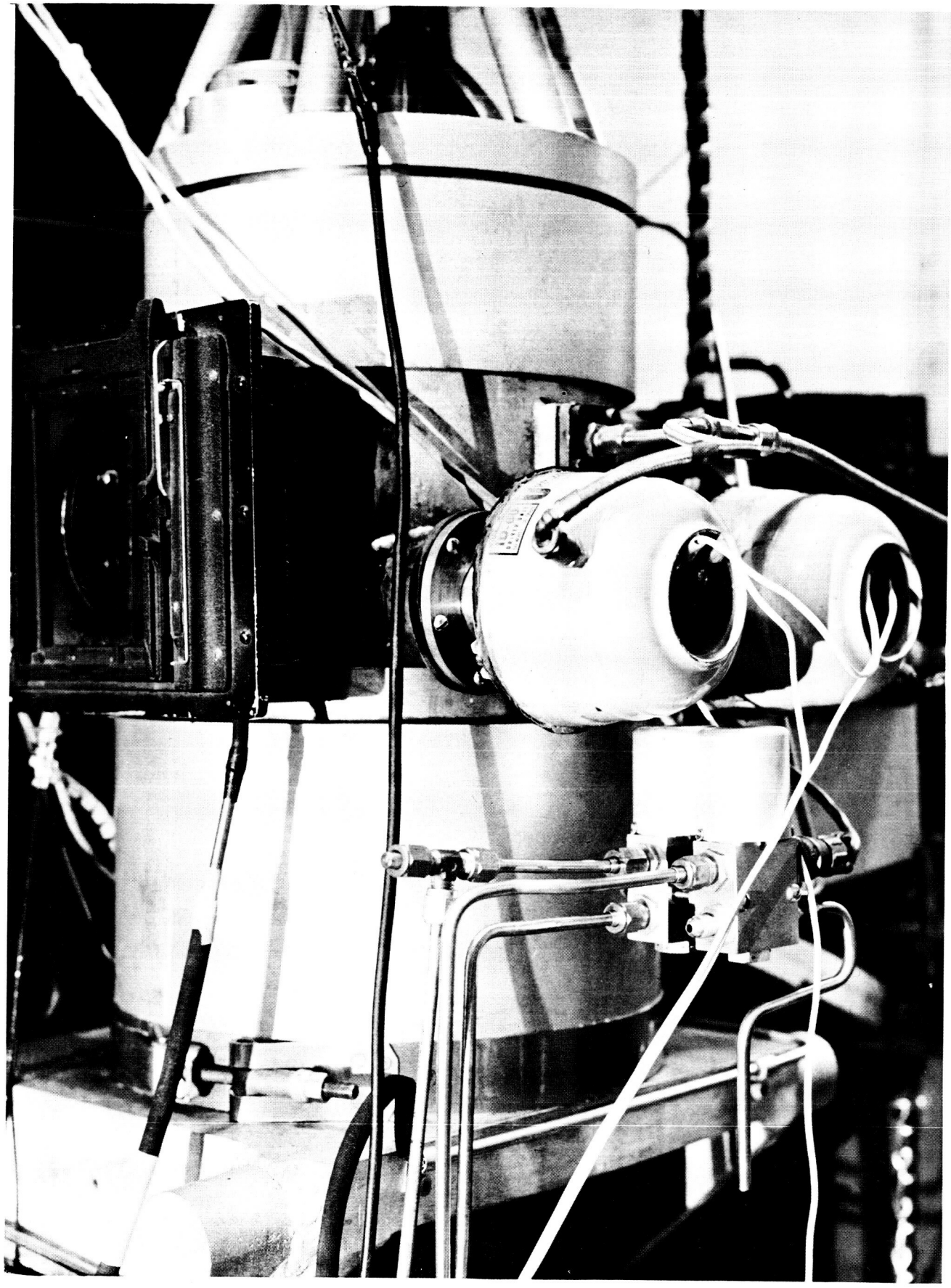

Pseudo rocket chamber

Figure 1

JP21-4127-66

Experimental apparatus schematic

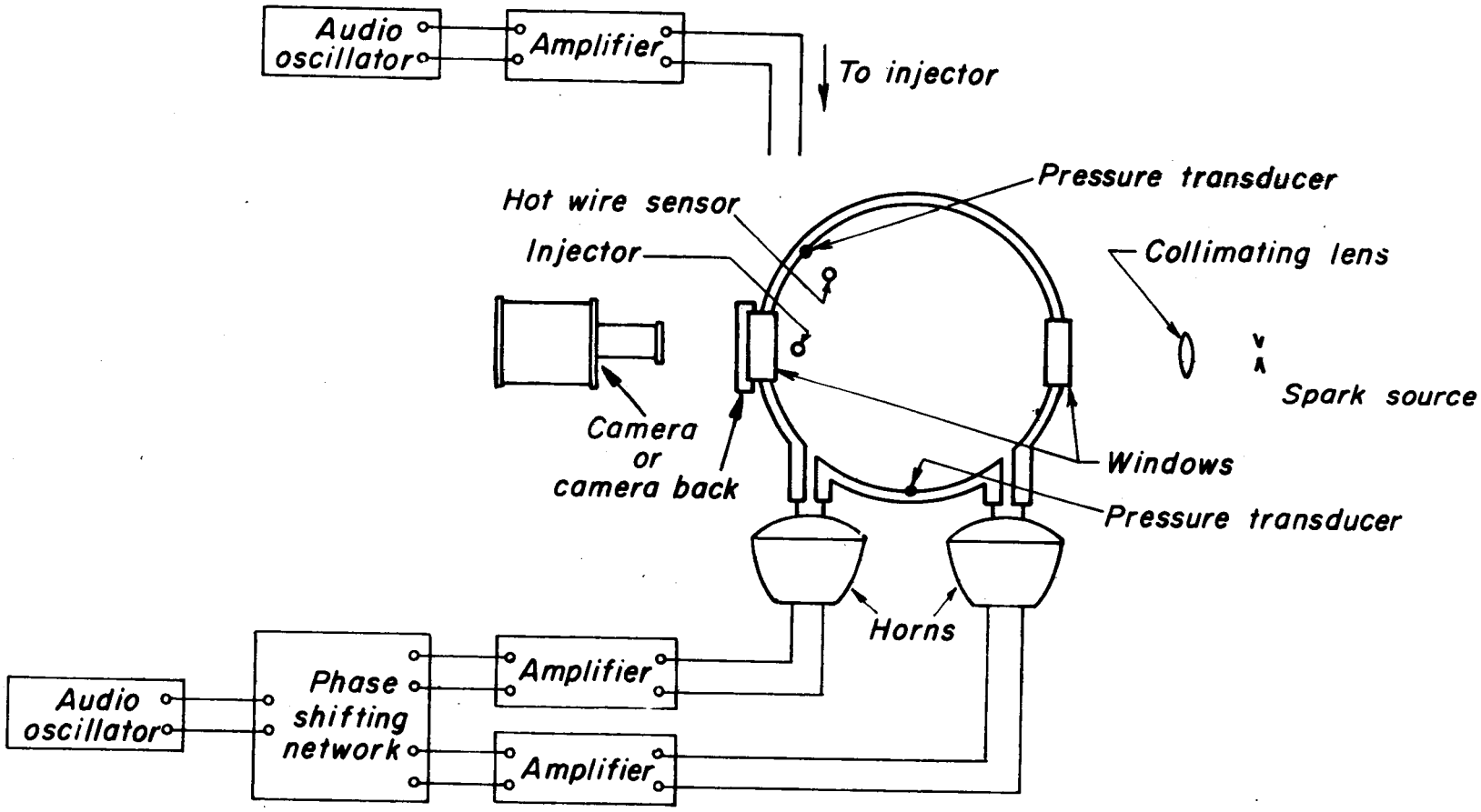


Figure 2

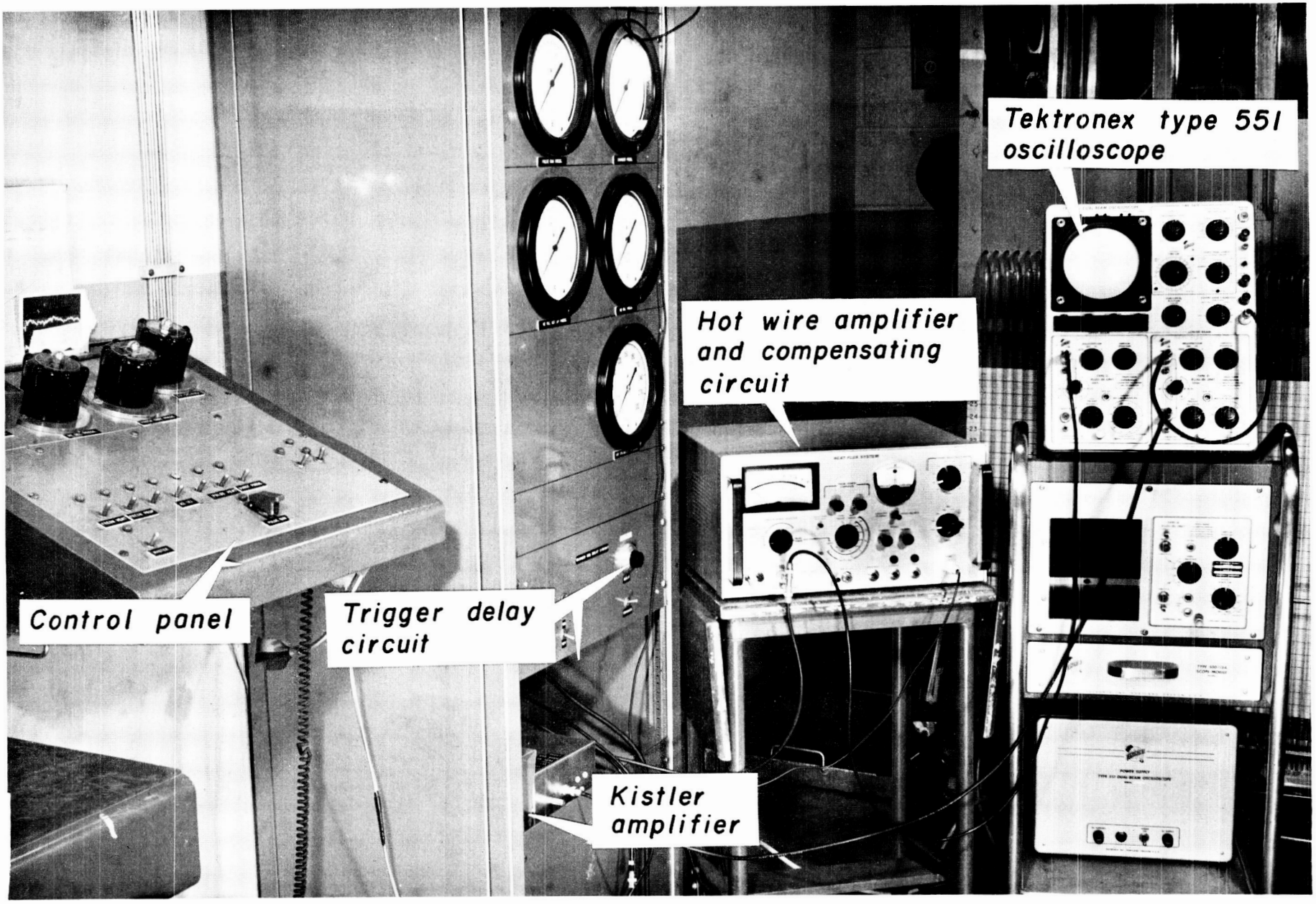


Figure 3

Hot-wire instrumentation and trigger delay circuit

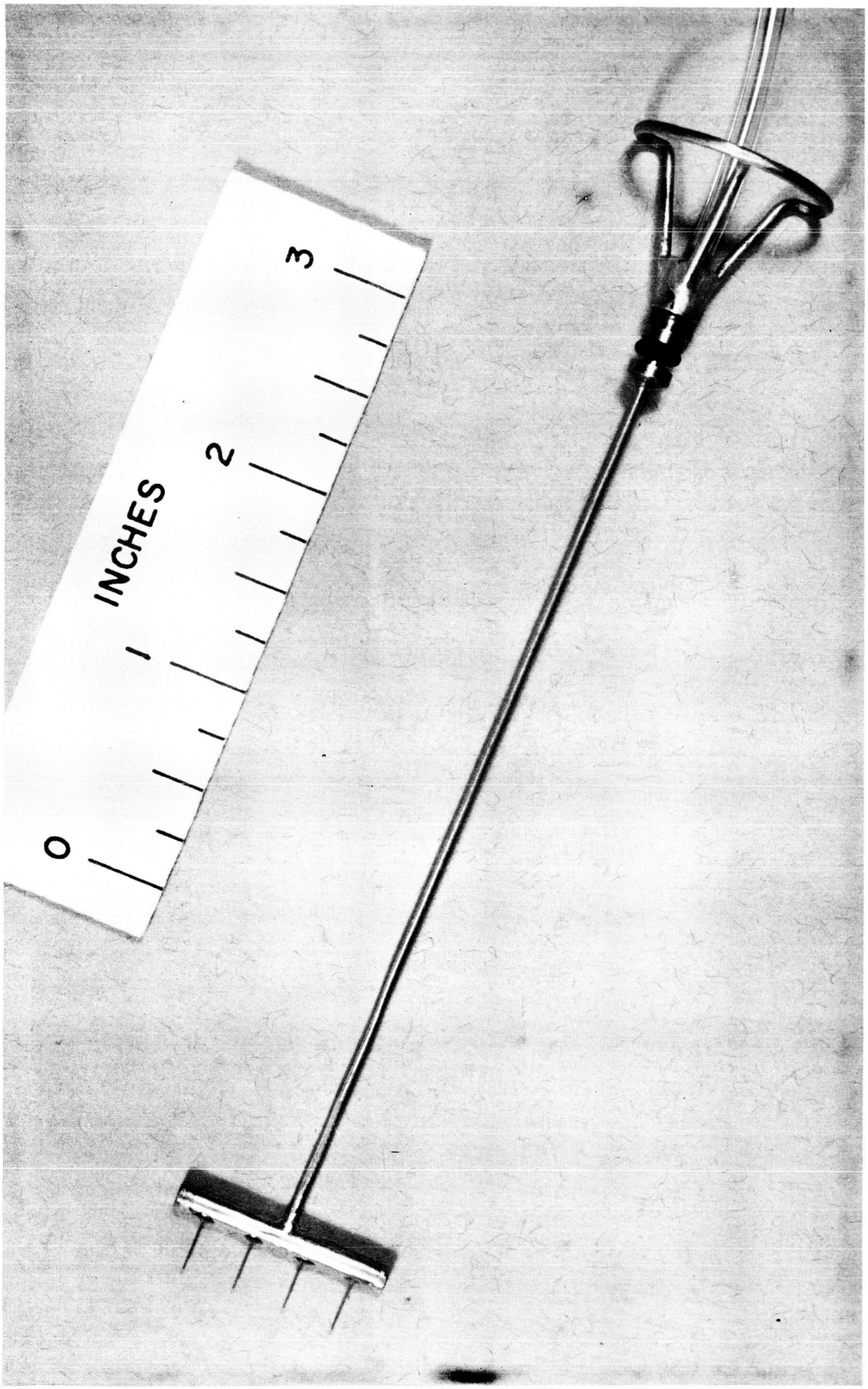


Droplet generator

Figure 4

JP21-P38-66

Terminal and minimum velocities for Freon 114 and $H_2O$ in nitrogen atmosphere

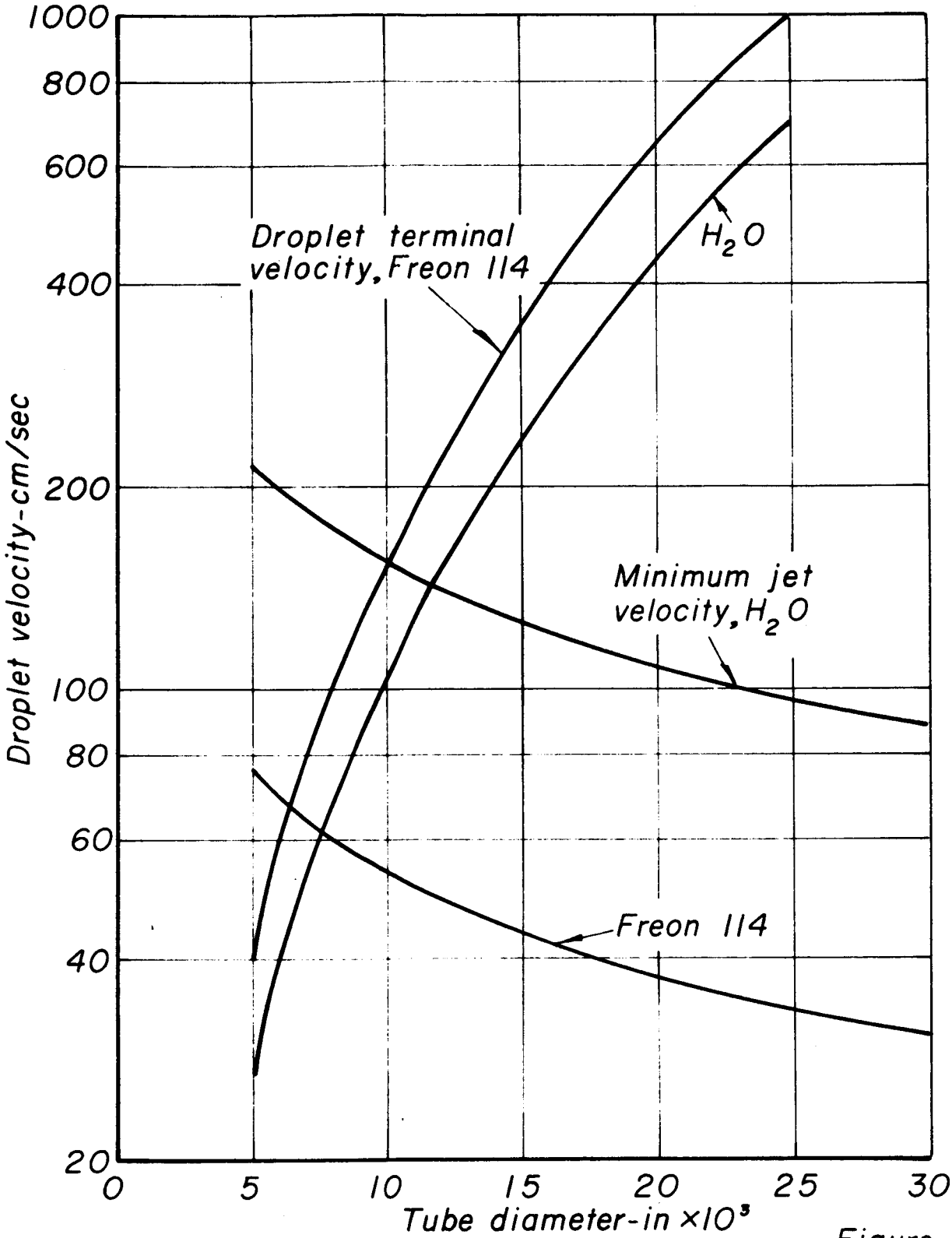


Figure 5

JP21-4117-66

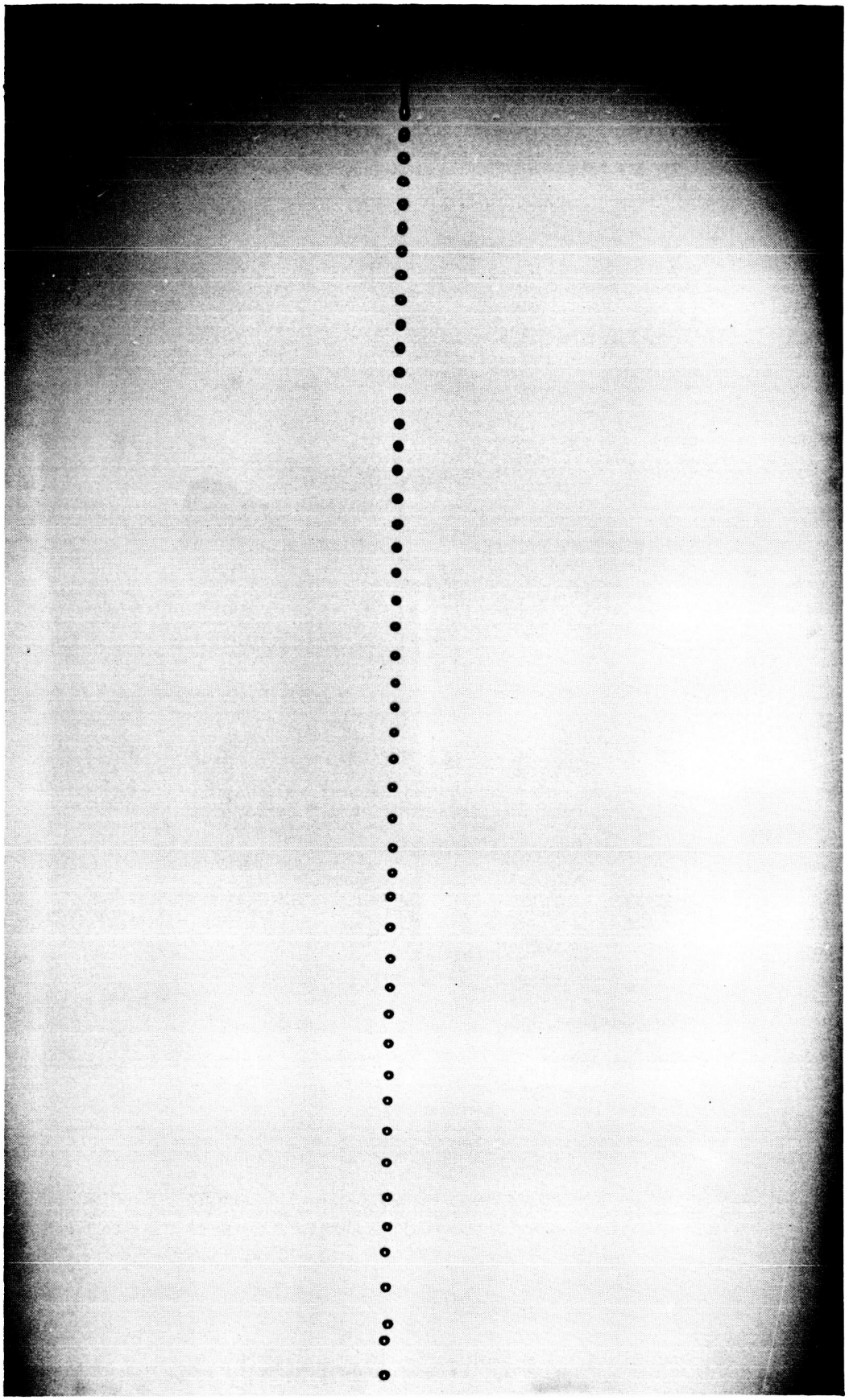

*Typical droplet stream*

*Figure 6*

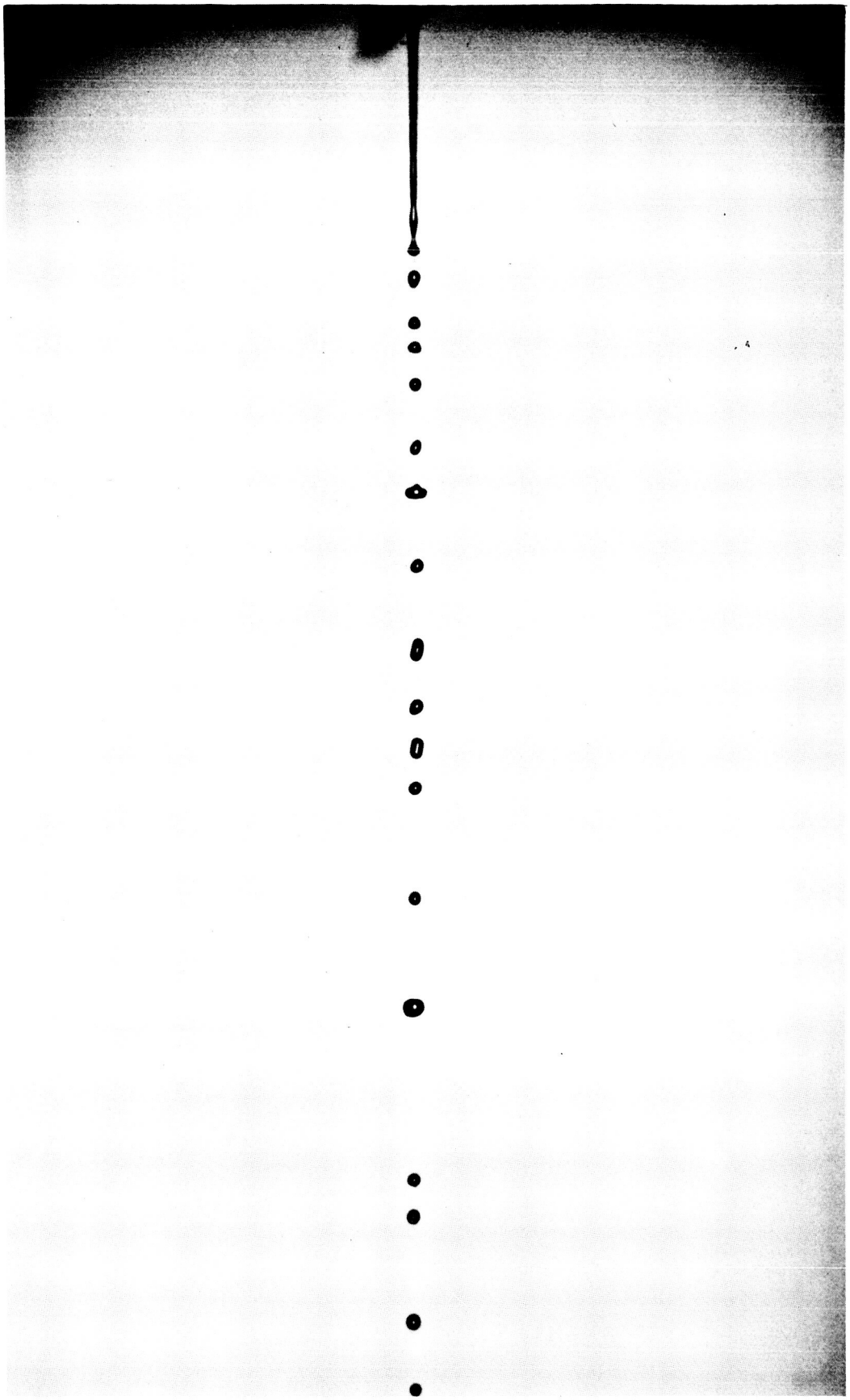

*Laminar jet breakup - quiescent chamber*

*Figure 7*

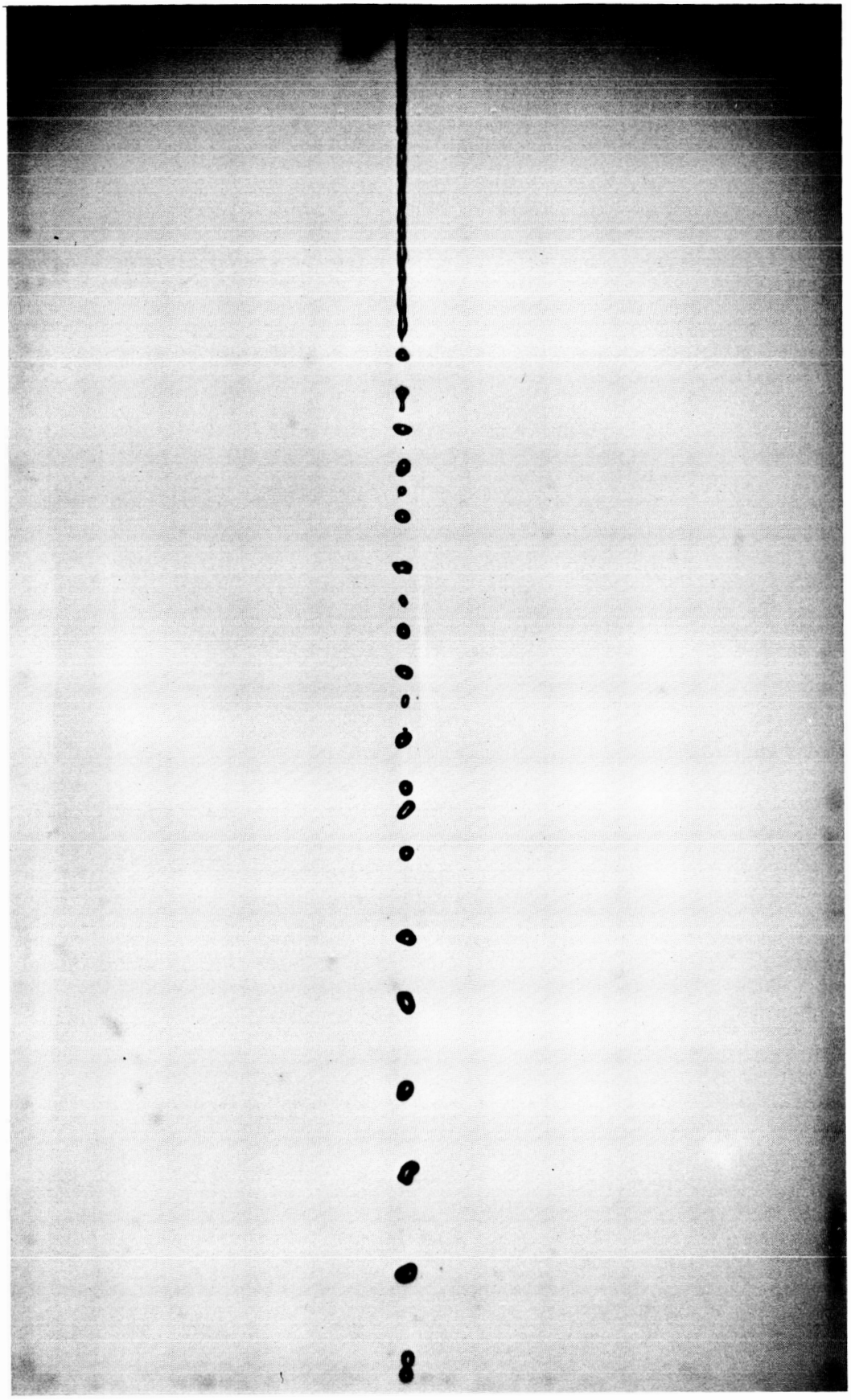

*Transition jet breakup - quiescent chamber*

*Figure 8*